Redox reactions and phase transformation processes at iron mineral surfaces studied by compound specific isotope analysis

Dissertation

zur Erlangung des Grades eines Doktors
der Naturwissenschaften

der Geowissenschaftlichen Fakultät
der Eberhard Karls Universität Tübingen

vorgelegt von
Anke Buchholz
aus Bad Saulgau

2009

Tag der mündlichen Prüfung: 05. Oktober 2009

Dekan: Prof. Dr. Peter Grathwohl

1. Berichterstatter: Prof. Dr. Stefan Haderlein

2. Berichterstatter: Prof. Dr. Stefan Peiffer

Erklärung

Hiermit versichere ich wahrheitsgemäß, dass ich die vorliegende
Arbeit selbständig verfasst, keine anderen als die angegebenen
Quellen und Hilfsmittel benutzt und wörtlich oder inhaltlich
übernommene Stellen als solche gekennzeichnet habe.

Danksagung

Abstract

Iron minerals are widely distributed in the subsurface due to the oxidation of aqueous ferrous iron released by weathering processes. They are known to support electron cycles and facilitate redox reactions in the anoxic subsurface. The high affinity of iron oxides for dissolved ferrous iron leads to accelerated oxidation of Fe(II) upon sorption which involves changes in the mineral structure. These highly reactive Fe(II) phases mostly present as mineral coatings, may act as electron donors and acceptors for chemical and microbial processes. During the oxidation of surface bound Fe(II) by the simultaneously transformation of contaminants, several environmental conditions, i.e., the mineral structure, the available amount of dissolved iron, pH and the occurrence of organic material, may affect the properties of the sorbed Fe(II) and the dynamics of the iron mineral surface. So far the *in situ* characterization of the properties of reactive Fe(II) species and the dynamics of mineral phases is very limited due to a lack of spectroscopic methods. Therefore this work focused on an indirect method, the *reactive isotope tracer approach*, which based on changes in the isotopic composition of probe compounds reacting with surface bound Fe(II) species.

In the second chapter, the iron minerals were characterized by different surface sensitive methods, i.e., μ-XRD, BET and SEM, and selected for the further experiments. This work was essential for the further experiments to guarantee well defined reaction conditions and the comparability with former studies.

The effect of different geochemical factors on the oxidation of surface bound Fe(II) were investigated in chapter 3 and 4. Therefore batch experiments with goethite, lepidocrocite, magnetite or hematite were performed under well defined conditions (50 m^2/L mineral, 1 mM aqueous Fe(II)$_{final}$, CCl$_4$ as

contaminant) and the effect of various pH values (5-8) was investigated in chapter 3. Initially the amount of sorbed Fe(II) decreased in the order: goethite > magnetite > hematite > lepidocrocite. The subsequent transformation of CCl_4 on the mineral/Fe(II) surface showed the fastest reaction rate constants for the goethite system for all pH values. Whereas in the goethite system the reductive dehalogenation of CCl_4 forms chloroform and carbon monoxide as products, only the formation of CO was observed in the hematite system at pH 7. Additionally sorbed Fe(II) on hematite was less oxidized (< 10 times) compared to goethite with different product distribution. All batch experiments showed no reactivity towards CCl_4 at pH 5 and 6 as well as the magnetite and lepidocrocite systems at pH 7. At pH 8 secondary iron mineral formation occurred in the lepidocrocite system during the addition of Fe(II) which was identified as magnetite by μ-XRD and Mössbauer spectroscopy. Only batch experiments with magnetite showed no reactivity towards CCl_4 at pH 8. A Mössbauer study demonstrated the non-stoichiometric nature of magnetite also in the presence of aqueous Fe(II) which could be responsible for the missing reactivity of this iron oxide.

In chapter 4 the influence of several environmental factors like different pH values, amounts of sorbed Fe(II) and sorption times of Fe(II) were investigated at the goethite surface. In general, the results indicated that the surface speciation of Fe(II) on goethite changed significantly already after a small fraction of Fe(II)$_{sorb}$ was oxidized by CCl_4. Thus, changes (i) in the product distribution monitored by the formation of chloroform, (ii) in reaction rate constants for CCl_4 and (iii) in the isotope fraction of CCl_4 could be observed. At the mineral surface two different "types" of reactive Fe(II) species could be identified as shown by the isotope fractionation factors: highly reactive Fe(II) species (ε = -10 to -15‰) and with the depletion of theses species less reactive Fe(II) sites (ε ~ -25‰), formed by readsorption of Fe(II) and/or further surface remodeling processes. The hypothesis of two different Fe(II) species could be further proven by Mössbauer spectroscopy.

Finally, the potential effect of the organic buffers MOPS and HEPES on reaction conditions in a goethite/Fe(II) system was examined in chapter 5. Although the application of these buffers is discussed controversially, many studies include organic buffers to control reaction conditions in batch experiments. Desorption of previously sorbed Fe(II) from the goethite surface in the presence of organic buffers occurred simultaneously with significant sorption of the organic buffers on the mineral/Fe(II) surface (MOPS > HEPES). These observations suggest an interaction between the organic buffers and the Fe(II)/mineral surface. This interaction showed various effects on the oxidation of Fe(II) by CCl_4 (i) with slower reaction rate constants and (ii) higher yield of chloroform with increasing organic sorbate concentrations. The type of interaction between MOPS/HEPES and Fe(II) was further characterized by investigating the competitive electrostatic and steric effects of model compounds (Ca^{2+} and two sulfonic acids). Neither desorption of Fe(II) nor significant sorption of Ca^{2+} and the two sulfonic acids were observed. *In situ* ATR-FTIR measurements of the organic buffers and aqueous Fe(II) excluded the involvement of C-H or C-C bonds in a complex formation and the precipitation of a buffer-Fe(II)-complex could not be observed. Therefore we postulated that free electron pairs of the nitrogen in the heterocyclic ring may form complexes with surface bound Fe(II).

Zusammenfassung

Durch die Oxidation von gelöstem zweiwertigem Eisen, das durch Verwitterungsprozesse freigesetzt wird, sind Eisenminerale in Böden und Sedimenten weit verbreitet. Sie sind bekannt dafür, dass sie Elektronenkreisläufe unterstützen und Redoxreaktionen im anoxischen Milieu ermöglichen. Die hohe Affinität der Eisenoxide zu gelöstem zweiwertigem Eisen führt zu einer beschleunigten Oxidation von reaktivem Fe(II) nach dessen Sorption, womit Veränderungen in der Mineralstruktur einhergehen. Diese hoch reaktiven zweiwertigen Eisenphasen, die meist als Mineralüberzug vorhanden sind, können als Elektronendonoren und –aktzeptoren für chemische und mikrobielle Prozesse agieren. Während der Oxidation von oberflächengebundenem Fe(II) können die Eigenschaften des sorbierten Eisens und die Dynamik der Eisenmineraloberflächen durch diverse umweltspezifische Bedingungen (pH, Mineralstruktur, gelöstes Eisen, organisches Material) beeinflusst werden. In Ermangelung spektroskopischer Methoden ist eine *in- situ* Charakterisierung von reaktiven Fe(II) Spezies und der Dynamik von Mineralphasen bisher nur sehr begrenzt möglich. Deshalb konzentriert sich die vorliegende Arbeit auf eine indirekte Methode, die so genannte „*reactive isotope tracer*" Methode. Diese basiert auf Veränderungen der Isotopenzusammensetzung von Testverbindungen, die mit oberflächengebundenen Fe(II) Spezies reagieren können.

Im zweiten Kapitel dieser Arbeit wurden die Eigenschaften von Eisenmineralen durch verschiedene Oberflächen sensitiven Methoden wie µ-XRD, BET und SEM bestimmt und aufgrund dessen für weitere Experimente ausgewählt. Diese Arbeit war von entscheidender Bedeutung für die weiteren Versuche, um gut definierte Reaktionsbedingungen und eine Vergleichbarkeit mit früheren Studien gewährleisten zu können.

Die Auswirkungen von verschiedenen geochemischen Faktoren auf die Oxidation von oberflächengebundenem zweiwertigem Eisen wurden in Kapitel 3 und 4 untersucht. Dafür wurden Versuche mit Goethit, Lepidokrokit, Magnetit oder Hämatit unter gut definierten Bedingungen (50 m^2/L Mineral, 1 mM gelöstes Fe(II)$_{final}$, CCl$_4$ als Schadstoff) durchgeführt. Zu Beginn wurden die Auswirkungen von unterschiedlichen pH-Werten (5-8) in Kapitel 3 bestimmt. Die Menge an sorbiertem zweiwertigem Eisen verringerte sich in der folgenden Reihenfolge: Goethit > Magnetit > Hämatit > Lepidokrokit. Der darauf folgende Abbau von CCl$_4$ an der Mineral/Fe(II) Oberfläche fand am schnellsten in den Ansätzen mit Goethit bei allen untersuchten pH-Werten statt. Während in den Ansätzen mit Goethit die reduktive Dehalogenierung von CCl$_4$ zu den Produkten Chloroform und Kohlenstoffmonoxid führte, war in den Ansätzen mit Hämatit bei pH 7 nur die Bildung von Kohlenstoffmonoxid zu sehen. Zusätzlich wurde bei pH 8 das sorbierte Fe(II) an Hämatit weniger schnell oxidiert und führte zu verschiedenen Produktverteilungen. Bei pH 5 und 6 konnten in allen Versuchen kein Abbau von CCl$_4$ beobachtet werden. Außerdem zeigten die Ansätze mit Magnetit und Lepidokrokit keine Reaktivität bei pH 7. Zusätzlich konnte bei pH 8 die Bildung einer zweiten Eisenmineralphase bei der Zugabe von gelöstem zweiwertigem Eisen im Lepidokrokitsystem beobachtet werden, welche mittels μ-XRD und Mössbauerspektroskopie als Magnetit identifiziert werden konnte. Nur die Ansätze mit Magnetit zeigten auch bei pH 8 keine Reaktivität. Eine Studie unter Verwendung der Mössbauerspektroskopie zeigte, dass es sich bei dem verwendeten Eisenoxid um ein nicht-stöchiometrisches Fe(II)/Fe(III)-Verhältnis des Magnetits handelt. Selbst in der Anwesenheit von wässrigem Fe(II) war das Magnetit unterstöchiometrisch, wodurch die fehlende Reaktivität des Magnetits sehr wahrscheinlich erklärt werden kann.

Aufgrund der vorangegangenen Ergebnisse wurden in Kapitel 4 weitere umweltrelevante Faktoren wie unterschiedliche pH-Werte, unterschiedliche

Mengen an sorbiertem zweiwertigen Eisen und verschiedene Sorptionsintervalle von Fe(II) an der Goethitoberfläche genauer untersucht. Zusammengefasst deuten die Ergebnisse dieser Experimente darauf hin, dass sich die an der Goethitoberfläche befindlichen Fe(II) Spezies bereits nach ein einer kleinen Menge durch CCl_4 oxidiertes Fe(II) deutlich verändern.

Dies konnte durch Veränderungen (i) in der Produktbildung durch die Bildung von Chloroform gezeigt, (ii) in den Reaktionsraten von CCl_4 und (iii) in der Isotopenfraktionierung von CCl_4 beobachtet werden. Zusätzlich konnten an der Mineraloberfläche zwei verschiedene „Typen" von reaktiven Fe(II) Spezies mit Hilfe der Isotopenfraktionierungsfaktoren identifiziert werden: hoch reaktive Fe(II) Spezies (ε = -10 bis -15‰) und mit der Verringerung dieser Spezies weniger reaktive Fe(II) Spezies ($\varepsilon \sim$ -25‰), welche durch Readsorption von Fe(II) und/oder durch weitere Veränderungen der Mineraloberfläche gebildet wurden. Die Hypothese, dass zwei verschiedene Fe(II) Spezies an der Mineraloberfläche vorhanden sind, konnte durch die Anwendung der Mössbauerspektroskopie weiter untermauert werden.

Zuletzt wurde in Kapitel 5 der potentielle Effekt der organischen Puffer MOPS und HEPES auf die Reaktionsbedingungen in einem Goethitsystem untersucht. Obwohl die Anwendung dieser Puffer kontrovers diskutiert wird, werden organische Puffer in vielen Studien benutzt um die Reaktionsbedingungen zu stabilisieren. Durch die Anwesenheit von organischen Puffern wurde bereits sorbiertes Fe(II) an der Goethitoberfläche desorbiert und gleichzeitig konnte eine bemerkenswerte Sorption der organischen Puffer an der Mineral/Fe(II)-Oberfläche beobachtet werden (MOPS > HEPES). Dies legt die Vermutung nahe, dass eine Wechselwirkung zwischen den organischen Puffern und der Fe(II)/Mineraloberfläche stattfindet. Durch diese Wechselwirkung konnten zahlreiche Effekte auf die Oxidation von Fe(II) durch CCl_4 beobachtet

werden: z.B. (i) langsamere Reaktionsraten und (ii) höhere Ausbeuten an Chloroform mit einer ansteigenden Konzentration an organischen Puffern. Die Art und Weise der Wechselwirkung zwischen MOPS und HEPES und Fe(II) wurde durch Modelsubstanzen (Ca^{2+} und zwei Sulfonsäuren) anstelle der Puffer im Goethitsystem untersucht. Dadurch konnten die möglichen kompetitiven elektrostatischen und sterischen Effekte der organischen Puffer bestimmt werden. Aber weder eine Desorption von sorbiertem Fe(II) noch eine eindeutige Sorption von Ca^{2+} und den beiden Sulfonsäuren an der Mineraloberfläche konnten festgestellt werden. *In situ* ATR-FTIR Messungen einer anoxischen Lösung von organischen Puffern und $Fe(II)_{aq}$ zeigten keine Beteiligung von C-H und C-C- Bindungen an einer Komplexbildung. Zudem konnte keine Ausfällung eines Puffer-Fe(II)-Komplexes beobachtet werden. Deshalb muss angenommen werden, dass durch die freien Elektronenpaare des Stickstoffatoms in dem Heterozyklus eine Komplexbildung mit dem oberflächengebundenem zweiwertigen Eisens zustande kommt.

Table of Contents

1. General Introduction

1.1 The biogeochemical cycle of iron

Iron is the most abundant transition element in the earth's crust (5-6%) and is released as ferrous iron by weathering processes of primary silicate and sulfide minerals. In surface environments the released ferrous iron is immediately oxidized by O_2 and hydrolyzed by H_2O and precipitates as ferric iron oxide (hematite, magnetite) and hydroxide minerals (ferrihydrite, goethite or lepidocrocite) (Cornell and Schwertmann, 2003). Depending on pH, the formation of Fe(III) minerals occurs as abiotic oxidation at higher pH values, whereas at pH < 3 the oxidation of dissolved Fe(II) to Fe(III) minerals is often mediated by microorganisms. The dissolution of these Fe(III) minerals can involve either microbial reduction (Roden and Urrutia, 2002) or chemical complexation (Stumm and Sulzberger, 1992) and produce aqueous Fe(II). Again the aqueous Fe(II) can reprecipitate as insoluble Fe(III) phases by oxidation and hydrolysis. These processes besides several other natural processes can explain the ubiquitous distribution of iron in the environment and the predominant occurrence of the ferrogenic zone besides the methanogenic, sulfidogenic and nitrate-reducing zone of the redox zonation in the environmental subsurface.

1.2 Iron minerals and surface bound Fe(II) species

In anoxic aquifers the role of solid iron minerals plays an important role as reductants, oxidants and electron transfer mediators in the overall electron transfer processes (Christensen et al., 2000). They may interact as an electron donor and acceptor for chemical and microbial processes due to their high

affinity for dissolved ferrous iron (Amonette et al., 2000; Coughlin and Stone, 1995; Stumm and Sulzberger, 1992; Zhang et al., 1992) which is shown as a simplified scheme (Figure 1.1).
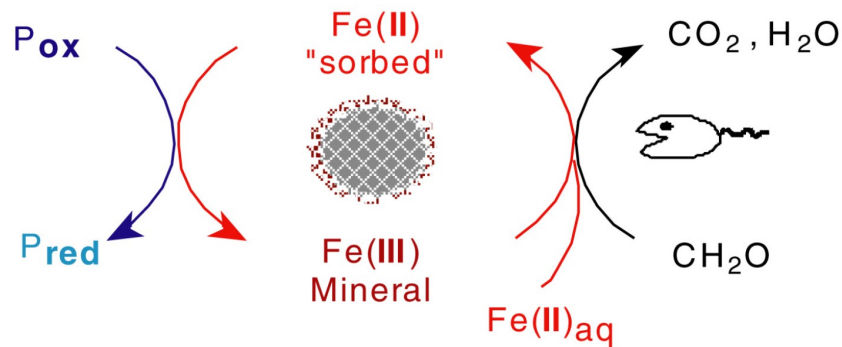
Figure 1.1: Dynamic processes taking place at iron mineral surfaces; oxidation of Fe(II) sorbed to iron minerals by an oxidant (left side) and reduction of Fe(III) and/or adsorption of aqueous Fe(II) induced by microorganisms (right side).

After the sorption of ferrous iron on the iron mineral surface, the surface bound iron becomes a reactive reductant and interacts with dissolved oxidants like O_2, NO_3^- or organic compounds (Heijman et al., 1995; Hofstetter et al., 1999; Klausen et al., 1995; Pecher et al., 2002; Postma, 1990). These freshly formed Fe(III) phases coating the underlying iron mineral are highly bioavailable and are reduced to Fe(II) phases by iron reducing microorganisms (Christensen et al., 2001; Heijman et al., 1995). The presence of aqueous Fe(II) and Fe(III) as bulk element may suggest that the redox cycle occurring on the mineral surface is self sustaining if additionally iron reducing bacteria and oxidants are present in the anoxic groundwater system.

Several studies in the past years have shown the importance of ferrous iron bound to iron mineral surfaces on the transformation processes of organic contaminants in the anoxic subsurface (Cervini-Silva et al., 2001; Haderlein and Pecher, 1998; Klausen et al., 1995; McCormick et al., 2002). They all conclude that surface bound ferrous iron is several orders of magnitude more reactive than dissolved ferrous iron. The high reactivity of surface

bound Fe(II) is based on the fact that Fe(II) and the underlying Fe(III) mineral form an inner sphere complex with the surface hydroxyl groups (Charlet et al., 1998). The formation of an inner sphere complex also increases the density of electrons around the adsorbed Fe(II) species (Stumm and Sulzberger, 1992) and supports an electron transfer between the sorbed Fe(II) species and the iron mineral. Besides the non reactive electrostatic attraction of aqueous Fe(II) and the oxidized Fe(II) species involved in the mineral structure, reactive Fe(II) species can be formed on the mineral surface by several remodeling processes resulting in a mixed valence iron surface (Coughlin and Stone, 1995; Pecher et al., 2002; Zhang et al., 1992).

The redox processes of the oxidation and reduction of surface bound iron species may take place simultaneously (Christensen et al., 2001; Heron et al., 1994; Postma and Jakobsen, 1996; Rugge et al., 1998), whereby the characterization of redox sensitive surface species in groundwater systems is very limited and difficult to observe due to a lack of spectroscopic methods.

1.3   Reactive isotope tracer approach

Due to limitations of spectroscopic methods to monitor the *in situ* oxidation of sorbed Fe(II) species on iron mineral surfaces in field and laboratory experiments, an indirect method has been suggested, the so called reactive isotope tracer approach. This indirect method relies on isotopic changes of an organic probe compound during the oxidation of reactive Fe(II) species on the mineral surface. Therefore carbon tetrachloride seems to be an optimal probe compound for transformation studies on iron minerals. Hence, the single carbon atom in CCl_4 is directly involved in electron

transfer simplifying the interpretation of isotope fractionation (Elsner et al., 2004; Zwank et al., 2003).

The principle of the isotope fractionation is based on changes of the isotope ratios during the transformation of contaminants. Bonds between light isotopes are broken more easily than bonds between heavy isotopes corresponding to the harmonic oscillator model. During the transformation of contaminants the substrate is enriched on its isotope composition during the progress of the reaction, whereas the products are depleted compared to the substrate.

Recently, several studies demonstrated the usefulness of the reactive isotope approach to determine the dynamics and properties of reactive iron species coating iron minerals (Elsner et al., 2004; Zwank et al., 2005). Elsner and co-workers (Elsner et al., 2004) and Zwank and co-workers (Zwank et al., 2005) could demonstrate that the surface normalized reactivity of organic contaminants on an mineral/Fe(II) surface varied within several orders of magnitude depending on the type of iron mineral (green rust, mackinawite, siderite, goethite, lepidocrocite, hematite and magnetite for example). However the reactivity of CCl_4 is dependent on the intermediate trichloromethyl radical, which should not have a great influence on the isotope fractionation of CCl_4 as it already occurs during first C-Cl bond cleavage. Therefore a direct correlation between reaction rate constants and the isotope fractionation may not be expected. Some indirect correlations between the isotope fractionation and the surface reactivity caused by interactions with the mineral surface might be feasible.

The carbon isotopic enrichment factors ε of CCl_4 could be divided into two "classes" (Zwank et al., 2005): for iron sulfides (mackinawite) the enrichment factor ε was about -15.9‰ and for iron oxides ε was -29‰, respectively. However, the enrichment factors of these batch experiments can only be applied in field studies if the enrichment factors did not change under different conditions (pH, amount of dissolved Fe(II)) which has not

been investigated till this day. Also a mixture of several iron minerals can complicate the interpretation of the carbon isotope fractionation of contaminants.

Zwank and co-workers (Zwank et al., 2005) also studied the reaction rates of CCl_4 at a hematite/Fe(II) surface. Even in a relatively short reaction time, the reaction rates increased during the progress of the reaction combined with a change in the isotope fractionation of CCl_4. These results suggest a change in the reaction mechanism of CCl_4 over the reaction time and subsequently a change in the surface properties of the reactive Fe(II) species. The oxidation of surface bound Fe(II) may form a fresh reactive phase, which is more reactive than the underlying hematite surface. Klausen and co-workers (Klausen et al., 1995) observed the formation of new reactive surface sites of uniform reactivity at iron mineral surfaces during the oxidation of sorbed Fe(II). These studies showed the potential applicability of the reactive isotope tracer approach in batch experiments.

1.4 Pathways for reductive dehalogenation of CCl_4

The transformation of carbon tetrachloride in anoxic aquifers may mostly occur as a reductive dehalogenation process either by the transformation in natural systems or in the presence of reactive Fe(0) barriers (Scherer et al., 2001). Especially due to its persistence under oxic conditions (high oxidation state), CCl_4 is often found in contaminated anoxic aquifers (Perlinger et al., 1998). The reductive dehalogenation of CCl_4 on surface bound Fe(II) forms a trichloromethyl radical by an electron transfer and the cleavage of a C-Cl bond (Figure 1.2).
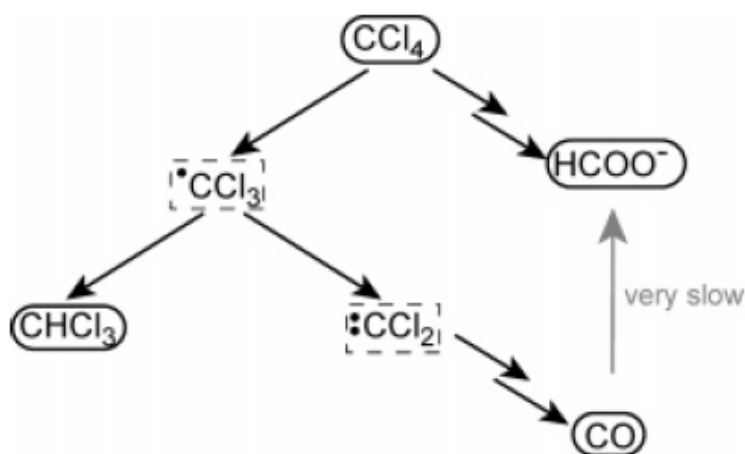
Figure 1.2: Simplified pathway for the surface mediated reductive dehalogenation of CCl₄ by Fe(II) on goethite (Elsner et al., 2004; Zwank et al., 2005).

The trichloromethyl radical can be transformed either to chloroform by a hydrogen radical transfer or to carbon monoxide and formate by a second electron transfer process and further dehalogenation and hydrolysis steps. Under anoxic conditions, chloroform is even more persistent than CCl₄ and enhances the problem of groundwater pollution. It seems that radicals and carbenes play a key role in the transformation mechanism of CCl₄.

1.5   Compound specific isotope analysis in environmental studies

Compound specific isotope analysis (CSIA) appears to be a promising tool to characterize and quantify transformation reactions in laboratory and field studies (Hayes et al., 1990; Hunkeler et al., 1999; Mancini et al., 2003; Meckenstock et al., 1999; Morasch et al., 2001; Schmidt et al., 2004). Furthermore, the carbon isotope fractionation of probe compounds provides mechanistic insights into heterogeneous redox reactions and phase transformation processes taking place at iron minerals under anoxic conditions.

By the coupling of a gas chromatograph (GC) and an isotope ratio mass spectrometer (IRMS) the isotope composition of single compounds in a mixture can be determined (Figure 1.3). In case of carbon isotope analysis the compounds are separated on a GC column and individually oxidized to CO_2 and H_2O in a combustion unit at 940 °C. Afterwards the separation of nitrogen-containing analytes in the reduction oven at 650 °C and the removal of water by a Nafion-membrane take place in the interface. In the isotope ratio mass spectrometer the CO_2 is ionized to $^{12}CO_2$ (m/z 44), $^{13}CO_2$ (m/z 45) and $^{12}C^{16}O^{18}O$ (m/z 46) and the ions are deviated by the magnetic field into Faraday cups.
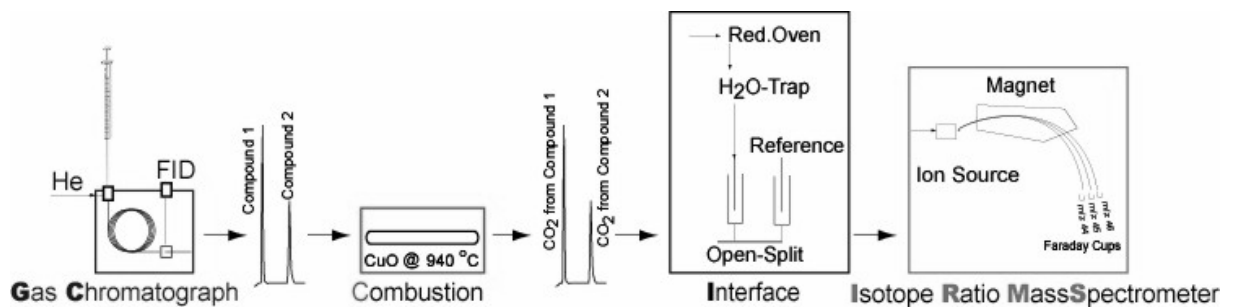
Figure 1.3: Assembly of a GC-IRMS system for the determination of the carbon isotope ratios of compounds (Schmidt et al., 2004).

The isotope composition of carbon is usually expressed in the δ-notation ($\delta^{13}C$):

$$\delta^{13}C = \left(\frac{R_{sample}}{R_{standard}} - 1 \right) \times 1000 \ [‰]$$

where R_{sample} and $R_{reference}$ are the ratios of heavy isotopes to light isotopes ($^{13}C/^{12}C$) of a compound and an international standard. For carbon isotope analysis the international standard is VPDB (Mariotti et al., 1981). The determination of mass 46 ($^{12}C^{16}O^{18}O$) is used for correction of the oxygen isotopes. Furthermore the isotope composition can be also determined of compounds containing hydrogen (Hunkeler et al., 2001; Morasch et al., 2001), nitrogen (Coffin et al., 2001) or chlorine

(Sakaguchi-Söder et al., 2007; Shouakar-Stash et al., 2003; van Warmerdam et al., 1995) for example. The isotope fractionation is expressed in the Rayleigh equation introduced by Mariotti et al. (Mariotti et al., 1981):

$$\left(\frac{R_t}{R_0}\right)=\left(\frac{C_t}{C_0}\right)^{(\alpha-1)}=f^{(\alpha-1)}$$

where α is the isotope fractionation factor, R_t and R_0 are the isotopic ratios of the remained and initial isotopic composition of a compound at the time point t and 0 and f corresponds to the remaining fraction of the substrate. In the literature isotope changes are often described by the enrichment factor ε which can be easily calculated by the following equation:

$$\varepsilon=(\alpha-1)\times1000$$

or can also be described by the linearized form of the Rayleigh equation:

$$\ln\left(\frac{R_t}{R_0}\right)=(\alpha-1)\ln f=\varepsilon\ln f\times1000$$

where ε can be determined by the slope of the regression line in a $\ln(R_t/R_0)$ vs. $\ln f$ diagram.

If the C-Cl bond cleavage during the reductive dehalogenation of CCl_4 is rate-limiting, the fractionation and the enrichment factor can be directly translated into the intrinsic isotope effect, KIE:

$$\alpha^{-1}=\left(1+\frac{\varepsilon}{1000}\right)^{-1}=KIE=\frac{^{12}k}{^{13}k}$$

where ^{12}k and ^{13}k are rate constants for the cleavage of a ^{12}C-Cl and ^{13}C-C bond.

1.6 Scope of the thesis

The main goal of the present work is to gain an improved understanding of heterogeneous redox reactions and phase transformation processes taking place at iron minerals in anoxic environments. In details the main objectives are (i) to monitor electron transfer processes at iron minerals by developing and applying the reactive isotope tracer approach, (ii) to characterize and investigate various iron minerals with respect to the oxidation of sorbed Fe(II) on the mineral surfaces and (iii) to evaluate the effects of geochemical conditions (pH, sorption time of Fe(II), organic sorbates) on the oxidation of Fe(II) on goethite surfaces and the isotope fractionation of the model oxidant CCl_4. The batch experiments are carried out under well defined conditions in the laboratory. The results may provide further insights into the occurrence and the dynamics of surface bound Fe(II) species involved in the redox reactions.

In chapter 2 the properties of the iron minerals are investigated to work in well defined batch systems for further investigations. Therefore, iron oxides (hematite, magnetite) and iron hydroxides (goethite, lepidocrocite) are purchased and synthesized. Afterwards all minerals are characterized regarding their purity (μ-XRD), specific surface areas, particle size and other properties (TOC, pH_{pzc}). Based on this data set, the purchased and synthesized minerals are compared and selected for the following batch experiments.

The effect of geochemical factors on the oxidation of sorbed Fe(II) and the dynamics of surface remodeling at iron minerals are studied to obtain a comprehensive data set in chapter 3 and 4. In chapter 3, both the adsorption of aqueous Fe(II) on these different iron minerals as well as the transformation of CCl_4 with respect to product distribution, reaction rate constants and the isotope fractionation of CCl_4 are investigated at different

pH values. Furthermore secondary iron mineral formation is studied by μ-XRD and Mössbauer techniques to gain further insights on the processes occurring on the mineral surfaces. Additionally in chapter 4, the electron transfer processes are examined with regard to the effect of different amounts of oxidized Fe(II) and the sorption time of Fe(II) in a goethite system. Again the product distribution, reaction rate constants and the isotope fractionation of CCl_4 are used to characterize mechanistic pathways of this redox process. Afterwards the dynamic of the goethite/Fe(II) surface is further investigated performing batch experiments with ^{57}Fe(II) sorbed on the goethite surface analyzed by Mössbauer spectroscopy.

In chapter 5, a study is performed concerning the effect of organic buffers on the oxidation of ferrous iron on goethite as these organic buffers are widely used in environmental studies. The influence of the zwitterionic amine buffers MOPS and HEPES on the reactivity of CCl_4 (product distribution, reaction rate constants) in a goethite/Fe(II) system is examined. Additionally, the possible sorption of these organic buffers on the goethite and/or goethite/Fe(II) surface is studied with respect to their influence on the sorbed Fe(II) species. Furthermore, model compounds are used instead of MOPS and HEPES to characterize and identify the possible complex formation of the organic buffers with ferrous iron or the goethite/Fe(II) surface.

1.7 References

Amonette, J. E., Workman, D. J., Kennedy, D. W., Fruchter, J. S. and Gorby, Y. A., Dechlorination of Carbon Tetrachloride by Fe(II) Associated with Goethite. *Environ. Sci. Technol.* **2000,** *34*, (21), 4606-4613.

Cervini-Silva, J., Larson, R. A., Wu, J. and Stucki, J. W., Transformation of Chlorinated Aliphatic Compounds by Ferruginous Smectite. *Environ. Sci. Technol.* **2001,** *35*, (4), 805-809.

Charlet, L., Silvester, E. and Liger, E., N-compound reduction and actinide immobilisation in surficial fluids by Fe(II): the surface =Fe^{III}OFe^{II}OH° species, as major reductant. *Chemical Geology* **1998,** *151*, (1-4), 85-93.

Christensen, T. H., Bjerg, P. L., Banwart, S. A., Jakobsen, R., Heron, G. and Albrechtsen, H.-J., Characterization of redox conditions in groundwater contaminant plumes. *Journal of Contaminant Hydrology* **2000,** *45*, (3-4), 165-241.

Christensen, T. H., Kjeldsen, P., Bjerg, P. L., Jensen, D. L., Christensen, J. B., Baun, A., Albrechtsen, H.-J. and Heron, G., Biogeochemistry of landfill leachate plumes. *Applied Geochemistry* **2001,** *16*, (7-8), 659-718.

Coffin, R. B., Miyares, P. H., Kelley, C. A., Cifuentes, L. A. and Reynolds, C. M., Stable carbon and nitrogen isotope analysis of TNT: two-dimensional source identification. *Environ Toxicol Chem* **2001,** *20*, (12), 2676-80.

Cornell, R. M. and Schwertmann, U., The iron oxides. *Wiley-VCH Verlag GmbH & Co. KGaA, Weinheim* **2003,** *second, completely revised and extended edition*, 664 pp.

Coughlin, B. R. and Stone, A. T., Nonreversible Adsorption of Divalent Metal Ions (MnII, CoII, NiII, CuII, and PbII) onto Goethite: Effects of Acidification, FeII Addition, and Picolinic Acid Addition. *Environ. Sci. Technol.* **1995,** *29*, (9), 2445-2455.

Elsner, M., Haderlein, S. B., Kellerhals, T., Luzi, S., Zwank, L., Angst, W. and Schwarzenbach, R. P., Mechanisms and products of surface-mediated reductive dehalogenation of carbon tetrachloride by Fe(II) on goethite. *Environ Sci Technol* **2004,** *38*, (7), 2058-66.

Elsner, M., Schwarzenbach, R. P. and Haderlein, S. B., Reactivity of Fe(II)-bearing minerals toward reductive transformation of organic contaminants. *Environ Sci Technol* **2004,** *38*, (3), 799-807.

Haderlein, S. B. and Pecher, K., Pollutant Reduction of Heterogenous Fe(II)/Fe(III)-Systems. *In: D.L. Sparks and T.J. Grundl, Editors, Mineral-Water Interfacial Reactions, American Chemical Society, Washington, DC* **1998,** *Chapter 17,* pp. 342-357.

Hayes, J. M., Freeman, K. H., Popp, B. N. and Hoham, C. H., Compound-specific isotopic analyses: A novel tool for reconstruction of ancient biogeochemical processes. *Organic Geochemistry* **1990,** *16*, (4-6), 1115-1128.

Heijman, C. G., Grieder, E., Holliger, C. and Schwarzenbach, R. P., Reduction of Nitroaromatic Compounds Coupled to Microbial Iron Reduction in Laboratory Aquifer Columns. *Environ. Sci. Technol.* **1995,** *29*, (3), 775-783.

Heron, G., Crouzet, C., Bourg, A. C. M. and Christensen, T. H., Speciation of Fe(II) and Fe(III) in Contaminated Aquifer Sediments Using Chemical Extraction Techniques. *Environ. Sci. Technol.* **1994,** *28*, (9), 1698-1705.

Hofstetter, T. B., Heijman, C. G., Haderlein, S. B., Holliger, C. and Schwarzenbach, R. P., Complete Reduction of TNT and Other (Poly)nitroaromatic Compounds under Iron-Reducing Subsurface Conditions. *Environ. Sci. Technol.* **1999,** *33*, (9), 1479-1487.

Hunkeler, D., Anderson, N., Aravena, R., Bernasconi, S. M. and Butler, B. J., Hydrogen and carbon isotope fractionation during aerobic biodegradation of benzene. *Environmental Science & Technology* **2001,** *35*, (17), 3462-3467.

Hunkeler, D., Aravena, R. and Butler, B. J., Monitoring microbial dechlorination of tetrachloroethene (PCE) in groundwater using compound-specific stable carbon isotope ratios: Microcosm and field studies. *Environmental Science & Technology* **1999,** *33*, (16), 2733-2738.

Klausen, J., Troeber, S. P., Haderlein, S. B. and Schwarzenbach, R. P., Reduction of Substituted Nitrobenzenes by Fe(II) in Aqueous Mineral Suspensions. *Environ. Sci. Technol.* **1995,** *29*, (9), 2396-2404.

Mancini, S. A., Ulrich, A. C., Lacrampe-Couloume, G., Sleep, B., Edwards, E. A. and Lollar, B. S., Carbon and hydrogen isotopic fractionation during anaerobic biodegradation of benzene. *Applied and Environmental Microbiology* **2003,** *69*, (1), 191-198.

Mariotti, A., Germon, J. C., Hubert, P., Kaiser, P., Letolle, R., Tardieux, A. and Tardieux, P., Experimental determination of nitrogen kinetic isotope fractionation: some principles; illustration for the denitrification and nitrification processes. *Plant Soil* **1981,** *62*, 413-430.

McCormick, M. L., Bouwer, E. J. and Adriaens, P., Carbon Tetrachloride Transformation in a Model Iron-Reducing Culture: Relative Kinetics of Biotic and Abiotic Reactions. *Environ. Sci. Technol.* **2002,** *36*, (3), 403-410.

Meckenstock, R. U., Morasch, B., Warthmann, R., Schink, B., Annweiler, E., Michaelis, W. and Richnow, H. H., C-13/C-12 isotope fractionation of aromatic hydrocarbons during microbial degradation. *Environmental Microbiology* **1999,** *1*, (5), 409-414.

Morasch, B., Richnow, H. H., Schink, B. and Meckenstock, R. U., Stable hydrogen and carbon isotope fractionation during microbial toluene degradation: Mechanistic and environmental aspects. *Applied and Environmental Microbiology* **2001,** *67*, (10), 4842-4849.

Pecher, K., Haderlein, S. B. and Schwarzenbach, R. P., Reduction of polyhalogenated methanes by surface-bound Fe(II) in aqueous suspensions of iron oxides. *Environ Sci Technol* **2002,** *36*, (8), 1734-41.

Perlinger, J. A., Buschmann, J., Angst, W. and Schwarzenbach, R. P., Iron Porphyrin and Mercaptojuglone Mediated Reduction of Polyhalogenated Methanes and Ethanes in Homogeneous Aqueous Solution. *Environmental Science & Technology* **1998,** *32*, (16), 2431-2437.

Postma, D., Kinetics of nitrate reduction by detrital Fe(II)-silicates. *Geochimica et Cosmochimica Acta* **1990,** *54*, (3), 903-908.

Postma, D. and Jakobsen, R., Redox zonation: Equilibrium constraints on the Fe(III)/SO4-reduction interface. *Geochimica et Cosmochimica Acta* **1996,** *60*, (17), 3169-3175.

Roden, E. E. and Urrutia, M. M., Influence of Biogenic Fe(II) on Bacterial Crystalline Fe(III) Oxide Reduction. *Geomicrobiology Journal* **2002,** *19,* (2), 209-251.

Rugge, K., Hofstetter, T. B., Haderlein, S. B., Bjerg, P. L., Knudsen, S., Zraunig, C., Mosbaek, H. and Christensen, T. H., Characterization of Predominant Reductants in an Anaerobic Leachate-Contaminated Aquifer by Nitroaromatic Probe Compounds. *Environ. Sci. Technol.* **1998,** *32,* (1), 23-31.

Sakaguchi-Söder, Jager, J., Grund, H. and Schüth, F. M. C., Monitoring and evaluation of dechlorination processes using compound-specific chlorine isotope analysis. *Rapid Communications in Mass Spectrometry* **2007,** *21,* (18), 3077-3084.

Scherer, M. M., Johnson, K. M., Westall, J. C. and Tratnyek, P. G., Mass transport effects on the kinetics of nitrobenzene reduction by iron metal. *Environ Sci Technol* **2001,** *35,* (13), 2804-11.

Schmidt, T. C., Zwank, L., Elsner, M., Berg, M., Meckenstock, R. U. and Haderlein, S. B., Compound-specific stable isotope analysis of organic contaminants in natural environments: a critical review of the state of the art, prospects, and future challenges. *Anal Bioanal Chem* **2004,** *378,* (2), 283-300.

Shouakar-Stash, O., Frape, S. K. and Drimmie, R. J., Stable hydrogen, carbon and chlorine isotope measurements of selected chlorinated organic solvents. *Journal of Contaminant Hydrology* **2003,** *60,* (3-4), 211-228.

Stumm, W. and Sulzberger, B., The cycling of iron in natural environments: Considerations based on laboratory studies of heterogeneous redox processes. *Geochimica et Cosmochimica Acta* **1992,** *56,* (8), 3233-3257.

van Warmerdam, E. M., Frape, S. K., Aravena, R., Drimmie, R. J., Flatt, H. and Cherry, J. A., Stable chlorine and carbon isotope measurements of selected chlorinated organic solvents. *Applied Geochemistry* **1995,** *10,* (5), 547-552.

Zhang, Y., Charlet, L. and Schindler, P. W., Adsorption of protons, Fe(II) and Al(III) on lepidocrocite ([gamma]-FeOOH). *Colloids and Surfaces* **1992,** *63,* (3-4), 259-268.

Zwank, L., Berg, M., Schmidt, T. C. and Haderlein, S. B., Compound-Specific Carbon Isotope Analysis of Volatile Organic Compounds in the Low-Microgram per Liter Range. *Anal. Chem.* **2003,** *75*, (20), 5575-5583.

Zwank, L., Elsner, M., Aeberhard, A., Schwarzenbach, R. P. and Haderlein, S. B., Carbon isotope fractionation in the reductive dehalogenation of carbon tetrachloride at iron (hydr)oxide and iron sulfide minerals. *Environ Sci Technol* **2005,** *39*, (15), 5634-41.

2. Properties, synthesis and characterization of iron minerals

2.1 Introduction

Iron minerals are widely distributed in natural environments especially in soils and sediments. Till today sixteen iron oxides, hydroxides or oxyhydroxides have been known. Dominant species of iron oxides are hematite and magnetite and the most widespread iron oxyhydroxides and hydroxides are identified as goethite, lepidocrocite, ferrihydrite and green rust. Overall they named iron oxides in this work which contain all types of iron oxides, hydroxides and oxyhydroxides. In general they consist of ferric iron and oxygen or hydroxide or a mixture of them. Divalent iron can be observed in magnetite and green rust in which a mixture of ferrous and ferric iron exists. Although many disciplines are dealing with iron oxides, less comprehensive reviews of the state of the art on this class of minerals can be found in literature. The two most comprehensive reviews were done by Fricke and Hüttig (Fricke and Hüttig, 1937) in the third decade of the 20th century and by Cornell and Schwertmann (Cornell and Schwertmann, 2003) in recent years.

The aim of this study was to characterize commercial and synthesized iron minerals which were used for batch experiments regarding redox reactions and phase transformation processes at the surface of these iron minerals. Therefore the iron minerals goethite, lepidocrocite, hematite and magnetite were bought and synthesized in our laboratories. The identification of the mineral properties was determined by several techniques like X-ray diffraction, BET and TOC measurements, scanning electron microscopy and titration experiments.

The synthesis and characterization of the iron minerals were performed in collaboration with Katrin Hellige and Stefan Peiffer, University of Bayreuth within the research group "Electron transfer processes of anoxic aquifers" of the German research foundation.

2.2 Properties

2.2.1 Goethite

Goethite is the most common iron oxide in soils and sediments under cool to moderate climatic conditions due to its thermodynamic stability. In warmer regions, goethite is often associated with hematite, another stable iron oxide. Recently, authigenic nanoparticles of goethite were shown to be the most common diagenetic iron oxyhydroxide in both marine and lake sediments (van der Zee et al., 2003). The formation of goethite can be stimulated either by the oxidation of ferrous iron released by the dissolution of solid Fe(II) compounds like iron carbonates or silicates or by the reduction of ferric iron phases in the subsurface. The color of the iron phase depends on its aggregation state. Massive aggregation of goethite ends up in black or brown colors whereas the powder of goethite has a yellow color. Therefore goethite is often used as pigment in industries. Goethite is named after Johann Wolfgang von Goethe, a famous German poet with a great interest in minerals.

The chemical formula of goethite is α-FeOOH and the crystals are needle shaped. In the goethite structure, each Fe(III) ion is surrounded by three O^{2-} and three OH^{-} ions resulting in $FeO_3(OH)_3$ octahedra. Double chains of octahedra placed by edge sharing are linked to adjacent double chains by corner sharing (Figure 2.1). The symmetry is set up by these double chains and resulted in an orthorhombic structure. Non-linear hydrogen bonds

extend diagonally across the empty cation sites in the goethite structure. These bonds help to stabilize the chains of octahedra.
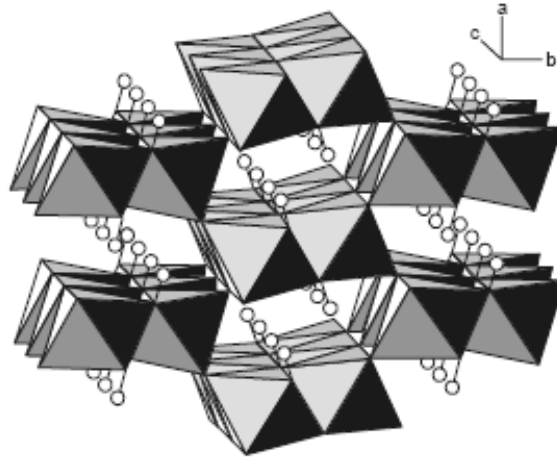
Figure 2.1: Arrangement of the goethite structure with octahedral double chains and hydrogen atoms (white atoms) (Cornell and Schwertmann, 2003).

Goethite crystals can range in length from several nanometers up to microns. Furthermore the specific surface area of goethite measured by BET can vary between 8-200 m²/g (Ardizzone and Formaro, 1985; Cornell et al., 1974; Koch and Moller, 1987; Morup, 1983; Schulze and Schwertmann, 1987; Schwertmann et al., 1985; Torrent et al., 1992) (see Appendix, Table A2.1).

2.2.2   *Lepidocrocite*

Lepidocrocite is less widespread than goethite and occurs in rock, soils and rust. It can be found from moderate to tropical climate and is metastable compared to goethite. Environments where an alteration of oxic and anoxic conditions can be observed by seasonal variability are typical for lepidocrocite formation. Anaerobic conditions are established during raining seasons and lead to the formation of ferrous iron. The oxidation of Fe(II) takes place during oxic conditions and often precipitates as lepidocrocite. The iron mineral lepidocrocite is orange colored.

The chemical formula of lepidocrocite is γ-FeOOH and the crystals are lath-like, tabular, diamond-shaped or rectangular depending on the crystallization conditions. The structure consists of double chains of octahedra as in the structure of goethite. In contrast with goethite which has a tunnel structure lepidocrocite possesses a layered structure. Each double chain shares edges with adjacent ones and is semi shifted with respect of their neighbors which form corrugated sheets of octahedra (Figure 2.2). These sheets just stick together through hydrogen bonds. The organization of ions is found as orthorhombic structure.
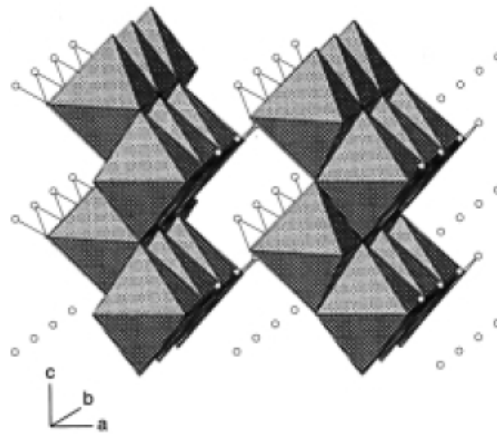
Figure 2.2: Arrangement of the lepidocrocite structure with octahedral double chains in corrugated layers, hydrogen atoms (white atoms) and hydrogen bonds between the layers (Cornell and Schwertmann, 2003).

The specific surface area of lepidocrocite can be found between 32.5-260 m²/g (Giovanoli and Brütsch, 1975; Gomez-Villacieros et al., 1984; Schwertmann and Taylor, 1979; Schwertmann and Thalmann, 1976) which is strongly pH dependent (see Appendix, Table A2.1).

2.2.3 Hematite

Hematite is the oldest known iron oxide. Due to its similar thermodynamic stability as goethite these minerals are often found as mixtures in soils and sediments. Nevertheless hematite is mostly present in subtropical and

tropical environments. Even to characterize soils the ratio of hematite to hematite and goethite (hematite/ (hematite + goethite)) is used either to be hematitic with red soils at lower latitudes or goethitic with brown soils at higher latitudes. Huge deposits of hematite can be found in the so-called banded iron formations or ore deposits. The formation of hematite in nature occurs during weathering processes in soils and is the end product of transformation processes of other iron hydroxides like ferrihydrite (Schwertmann et al., 1999). It is often used as pigment due to the red color of the powder or appears blackish if the mineral is highly aggregated.

The chemical formula of hematite is Fe_2O_3 and the crystal forms are plates, discs, rods, spindles, cubes, ellipsoids or spheres. Due to the arrangement of the cations the hematite structure consists of pairs of $Fe(O)_6$ octahedra. Each octahedron is arranged by edge sharing with three other octahedra in the same plane and by face sharing with another octahedron in an adjacent plane (Figure 2.3). The absence of hydrogen bonds follows in a compact structure with a high density and crystallinity.
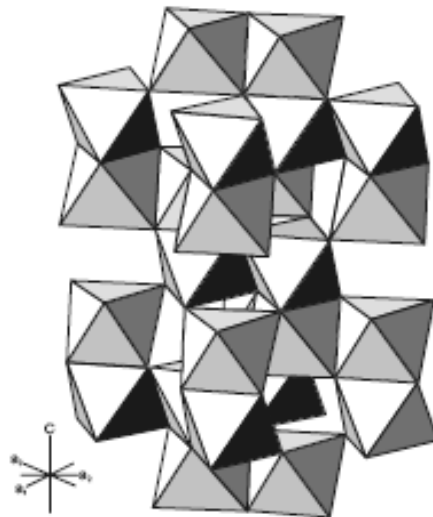
Figure 2.3: Arrangement of the hematite structure with pairs of face-sharing octahedra (Cornell and Schwertmann, 2003).

Depending on the environmental conditions the specific surface area of hematite can be found within 2-200 m²/g (Cornell and Schwertmann, 2003; Schwertmann et al., 1999; Torrent et al., 1994; Torrent et al., 1987) (see Appendix, Table A2.1).

2.2.4 Magnetite

Magnetite is a ferrimagnetic mineral and as important as iron ore. In nature it can be found in deposits of banded iron formations or in large quantities in beach sands. Due to its ferrimagnetic properties magnetite is responsible for the magnetic behavior in soils together with titanomagnetite. In biological systems magnetite is formed in organisms where it is used as orientation aid. The color of magnetite is blackish and it is also often used as pigment in industries.

The chemical formula of magnetite is Fe_3O_4 and the crystal form is orientated as octahedral crystals. Both Fe(II) and Fe(III) are present in the magnetite structure. Therefore it has an inverse spinel structure which is different to most other iron oxides. The ferric iron occupies both tetrahedral and octahedral sites and the tetrahedral sites are distributed between Fe(II) and Fe(III). The structure is composed of octahedral and mixed tetrahedral-octahedral layers (Figure 2.4). Magnetite is often found to be non-stoichiometric. The normal relationship between Fe(II) and Fe(III) is 0.5 but Fe(II) is often partly or fully replaced by other divalent ions.
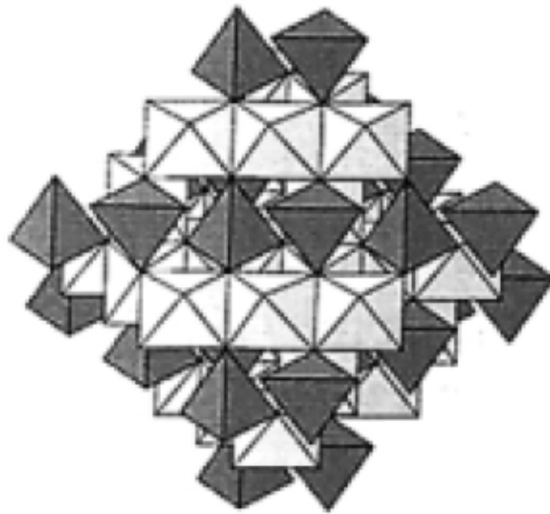
Figure 2.4: Arrangement of the magnetite structure with alternating octahedra and tetrahedral octahedra layers (Cornell and Schwertmann, 2003).

The specific surface area of magnetite can be set between 4-100 m²/g (Cornell and Schwertmann, 2003; Mannweiler, 1966) (see Appendix, Table A2.1).

2.3   Commercial available iron minerals

The iron minerals goethite, lepidocrocite and magnetite were purchased from Lanxess Germany GmbH, Leverkusen. The trade names are Bayferrox 920 Z for goethite, Bayferrox 943 for lepidocrocite and Bayoxide E 8710 for magnetite. These minerals are mostly used in the automotive industry and similar branches of industry as pigments or colorants. In our laboratories the storage was dry and cool as received under lab atmosphere. Additionally hematite was synthesized by heating magnetite up to 900°C for one hour and holding the temperature for another two hours in a muffle furnace. After cooling the hematite was treated like the other commercial iron minerals.

2.4 Synthesis of iron minerals

2.4.1 Goethite

360 mL 5 M KOH were added to 200 mL 1 M $Fe(NO_3)$ solution to precipitate ferrihydrite. The suspension was diluted to 4 L with Millipore water and held in several closed polypropylene flask in a 70°C oven for 60 hours. During this time the voluminous red-brown ferrihydrite suspension transformed into a compact yellow precipitate of goethite. The product was washed three times and frozen-dry. The yield of goethite was between 15.9 g and 16.7 g which was about 88.3-92.8% recovery (Cornell and Schwertmann, 2003).

2.4.2 Lepidocrocite

At pH 7 a 0.06 M $FeCl_2$ solution was precipitated with 120 mL NaOH. Afterwards the suspension was oxidized with air at a rate of 200 mL/min. If the pH dropped lower than 7 further NaOH was added to maintain the pH. The reaction was performed at room temperature, stirred and was completed within 3 hours. The suspension was washed three times and also frozen-dry. The yield of the thin, lathlike crystals was less than 1 g with a very small recovery rate (Cornell and Schwertmann, 2003).

Therefore another method for the synthesis of lepidocrocite was chosen according to Gupta (Gupta, 1976). 120 g $FeCl_2$ x 4 H_2O was dissolved in 3 L of Millipore water and filtered. 16.8 g hexamethylenetetramine (urotropine) was suspended in 600 mL of Millipore water and filtered. Under stirring the two solutions were mixed and a blue-green precipitate ($Fe(OH)_2$) was formed. 42 g $NaNO_2$ in 600 mL Millipore water was added to the suspension and heated up to 60°C with stirring. After reaching the set-point temperature the suspension equilibrated for another 3 hours. The supernatant was removed and the precipitate was washed with

Millipore water to remove chloride until the conductivity was less than 20 μS/cm. The product was frozen-dry and a yield of 34 g was achieved.

2.4.3 Hematite

A 1.5 L solution of 0.002 M HCl was preheated to 98°C and by the addition of 12.45 g $Fe(NO)_3 \times 9\,H_2O$ a 0.02 M solution was achieved. Again the solution was heated to 98°C for 7 days. During that time a compact, bright red precipitate was formed. The suspension was centrifuged and the precipitate was washed and centrifuged several times and then frozen-dry. Eventually, around 2 g of fairly uniform, rhombohedral crystals were formed (Cornell and Schwertmann, 2003).

2.4.4 Magnetite

A solution of 0.3 M Fe(II) sulphate (560 mL) was preheated to 90°C and 240 mL of a mixture of 3.33 M KOH and 0.27 M KNO_3 was added drop wise over a few minutes. The suspension was stirred for 60 minutes and the black precipitate was cooled, washed and dried. It was essential to carry out the entire preparation under an atmosphere of nitrogen (N_2) and that all solutions were degassed with N_2 before usage (Cornell and Schwertmann, 2003).

Alternatively, another synthesis pathway was performed according to Yu and co-workers (Yu et al., 2006). Under stirring an anoxic 3.2 M NaOH solution was heated up to 60°C and an anoxic stoichiometric volume of 0.8 M $Fe(SO)_4 \times 7\,H_2O$ solution was added with 10 mL/min during further stirring at 500 rpm. Afterwards the suspension was further stirred for 5 minutes to remove possible sodium sulphate. At last an anoxic 0.8 M $NaNO_3$ solution was added with 10 mL/min until at the fringe of the solution a blackish precipitate began to form. Subsequently the suspension was stirred at 80°C for 5 hours. Afterwards the supernatant was removed

and the precipitate was washed five times with Millipore water and ethanol. The product was frozen-dry and 14.78 g of a magnetic product was gained.

2.5   Sample preparation and technical equipment

The commercial available and the synthesized iron minerals were handled in the same way for the different analytical characterization methods. All minerals were characterized determing the purity by µ-XRD, the specific surface area by BET measurements, the particle size and crystal shape by scanning electron microscopy, the carbon content by TOC measurements and the point of zero charge by titration experiments.

2.5.1   µ-XRD

For the identity of the iron minerals and the exclusion of impurities the samples were ground and put on a silica-waver directly before the measurements. The surface of the minerals supposed to be as flat as possible to reach a maximum intensity in the X-ray diffractogram. The instrument was called Bruker-D8 with GADDS system (Bruker AXS GmbH, Karlsruhe).

2.5.2   BET measurements

To determine the specific surface area of each mineral by BET measurements developed by S. *B*runauer, P.H. *E*mmett and E. *T*eller (Brunauer et al., 1938), the samples were ground and heated at 105°C for two hours to remove any water residues. The measurements were performed using a Gemini 2375 Surface Area Analyzer (Micromeritics GmbH, Mönchengladbach) and nitrogen as carrier gas.

2.5.3 SEM

The particle size of the iron mineral and the possible existence of impurities were detected by scanning electron microscopy (SEM). Therefore the minerals were ground and given on a round graphite tape fixed on a special sample holder. For the commercially available minerals the scanning electron microscopes was a LEO 1550 VP and for the synthesized minerals a LEO 1450 VP (Carl Zeiss SMT, Oberkochen).

2.5.4 TOC

To analyze the content of organic carbon the samples were ground and put in the sample holders of a Horiba P100 with a TOC Boat Sampler (Elementar Analysensysteme GmbH, Hanau).

2.5.5 pH_{pzc}

The point of zero charge was determined by acid-base titrations according to Liu (Liu et al., 2007). Therefore the minerals were washed several times with anoxic 0.01 M $NaNO_3$ to stabilize the pH and resuspended in anoxic 0.01 M $NaNO_3$. The suspension was adjusted to pH 8.5 with anoxic NaOH and titrated with HNO_3.

2.6   Characterization

2.6.1   Goethite

The purity of the commercial and the synthesized goethite was shown by μ-XRD measurements (Figure 2.5). Furthermore the specific surface area of the synthesized goethite was measured to be three times higher than the commercial one (Table 2.1).
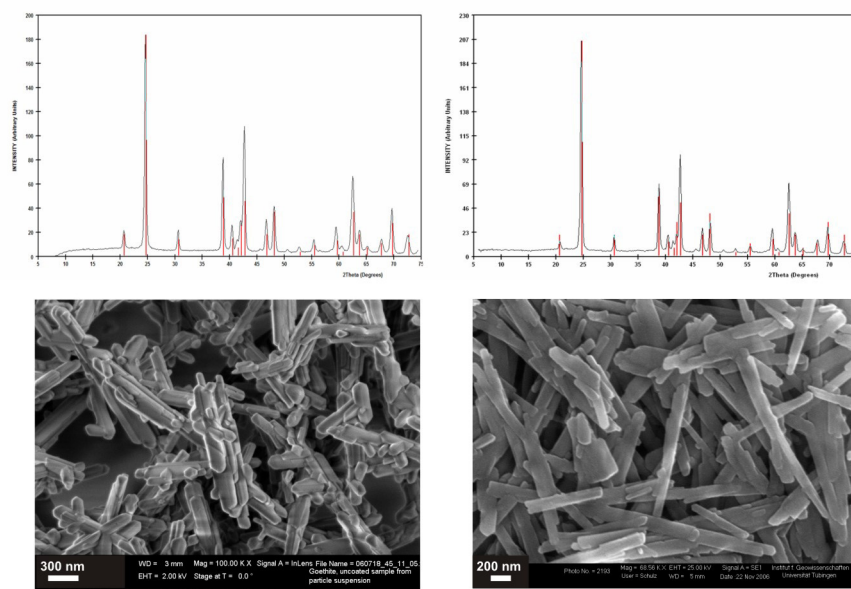
Figure 2.5: μ-XRD spectra (top) and SEM images (bottom) of goethite; left side: commercial goethite, right side: synthesized goethite (Cornell and Schwertmann, 2003); red lines in XRD spectra indicate reference lines of goethite (card 170536).

In comparison with literature values which are in the range of 8-200 m²/g (Ardizzone and Formaro, 1985; Cornell et al., 1974; Koch and Moller, 1987; Morup, 1983; Schulze and Schwertmann, 1987; Schwertmann et al., 1985; Torrent et al., 1992) (see Appendix, Table A2.1), both minerals were at the lower end of the expected range.

The crystal shape was identified as uniform needles in both cases and the particle size distribution was slightly higher for the synthesized goethite (Figure 2.5). Furthermore the total organic carbon (TOC) content was found

7 times higher for the synthesized one, but still in a very low concentration range. At the end the point of zero charge was determined ending up in values of 6.5 for the commercial and 6.4 for the synthesized goethite. It should be noticed that the initial pH_{pzc} for the commercial goethite was 5.5 before washing the mineral twice with Millipore water to remove any sulphate present at the mineral surface. Both values were in the lower sector of reported data (6.1 – 9.5) (Cornell and Schwertmann, 2003; Sigg, 1979).

Table 2.1: Characterization of commercial and synthesized goethite.

properties	goethite	
	commercial	synthesized
purity	pure	pure
specific surface area [m²/g] [a]	8.983 9.214 12.464	26.508 27.020 36.429
particle size [µm]	0.6 - 0.9	0.7 - 1.5
TOC [%] [b]	0.013	0.098
pH_{pzc}	6.5 [c]	6.4

[a] three BET measurement techniques: single point/multiple point/ Langmuir
[b] detection limit of TOC: 0.006%
[c] after washing twice with Miilipore water for sulphate removal
   (initial pH_{pzc} = 5.5)

In summary the commercial goethite was used for the following experiments with respect of the gained information and the available amount of the commercial mineral.

2.6.2 Lepidocrocite

Three different kinds of lepidocrocite were investigated: one commercial and two synthesized minerals. The µ-XRD spectra of the commercial lepidocrocite showed impurities of goethite (5-10%) whereas the synthesized minerals could be identified as pure phases (Figure 2.6). Additionally the lepidocrocite after Gupta (Gupta, 1976) seemed to be less crystalline indicated by broader reflexes of the sample. However the SEM image of the lepidocrocite (Gupta) showed fairly crystalline particles.
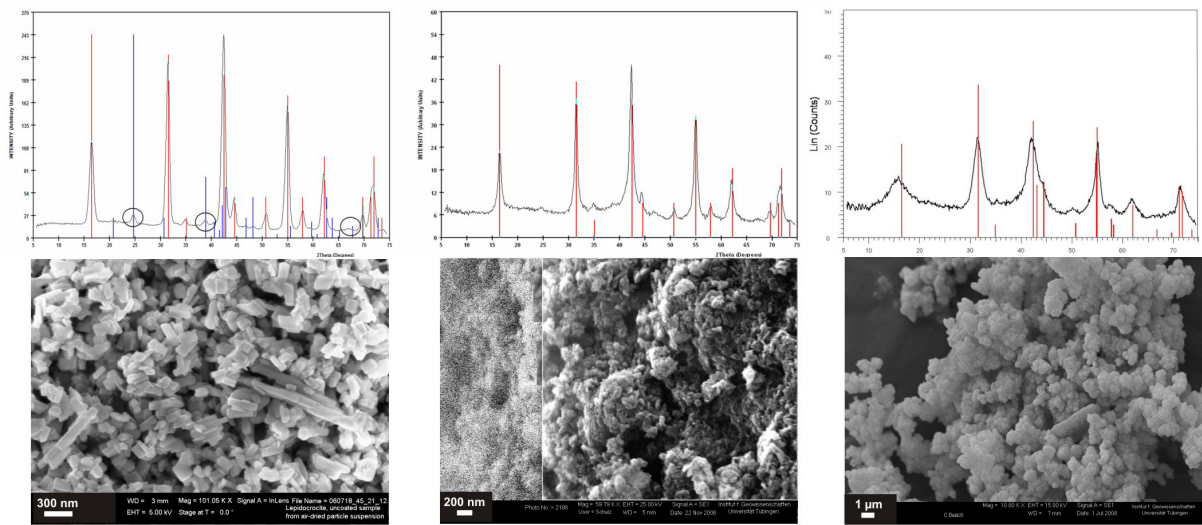
Figure 2.6: μ-XRD spectra (top) and SEM images (bottom) of lepidocrocite; left side: commercial lepidocrocite, middle: synthesized lepidocrocite, Cornell et al. (Cornell and Schwertmann, 2003), right side: synthesized lepidocrocite, Gupta (Gupta, 1976), red/blue lines in XRD spectra indicate reference lines of lepidocrocite (card 080098)/ goethite (card 170536).

The specific surface of the minerals differed with around 17 m²/g for the commercial lepidocrocite and 129-169 m²/g for the synthesized minerals (Table 2.2). The small specific surface of the commercial mineral could be explained by the presence of goethite due to reported values of lepidocrocite are normally in the range of 32.5-260 m²/g (Giovanoli and Brütsch, 1975; Gomez-Villacieros et al., 1984; Schwertmann and Taylor, 1979; Schwertmann and Thalmann, 1976) (see Appendix, Table A2.1). The impurity of the commercial lepidocrocite could also be seen in the SEM image where besides small orthorhombic crystals of lepidocrocite also needles of goethite could be observed (Figure 2.6). Furthermore the particle size was quite small with 0.2-0.6 μm compared to the goethite particles. The total organic carbon content was found to be higher for the synthesized minerals but still less than 0.5%. Again the point of zero charge (pH$_{pzc}$) of the synthesized mineral was smaller than expected due to the presence of goethite. The pH$_{pzc}$ of the lepidocrocite after Gupta was found in the expected range of 6.7-7.5 according to Cornell and Schwertmann (Cornell

and Schwertmann, 2003) and Sigg (Sigg, 1979) and the pH_{pzc} of the other synthesized mineral was not measured due to little recovery.

Table 2.2: Characterization of commercial and synthesized lepidocrocite.

properties	commercial	lepidocrocite synthesized (Cornell et al.)	synthesized (Gupta)
purity	impure (5-10% goethite)	pure	pure
specific surface area [m²/g] [a]	17.042 17.338 23.331	124.794 129.089 175.571	158.836 169.598 235.231
particle size [µm]	0.2 - 0.4	0.2 - 0.5	0.2 - 0.6
TOC [%] [b]	0.011	0.451	0.058
pH_{pzc}	4.65	n.m. [c]	6.85

[a] three BET measurement techniques: single point/multiple point/ Langmuir
[b] detection limit of TOC: 0.006%
[c] not measured due to less recovery

Since the commercial lepidocrocite was contaminated with goethite and the synthesized lepidocrocite after Cornell and Schwertmann was limited due to less recovery, the lepidocrocite after Gupta was used for the following experiments, also having typical properties.

2.6.3 Hematite

Neither the commercial (from commercial magnetite) nor the synthesized hematite showed impurities and both minerals were well crystalline in the µ-XRD spectra (Figure 2.7). As the literature values are given with 2-200 m²/g (Cornell and Schwertmann, 2003; Schwertmann et al., 1999; Torrent et al., 1994; Torrent et al., 1987) the specific surface area could be found within this range with 2 m²/g for the commercial and 44 m²/g for the synthesized mineral (Table 2.3 and see Appendix, Table A2.1). The particle size was quite small with 100-300 nm and well-formed crystalline particles could also be observed in the SEM images.
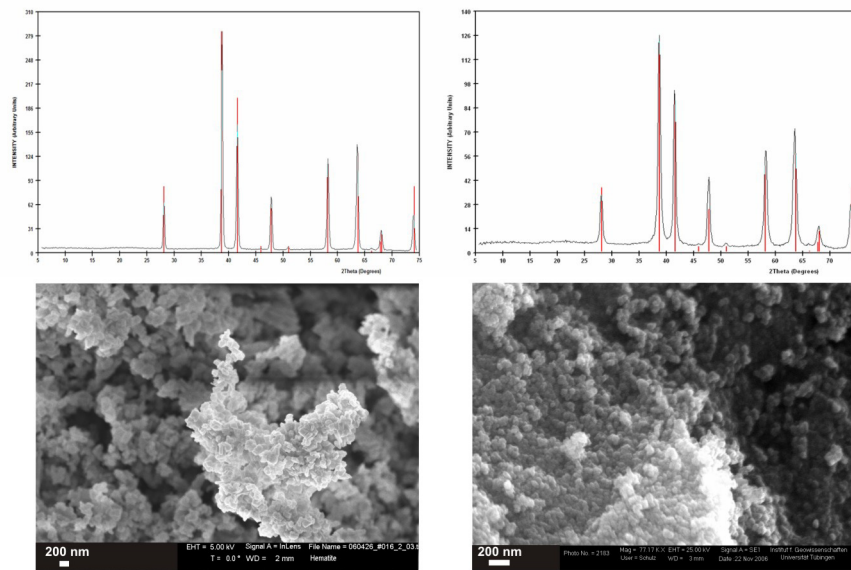
Figure 2.7: μ-XRD spectra (top) and SEM images (bottom) of hematite; left side: hematite from commercial magnetite, right side: synthesized hematite (Cornell and Schwertmann, 2003); red lines in XRD spectra indicate reference lines of hematite (card 330664).

Furthermore the total organic carbon content achieved less than 0.08% for the synthesized hematite and was even below the detection limit ($\leq 0.006\%$) for the commercial hematite. Interestingly the point of zero charge (pH_{pzc}) of the two minerals showed a difference of 3 pH units (5.7 vs. 8.7). Normally the pH_{pzc} can be found in the range of 8.0-9.5 after Cornell and Schwertmann (Cornell and Schwertmann, 2003) and Sigg (Sigg, 1979).

Table 2.3: Characterization of commercial and synthesized hematite.

properties	hematite	
	commercial	synthesized
purity	pure	pure
specific surface area [m²/g] [a]	2.017 2.068 2.800	43.324 44.377 60.070
particle size [μm]	0.1 - 0.3	~ 0.1
TOC [%] [b]	0.006	0.075
pH_{pzc}	5.7	8.7

[a] three BET measurement techniques: single point/multiple point/ Langmuir
[b] detection limit of TOC: 0.006%

Nevertheless the decision which hematite will be used in the experimental setups was driven by the fact that the synthesis of hematite (Cornell and Schwertmann, 2003) was a very time consuming method (7 days) and just a small amount of product (~ 2 g) were obtained. Therefore the commercial hematite was used in the following experiments.

2.6.4 Magnetite

In addition to the commercial magnetite two other syntheses of magnetite were conducted. μ-XRD patterns showed pure magnetite of the commercial and the synthesized iron oxide according to Cornell and Schwertmann (Cornell and Schwertmann, 2003). For the second synthesis product (Yu et al., 2006) a mixture of magnetite and goethite could be determined in a ratio of 1:1 (Figure 2.8). This observation was proven in the SEM image (Figure 2.8; bottom, right part) where also a mixture of octahedral crystals of magnetite and needle-like crystals of goethite was found in the same proportion.

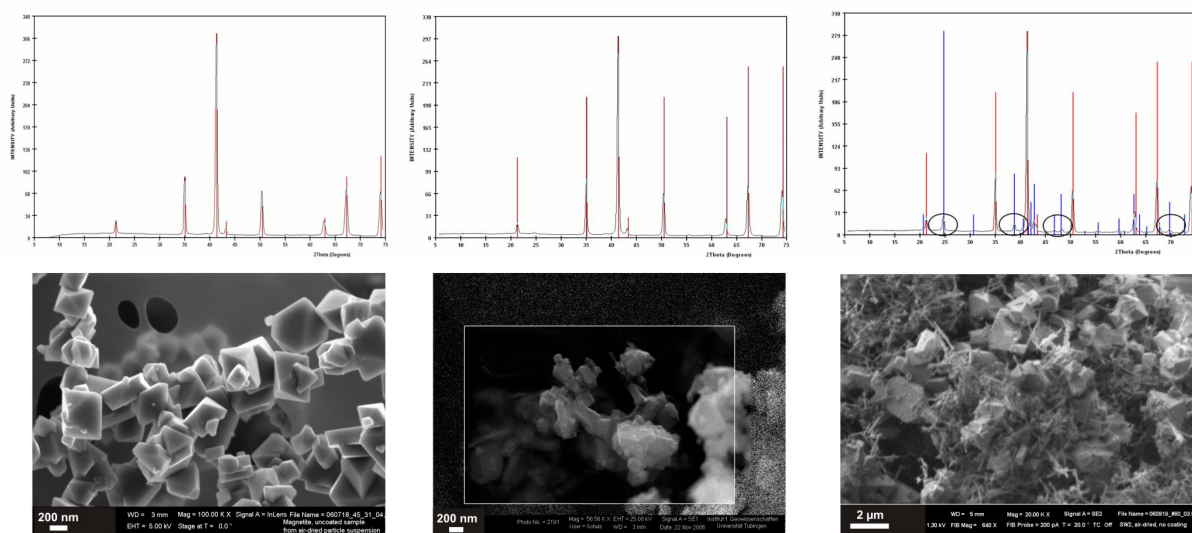**Figure 2.8: μ-XRD spectra (top) and SEM images (bottom) of magnetite; left side: commercial magnetite, middle: synthesized magnetite, Cornell and Schwertmann (Cornell and Schwertmann, 2003), right side: synthesized magnetite, Yu and co-workers (Yu et al., 2006), red/blue lines in XRD spectra indicate reference lines of magnetite (card 190629)/goethite (card 170536).**

The specific surface area of magnetite particles turned up between 4-100 m²/g in the literature (Cornell and Schwertmann, 2003; Mannweiler, 1966) (see Appendix, Figure A2.1). In our cases a specific surface area at the lower end of the reported values could be measured (Table 2.4). The synthesized minerals had up to three times higher surface areas than the commercial magnetite. In addition for hints of impurities like goethite the SEM images were used to determine the particle size of the minerals. The particle size for the two pure iron phases was between 0.3-0.6 μm. For the impure phase the particle size determination was not performed. Furthermore the total organic carbon content of the commercial minerals was found near the detection limit and for the synthesized minerals under 0.06%. Again the point of zero charge (pH_{pzc}) of the two pure phases was similar and ranged at the lower end of the published data (6.4-7.1) after Cornell and Schwertmann (Cornell and Schwertmann, 2003) and Sigg (Sigg, 1979). The pH_{pzc} of the contaminated magnetite was not determined due to the impurity with goethite.

Table 2.4: Characterization of commercial and synthesized magnetite.

properties	commercial	magnetite synthesized (Cornell et al.)	synthesized (Yu)
purity	pure	pure	impure (~ 50% goethite)
specific surface area [m²/g] [a]	3.635 3.756 5.107	8.976 9.314 12.705	6.575 6.575 9.417
particle size [μm]	0.3 - 0.6	0.3- 0.6	n.c. [c]
TOC [%] [b]	0.006	0.057	0.025
pH_{pzc}	6.25	6.50	n.m. [c]

[a] three BET measurement techniques: single point/multiple point/ Langmuir
[b] detection limit of TOC: 0.006%
[c] not calculated/measured due to impurities

Summing up all parameters above and considering the higher availability of the commercial mineral the commercial magnetite was used for the following experimental approaches.

2.7   Conclusion

The characterization of the mineral properties regarding purity, specific surface area, crystal form, particle size, organic carbon content and the point of zero charge resulted in the following minerals: commercial goethite, hematite and magnetite and synthesized lepidocrocite. An overview of the properties of the commercial and synthesized minerals is shown in the Appendix (Figure A2.2 and A2.3).

These minerals were used for batch experiments concerning redox reactions and phase transformation processes that occur on the mineral surface. By the identification of impurities in commercial as well as synthesized mineral batches, the importance of a careful characterization concerning the properties of the iron minerals could be demonstrated. The characterization of iron minerals can be highly recommended for all experiments where iron minerals are involved.

2.8 References

Ardizzone, S. and Formaro, L., Hydrothermal preparation of goethite crystals. *Surface Technology* **1985,** *26*, 269-274.

Brunauer, S., Emmett, P. H. and Teller, E., Adsorption of Gases in Multimolecular Layers. *Journal of the American Chemical Society* **1938,** *60*, (2), 309-319.

Cornell, R. M., Posner, A. M. and Quirk, J. P., Crystal morphology and the dissolution of goethite. *Journal of Inorganic and Nuclear Chemistry* **1974,** *36*, (9), 1937-1946.

Cornell, R. M. and Schwertmann, U., The iron oxides. *Wiley-VCH Verlag GmbH & Co. KGaA, Weinheim* **2003,** *second, completely revised and extended edition*, 664 pp.

Fricke, R. and Hüttig, G. F., Hydroxyde and Oxydhydrate *The Journal of Physical Chemistry* **1937,** *41*, (5), 768-768.

Giovanoli, R. and Brütsch, R., Kinetics and mechanism of the dehydration of [γ]-FeOOH. *Thermochimica Acta* **1975,** *13*, (1), 15-36.

Gomez-Villacieros, R., Hernan, L., Morales, J. and Tirado, J., Textural evolution of synthetic [gamma]-FeOOH during thermal treatment by differential scanning calorimetry. *Journal of Colloid and Interface Science* **1984,** *101*, (2), 392-400.

Gupta, S. K., Über die Phosphat-Elimination in den Systemen HPO-γ-FeO(OH) und HPO-FeCl und die Eigenschaften von Klärschlamm-Phosphat. *Dissertation* **1976,** *Universität Bern*, 138pp.

Koch, C. J. W. and Moller, P. J., Adsorption of nitrogen and water vapour onto goethite surfaces. *Thermochimica Acta* **1987,** *114*, (1), 139-144.

Liu, C., Zachara, J. M., Foster, N. S. and Strickland, J., Kinetics of Reductive Dissolution of Hematite by Bioreduced Anthraquinone-2,6-disulfonate. *Environmental Science & Technology* **2007,** *41*, (22), 7730-7735.

Mannweiler, U., Vergleich dreier Methoden zur Bestimmung von spezifischen Oberflächen in Pulvern. *Chimia* **1966,** *20*, 363-364.

Morup, S., Mossbauer spectroscopy studies of suspensions of Fe3O4 microcrystals. *Journal of Magnetism and Magnetic Materials* **1983,** *39*, (1-2), 45-47.

Schulze, D. G. and Schwertmann, U., The influence of aluminium on iron oxides; XIII, Properties of goethites synthesised in 0.3 M KOH at 25 degrees C. *Clay Minerals* **1987,** *22*, (1), 83-92.

Schwertmann, U., Cambier, P. and Murad, E., Properties of goethites of varying crystallinity. *Clays and Clay Minerals* **1985,** *33*, (5), 369-378.

Schwertmann, U., Friedl, J. and Stanjek, H., From Fe(III) Ions to Ferrihydrite and then to Hematite. *J Colloid Interface Sci* **1999,** *209*, (1), 215-223.

Schwertmann, U. and Taylor, R. M., Natural and synthetic poorly crystallized lepidocrocite. *Clay Minerals* **1979,** *14*, (4), 285-293.

Schwertmann, U. and Thalmann, H., The influence of Fe (II), Si, and pH on the formation of lepidocrocite and ferrihydrite during oxidation of aqueous FeCl2 solutions. *Clay Minerals* **1976,** *11*, 189-200.

Sigg, L. M., Die Wechselwirkung von Anionen und schwachen Säuren mit alpha-FeOOH (Goethit) in wässriger Lösung. *Dissertation* **1979,** *ETH Zürich*, (Nr. 6417), 141pp.

Torrent, J., Schwertmann, U. and Barron, V., The reductive dissolution of synthetic goethite and hematite in dithionite. *Clay Minerals* **1987,** *22*, (3), 329-337.

Torrent, J., Schwertmann, U. and Barron, V., Fast and slow phosphate sorption by goethite-rich natural materials. *Clays and Clay Minerals* **1992,** *40*, (1), 14-21.

Torrent, J., Schwertmann, U. and Barron, V., Phosphate sorption by natural hematites. *European Journal of Soil Science* **1994,** *45*, (1), 45-51.

van der Zee, C., Roberts, D. R., Rancourt, D. G. and Slomp, C. P., Nanogoethite is the dominant reactive oxyhydroxide phase in lake and marine sediments. *Geology* **2003,** *31*, (11), 993-996.

Yu, W., Zhang, T., Zhang, J., Qiao, X., Yang, L. and Liu, Y., The synthesis of octahedral nanoparticles of magnetite. *Materials Letters* **2006,** *60*, (24), 2998-3001.

2.9 Appendix

The appendix contains several overviews: specific surface area of iron minerals according to the literature (Table A2.1), the characterization of commercial iron oxides (Table A2.2) and the characterization of synthesized iron oxides (Table A2.3).

Table A2.1: Overview of specific surface area of the iron minerals goethite, lepidocrocite, hematite and magnetite according to the literature.

mineral	specific surface area [m²/g]	synthesis	conditions	reference
goethite	10	Fe-salt with hydroxylamine	pH 4 - 7,5, 85°C	Ardizzone and Formaro, 1985
	9	ferrihydrite	0.7 M KOH, 60-90°C	Schwertmann et al., 1985
	153		0.7 M KOH, 4°C	
	30 - 90	ferrihydrite	pH 12, 70°C	Cornell et al., 1974
	26 - 52	ferrihydrite	0.3 M KOH, 25°C	Schulze and Schwertmann, 1987
	30	oxidation of Fe(II) systems	pH 12, 20°C	Torrent et al., 1992
	80 - 150	-	pH 6 - 7, 20°C	Koch and Moller, 1987
	71	hydrolysis of Fe(III) solution	-	Morup et al., 1983
	100		acid pH	Schwertmann and Taylor, 1979
				Giovanoli and Brütsch, 1975
				Schwertmann and Thalmann,
	low	oxidation of Fe(II) systems	pH 6-7	Schwertmann and Taylor, 1979
lepidocrocite	17 - 58	-	recrystallisation in KOH, silicate	Gomez-Villacieros et al., 1984
	32.5 - 68	-	20°C - 300°C	Schwertmann and Thalmann, 1976
	> 100	-	in the presence of organics and silikates	Gomez-Villacieros, 1984
hematite	2	solution	alkaline	Torrent et al., 1987
	< 5	-		Schwertmann et al, 1999
	10 - 36,0	-	800 - 900°C	Cornell and Schwertmann, 2003
	10 - 90,0	solution	-	Torrent et al., 1994
	< 200	dehydroxylation of FeOOH	< 100°C	Cornell and Schwertmann, 2003
			500 - 600°C	Cornell and Schwertmann, 2003
magnetite	5.6 - 6.6	reduction of hematite	-	Mannweiler, 1966

Table A2.2: Overview of the characterization of commercial iron oxides.

properties	goethite Bayferrox 920Z	lepidocrocite Bayferrox 943	hematite from magnetite	magnetite Bayoxide E8710
purity	pure	impure (5-10% goethite)	pure	pure
specific surface area [m²/g] [a]	8.983 9.214 12.464	17.042 17.338 23.331	2.017 2.068 2.800	3.635 3.756 5.107
particle size [µm]	0.6 - 0.9	0.2 - 0.4	0.1 - 0.3	0.3 - 0.6
TOC [%] [b]	0.013	0.011	0.006	0.006
pH_{pzc}	6.5 [c]	4.65	5.7	6.25

[a] three BET measurement techniques: single point/multiple point/ Langmuir
[b] detection limit of TOC: 0.006%
[c] after washing twice with $water_{Millipore}$ for sulphate removal (initial pH_{pzc} = 5.5)

Table A2.3: Overview of the characterization of synthesized iron oxides.

properties	goethite (Cornell et al.)	lepidocrocite (Cornell et al.)	lepidocrocite (Gupta)	hematite (Cornell et al.)	magnetite (Cornell et al.)	magnetite (Yu et al.)
purity	pure	pure	pure	pure	pure	impure (~ 50% goethite)
specific surface area [m²/g] [a]	26.508 27.020 36.429	124.794 129.089 175.571	158.836 169.598 235.231	43.324 44.377 60.070	8.976 9.314 12.705	6.575 6.575 9.417
particle size [µm]	0.7 - 1.5	0.2 - 0.5	0.2 - 0.6	~ 0.1	0.3 - 0.6	n.c. [d]
TOC [%] [b]	0.098	0.451	0.058	0.075	0.057	0.025
pH$_{pzc}$	6.4	n.m. [c]	6.85	8.7	6.50	n.m. [d]

[a] three BET measurement techniques: single point/multiple point/ Langmuir
[b] detection limit of TOC: 0.006%
[c] not measured due to less recovery
[d] not calculated/measured due to impurities

3. Effect of pH on the transformation of CCl₄ at different iron mineral surfaces

3.1 Abstract

Different iron oxide and hydroxide minerals which are able to react as a reductant during the transformation of contaminants like chlorinated hydrocarbons are present in the subsurface. For these transformation processes aqueous Fe(II) is required in the anoxic environment. These minerals could form highly reactive surfaces with aqueous Fe(II) in different amounts depending on the concentration of aqueous Fe(II), their surface properties and general environmental conditions (e.g. pH). The amount of sorbed Fe(II) to iron hydroxides (goethite, lepidocrocite) and to iron oxides (magnetite, hematite) was investigated in batch experiments (50 m^2/L mineral, 1 mM aqueous Fe(II)$_{final}$, 30 μM CCl₄ as contaminant) at different pH values (5–8). The amount of sorbed Fe(II) increased at pH 7 in the order: lepidocrocite < hematite < magnetite < goethite. With increasing pH values the amount of sorbed Fe(II) enhanced for all minerals. All of the batch experiments at pH 5 and 6 showed no reactivity towards CCl₄. While goethite showed a significant transformation of CCl₄ at pH 7, hematite reacted 10 times slower with a different product distribution and isotope fractionation. Both other minerals did not indicate any transformation of CCl₄. At pH 8, goethite was again found to be the most reactive iron mineral followed by hematite. Lepidocrocite showed the formation of a secondary iron mineral during Fe(II) addition which was identified as magnetite by μ-XRD and Mössbauer spectroscopy. The reactivity of the lepidocrocite and/or the newly formed magnetite towards CCl₄ was slower compared to hematite. Only magnetite was even non reactive at pH 8. A Mössbauer study demonstrated the existence of a

non-stoichiometric magnetite also in the presence of aqueous Fe(II) which could be responsible for the non reactivity of this iron oxide.

3.2   Introduction

In the subsurface the attenuation of contaminants can refer to dilution, sorption, ion exchange, precipitation, redox reactions and transformation processes (Christensen et al., 2001). Especially the redox reactions and transformation processes on different iron minerals were studied intensively (Hofstetter et al., 1999; Klausen et al., 1995; McCormick and Adriaens, 2004). Furthermore aqueous Fe(II) plays a key role in these redox reactions (Stumm and Sulzberger, 1992) due to its high affinity to sorb on the mineral surface (Coughlin and Stone, 1995; Rugge et al., 1998; Zhang et al., 1992). Such iron phases, present as surface coatings, support an electron cycle by catalyzing heterogeneous oxidation and reduction processes. The underlying iron minerals can act as electron acceptors and electron donors depending on their chemical composition and structure (Heijman et al., 1995; Williams and Scherer, 2004).

Few studies are known considering the oxidation of Fe(II) on iron mineral surfaces and the transformation of chlorinated hydrocarbons (Amonette et al., 2000; Elsner et al., 2004; Lee and Batchelor, 2002; Pecher et al., 2002; Zwank et al., 2005). Amonette and others (Amonette et al., 2000) as well as Pecher and co-workers (Pecher et al., 2002) investigated principle interactions between goethite and Fe(II). Whereas Amonette and co-workers (Amonette et al., 2000) showed the catalytic behaviour of goethite during the oxidation of Fe(II), Pecher and others (Pecher et al., 2002) assumed that several Fe(II) species can be found at the goethite surface. The reactivity of sorbed Fe(II) on different iron minerals depends also greatly on the mineral properties. The iron hydroxides goethite and lepidocrocite and the iron

oxide hematite, all pure Fe(III) phases, have typical crystal structures and surfaces. Thus the adsorption of aqueous Fe(II) and later on the reactivity of sorbed Fe(II) may differ. Magnetite consists of a mixed Fe(II)/Fe(III) phase, which may show a different reactivity of sorbed Fe(II) due to the ferrous iron in the mineral lattice (Elsner et al., 2004). Elsner and co-workers (Elsner et al., 2004) investigated in general the different reactivities of Fe(II)-bearing iron minerals, in which the iron oxides were more reactive than iron carbonate and less reactive compared to iron sulfides. At pH 7.2 slightly different reaction rate constants of chlorinated hydrocarbons were observed even within the class of iron oxides. The influence of different iron minerals on the sorption of Fe(II) and the transformation of CCl$_4$ was studied by Zwank et al. (Zwank et al., 2005). They observed different amounts of sorbed Fe(II) at surface-normalized iron minerals, different reaction rate constants and product distributions not correlating with similar enrichment factors. Therefore the electron transfer between the sorbed Fe(II) species and CCl$_4$ controls the reaction rates for these iron minerals. However no studies are available so far in which the potential effect of different geochemical conditions like the pH values on several iron containing minerals was examined.

In this chapter the effect of different pH values on the transformation of CCl$_4$ at several iron mineral surfaces was investigated. The oxidant carbon tetrachloride was chosen as model compound. The progress of the redox reaction could be followed by compound specific isotope analysis of the single carbon atom of CCl$_4$ and the transformation product CHCl$_3$. The main objectives of this work were (i) to analyze the influence of pH values on the adsorption of aqueous Fe(II), (ii) to determine the effect of pH values regarding product distribution, reaction rate constants and carbon isotope fractionation and (iii) to investigate possible secondary iron mineral formation on the mineral surfaces by μ-XRD and/or Mössbauer spectroscopy.

3.3 Materials and Methods

3.3.1 Chemicals

Carbon tetrachloride CCl_4 (99+%), tetrachloroethylene C_2Cl_4 (99.9+%) and 1-chloro-4-nitrobenzene (99%) were purchased from Aldrich (Steinheim, Germany), chloroform $CHCl_3$ (≥99.5%) from Fluka (Buchs, Switzerland) respectively. Sodium hydroxide (1 M), hydrochloric acid (1 M) and metal iron Fe(0) were obtained from Merck (Darmstadt, Germany). The ferrozine solution was made with 0.1% (w/v) 3-(2-pyridyl)-5-6-diphenyl-1,2,4-triazine-p,p'-disulfonic acid in 50% (w/v) ammonium acetate (Acros, ≥98.0%). All stock solutions or dilutions were prepared using Millipore water.

3.3.2 Minerals

The iron oxides hematite and magnetite and the iron oxyhydroxides goethite and lepidocrocite were used for the experiments. While goethite and magnetite were ordered from Lanxess Germany GmbH the hematite was obtained by heating commercial magnetite and lepidocrocite was synthesized according to Gupta (Gupta, 1976). The storage conditions were cool under lab atmosphere. The characterization of the iron minerals was performed by μ-XRD, BET and TOC measurements and titration experiments (Liu et al., 2007) (Table 3.1).

Table 3.1: Overview of the characterization of the iron minerals used in this study.

properties	goethite Bayferrox 920Z	magnetite Bayoxide E8710	hematite (from magnetite)	lepidocrocite (Gupta)
purity	pure	pure	pure	pure
specific surface area $[m^2/g]$ [a]	8.983 9.214 12.464	3.635 3.756 5.107	2.017 2.068 2.800	158.836 169.598 235.231
particle size [µm]	0.6 - 0.9	0.3 - 0.6	0.1 - 0.3	0.2 - 0.6
TOC [%] [b]	0.013	0.006	0.006	0.058
pH_{pzc}	6.5 [c]	6.25	5.7	6.85

[a] three BET measurement techniques: single point/multiple point/ Langmuir
[b] detection limit of TOC: 0.006%
[c] after washing twice with water$_{Millipore}$ for sulphate removal (initial pH_{pzc} = 5.5)

For further information regarding the synthesis and characterization of iron minerals see chapter 2 "Properties, synthesis and characterization of iron minerals".

3.3.3 Fe(II) Stock Solution

The iron stock solution was prepared exactly in the same way as Elsner and co-workers. (Elsner et al., 2004) using metal iron Fe(0) and 1 M HCl. The exact content of Fe(II) was determined photometrically (562 nm) by the ferrozine assay (Stookey, 1970). For more details see chapter 4 "Effect of environmental factors on the oxidation of Fe(II) at goethite monitored by the isotope fractionation of CCl₄".

3.3.4 pH and Fe(II)$_{aq}$ in goethite suspension

All preparation steps in which Fe(II) was involved were conducted in a glove box (Unilab, Braun, Garching, Germany) to work strictly under anoxic conditions and avoid any oxidation of Fe(II). The general procedure preparing a mineral/Fe(II) suspension is described by Zwank et al. (Zwank et al., 2005) and is also described in chapter 4. The mineral suspension was

adjusted to a considered pH (pH 5.01, 6.01, 7.01 and 8.01 ± 0.05), Fe(II) stock solution was added and after an equilibration time of 18 hours the $Fe(II)_{aq}$ concentration was determined by the ferrozine assay (Stookey, 1970). If necessary these steps were repeated to reach a $Fe(II)_{aq}$ concentration of 1 mM and a considered pH after a total equilibration time of at least 48 hours. Instead of organic buffers the intrinsic buffer capacity of goethite was used to stabilize the suspension (Elsner et al., 2004), since the influence of organic buffers on the transformation of contaminants is discussed controversially and was studied in chapter 5.

3.3.5 Batch Experiments

First aqueous stock solutions of carbon tetrachloride (CCl_4) and tetrachloroethylene (C_2Cl_4, internal standard) were prepared. Serum bottles with 100 mL of Millipore water closed with butyl rubber stoppers were flushed with N_2 for 30 minutes through a syringe needle before aliquots of the pure chemicals were added to obtain carbon tetrachloride concentrations of 30 µM. Before the additions of the pure chemicals the rubber stoppers were quickly opened and afterwards replaced by Viton stoppers during a gentle nitrogen stream in the headspace of the vials (removal of any oxygen while adding) and immediately transferred into the glove box.

The equilibrated and stirred mineral/Fe(II) suspension was divided in 42 mL aliquots within 50 mL serum bottles inside the glove box. The reaction was started by adding 6 mL of the aqueous stock solution. The serum bottles were immediately closed with Viton stoppers. Serum bottles with 42 mL water instead of the goethite/Fe(II) suspension were prepared and treated in the same way as the samples to analyze the total concentration of CCl_4 and C_2Cl_4. The serum bottles were placed on a horizontal shaker (140 rpm, 25°C, in the dark) outside the glove box. All experiments were carried out in duplicates.

3.3.6 Sampling

For each sampling campaign the serum bottles closed with Viton stoppers (duplicates) were centrifuged (Hermle Z320, Hermle, Gosheim, Germany) at 2000 rpm for 10 minutes, individually opened and quickly divided into the vials for GC-MS and GC-IRMS measurements. For GC-IRMS measurements a threefold dilution was necessary due to the limited linear range of the instrument. These steps were repeated for each sampling point and the interval of each sampling campaign ranged from hours to days depending on reaction conditions.

3.3.7 Mössbauer spectroscopy

The iron minerals and mineral/Fe(II) suspensions were investigated with Mössbauer spectroscopy to determine possible secondary iron mineral formation. The mineral suspensions were treated in the same way as the mineral/Fe(II) suspensions where the sample preparation had to be performed under strictly anoxic conditions inside a glove box. The suspensions were filtered and prepared as described by Larese-Casanova (Larese-Casanova and Scherer, 2007). The instrument was a MB-500 with a ^{57}Co Mössbauer source (Wissenschaftliche Elektronik GmbH, Starnberg, Germany).

3.3.8 Analytical Methods

For quantitative analyses of CCl4, CHCl3 and C2Cl4 a TraceGC 2000 gas chromatograph coupled to a TraceDSQ single quadrupole mass spectrometric detector (Thermo Finnigan) was used. The injection was performed with a 2.5 mL headspace syringe (CTC-CombiPAL autosampler) and a split ratio of 1:50. For separation of the compounds an Rtx-VMS capillary column (60 m × 0.32 mm I.D., 1.8 μm film thickness, Restek) was installed. The temperature of the column was initially hold at 40°C for

4 min, heated up to 100°C with a rate of 7°C/min and maintained at 150°C for another 5 min.

The compound-specific isotope ratios ($\delta^{13}C$ values) were determined using a Trace gas chromatograph coupled to a combustion interface (GC Combustion III) maintained at 940°C and an isotope ratio mass spectrometer (DeltaPLUS XP; all Thermo Finnigan). As extraction technique a solid phase microextraction (SPME) with an 85 μm Carboxen™/PDMS Stable Flex™ fiber (Supelco) was used. The extraction time was 20 min at 35°C and the following desorption time was 0.5 min at 270°C. An Rtx-VMS capillary column (same as above) and as carrier gas Helium 5.0 (Air Liquide) were used at several column and split flows. The baseline separation of the compounds were reached using a temperature profile (40°C for 2 min, 100°C for 1 min and 200°C for 5 min to avoid any carry over). An example of a GC-IRMS chromatogram is given in the Appendix (Figure A3.1). Isotopic ratios were determined to a referenced CO_2 standard relative to Vienna Pee Dee Belemnite (VPDB). Reoxidation of the catalyst was carried out regularly after 40-50 measurements. All samples were run in triplicates with standards in between to exclude variability of the instrument (for further details see Chapter 4).

3.4 Results and Discussion

3.4.1 Adsorption of Fe(II) on iron minerals

Several parameters influence the adsorption of Fe(II) on iron minerals. On the one hand non changeable factors in an existing system like the properties of the minerals (e.g. point of zero charge pH$_{pzc}$ or the specific surface area) and on the other hand changeable factors like the concentration of aqueous Fe(II) and the pH. For comparable results the total surface concentration of all minerals was equalized to 50 m^2/L and at the endpoint of the adsorption of Fe(II) the remaining Fe(II)$_{aq}$ content kept constant at 1 mM. To estimate the amount of sorbed Fe(II) the pH$_{pzc}$ values were taken into account. The point of zero charge of all minerals could be measured between 5.7 for hematite and 6.85 for lepidocrocite. In general the surface loading would be negatively charged above these values and vice versa below these values. It could be expected that at higher pH values the sorption of aqueous Fe(II) to the mineral surfaces increases through electrostatic attraction. Additionally a direct interaction between the sorbed Fe(II) and the underlying iron mineral and following surface remodeling could be shown by Hiemstra and van Riemsdijk (Hiemstra and van Riemsdijk, 2007). They investigated the adsorption of ferrous iron on goethite and observed two adsorption steps with or without an electron transfer. In this study the total adsorption of Fe(II) was measured including adsorption of Fe(II)$_{aq}$ due to electrostatic attraction and through electron transfers.

The adsorption of aqueous Fe(II) may be distinguished into two classes towards the transformation of contaminants (Scheme 1): non reactive Fe(II) species like electrostatic attached Fe(II), ^{ie}Fe(II)$_{sorb}$, and oxidized Fe(II) through the underlying goethite, ^{ox}Fe(II)$_{sorb}$, and reactive Fe(II) species like

reactive sorbed Fe(II), ^{react}Fe(II)$_{sorb}$, and less reactive sorbed Fe(II) after surface remodeling processes, ^{remod}Fe(II)$_{sorb}$.

Scheme 1:
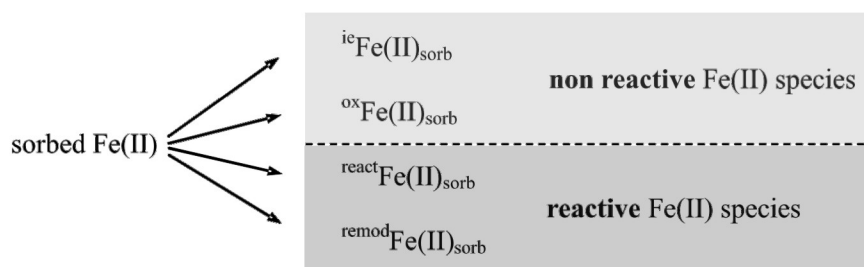
The adsorption of aqueous Fe(II) on the used iron oxides and hydroxides showed that the highest amount of Fe(II)$_{aq}$ sorbed on the goethite surface at all investigated pH values (Figure 3.1 and Appendix, Table A3.1). As a general trend, the concentration of sorbed Fe(II) increased in the order lepidocrocite < hematite < magnetite < goethite. At pH 6 the amount of sorbed Fe(II) turned between hematite and magnetite. The data set at pH 5 will be not discussed here since only the goethite system was investigated at pH 5.
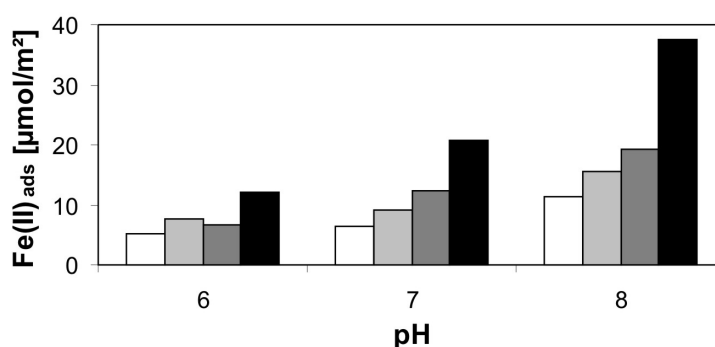
Figure 3.1: Adsorption of aqueous Fe(II) on different iron minerals at pH 6-8; Lepidocrocite (white), hematite (light grey), magnetite (dark grey) and goethite (black)

The adsorption of Fe(II) on different mineral surfaces was compared to a study by Zwank and co-workers (Zwank et al., 2005). Although they used the same iron minerals the sorption behavior of aqueous Fe(II) was different at pH 7.2 – 7.3. The amount of sorbed Fe(II) increased in the order goethite < hematite < magnetite ≤ lepidocrocite. Due to a lack of the given mineral properties (pH_{pzc}, impurities, particle size), it is not feasible to distinguish which parameters are responsible for the different adsorption behavior of Fe(II) on the mineral surfaces.

3.4.2   Effect of pH on the transformation of CCl₄

The transformation of CCl₄ is dominated by two reaction pathways (Elsner et al., 2004; Pecher et al., 2002). Initially reductive dehalogenation to a trimethyl radical occurs driven by an electron transfer between sorbed reactive Fe(II) species and CCl₄. The further transformation of the trimethyl radical continues either by a hydrogen radical transfer that delivers chloroform as product or by a second electron transfer and further dehalogenation steps to CO and the formation of a trichloromethylene anion. Here, the formation of chloroform was investigated although the existence of CO was qualitatively proven in several batch reactors.

The transformation of CCl₄ could not be observed in all batch experiments at pH 5 and 6. At pH 7 the transformation could be measured in the goethite and hematite systems. However the reaction time (> 90% transformation of CCl₄) was much longer for hematite (940 h) than for goethite (100 h) (Figure 3.2). Additionally the product distribution was totally different. For hematite only the formation of CO was observed while 44.8% CHCl₃ was found in the goethite system. Former studies (Zwank et al., 2005) showed the formation of CHCl₃ on goethite (30-33%) and even on hematite (17.5%). Although the initially adsorption of Fe(II) was decreased for hematite in our system, the result may indicate that over the total reaction

time further reactive Fe(II) species are formed and only CO was yielded. At pH 8 the product distribution changed again in all cases. For goethite a decrease of the relative CHCl$_3$ formation (31.8%) occurred while for hematite over 70% chloroform was formed. Even in the lepidocrocite system, where secondary mineral formation occurred (see next paragraph) during the addition of Fe(II), 37% CHCl$_3$ could be detected. Again the magnetite showed no reactivity, which was further investigated in this chapter. The assumption that at higher pH conditions more highly reactive surface sites of Fe(II) are present and subsequently more CO would be formed, is only applicable for the goethite system. Hematite showed the opposite behaviour although in all mineral systems (besides magnetite) the total reaction time decreased due to higher Fe(II) adsorption (Figure 3.2).
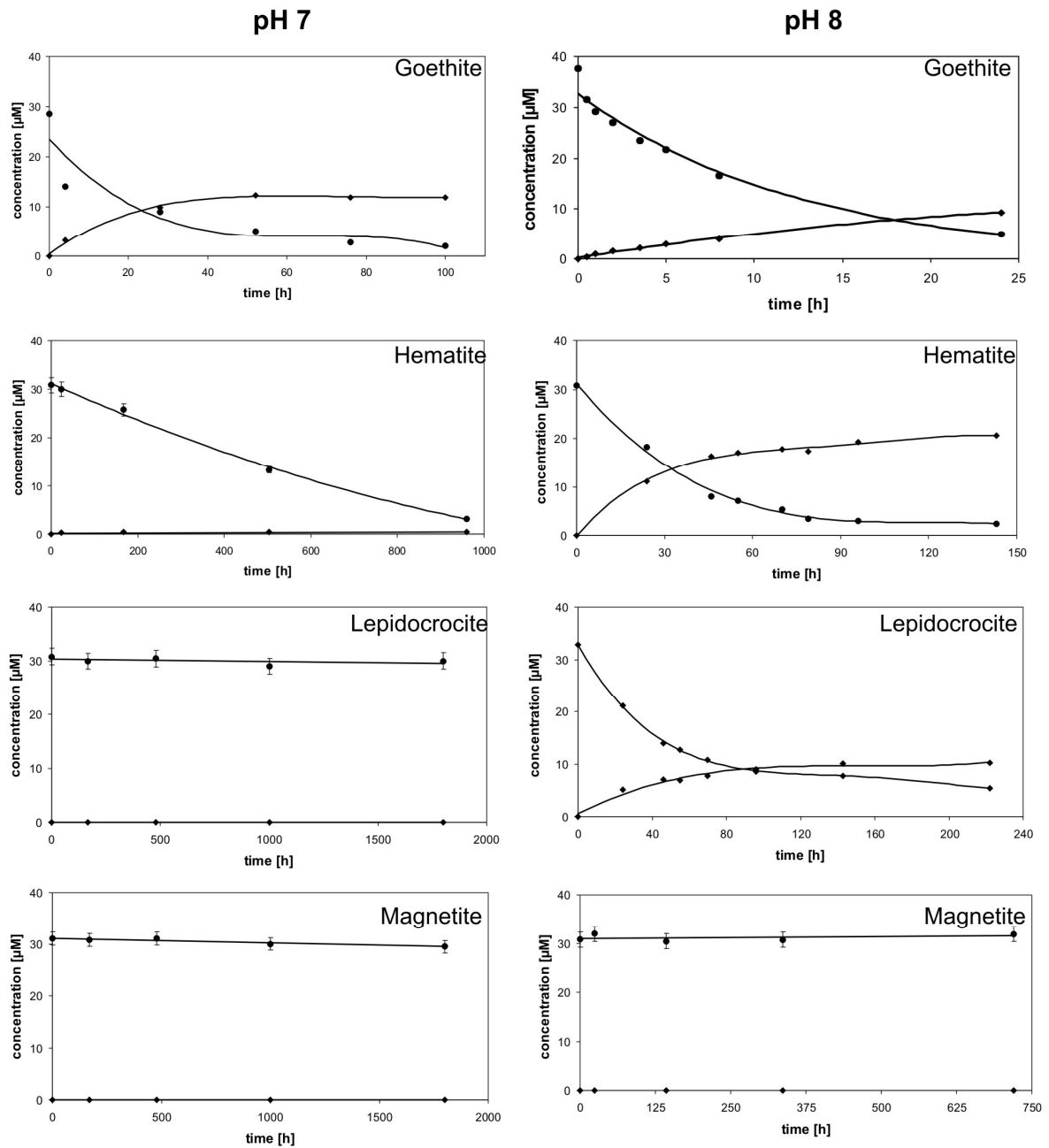
Figure 3.2: Transformation of CCl₄ and simultaneously formation of the product CHCl₃ at pH 7 (left) and pH 8 (right); CCl₄ (●), CHCl₃ (◆); Note the different time scale for the x-axes.

The transformation of CCl₄ followed pseudo-first order kinetics, if a reaction took place at all. The reaction rate constant k'_{obs} (normalized to the total surface area of 50 m²/L) spanned several orders of magnitude at both pH values taking into account earlier studies (Elsner et al., 2004; Zwank et al., 2005) this range could be expected. At pH 7 the k'_{obs} for goethite was

5.3×10^{-4} $h^{-1}m^{-2}L$ and for hematite 2.2×10^{-5} $h^{-1}m^{-2}L$ which agrees with less adsorption of aqueous Fe(II) on hematite. The order of reaction rate constants of iron minerals was identical to pH 7 with goethite > hematite > lepidocrocite + secondary mineral formation > magnetite (non reactive) (Figure 3.3). Additionally the effect was proven that at higher pH values the reaction rates increased compared with values at pH 7 within one iron mineral system. Two different kinds of reactive Fe(II) species might be present at different pH values.
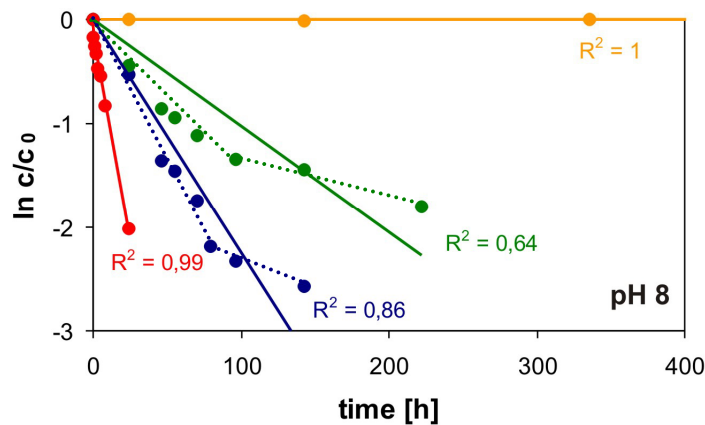
Figure 3.3: Reaction kinetics of CCl₄ in different mineral systems at pH 8; goethite (red), hematite (blue), lepidocrocite (green) and magnetite (orange).

The assumption of only one reaction rate expressing the transformation of CCl₄ at hematite and lepidocrocite might be too general. Two reaction rates of the transformation of CCl₄ at hematite and lepidocrocite surfaces could be also interpreted at pH 8. At the beginning of the transformation of CCl₄ initial reaction rates could be observed where more reactive Fe(II) species were existent. At the end of the reaction lower reaction rates could be measured due to several oxidation steps of sorbed Fe(II) and less reactive Fe(II) species present on the mineral surfaces. However these considerations are the opposite of the observation of Zwank and others. (Zwank et al., 2005). They assumed also two reaction rates for the transformation of CCl₄ at hematite at pH 7.2, but the initial reaction rate seemed to be slower than

the endpoint reaction rate. Again these results are difficult to compare due to slightly differences in the pH value and different iron mineral batches. Isotope fractionation measurements were performed to show the existence of two different reactive Fe(II) species on the mineral surfaces. Based on the Rayleigh model the enrichment factor ε for the goethite system changed from -21.9‰ (pH 7) to -13.8‰ (pH 8) (Figure 3.4). It can be concluded that more reactive Fe(II) species, ^{react}Fe(II)$_{sorb}$, must be present at higher pH values. Due to very few experimental points the interpretation of the isotope fractionation of CCl₄ on hematite at pH 7 is hardly feasible and will not be considered in the discussion. At pH 8 the isotope fractionation of CCl₄ on hematite and lepidocrocite seemed to be similar with $\varepsilon = $ -16.5‰ (hematite) and -16.8‰ (lepidocrocite). If two different isotope fractionation factors within each mineral system might be considered just the initial ε stayed in a similar range ($\varepsilon_{initial} = $ -14.2‰ and -13.2‰). The isotope fractionation of CCl₄ changed during the experiments ($\varepsilon_{end} = $ -20.2‰ and -37.9‰) resulting from a change of the reaction mechanism. The reactive Fe(II) species, ^{remod}Fe(II)$_{sorb}$, altered during the progress of the reaction in the case of lepidocrocite possibly through further secondary mineral formation.
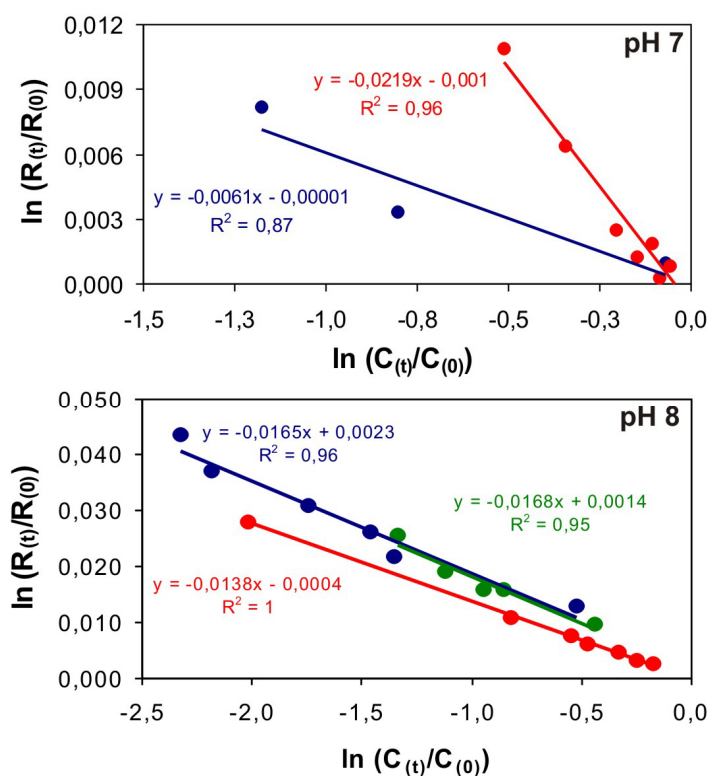
Figure 3.4: Rayleigh plots corresponding to pH 7 (top) and pH 8 (bottom); goethite (red), hematite (blue) and lepidocrocite (green). The enrichment factor ε can be determined from the slope of the regression line. Due to no reactivity of the batch experiments containing magnetite, magnetite is not shown here.

For more detailed information about the reaction mechanism and the goethite system see chapter 4: "Effect of environmental factors on the oxidation of Fe(II) at goethite monitored by the isotope fraction of CCl_4".

3.4.3   *Secondary iron mineral formation on lepidocrocite at pH 8*

The lepidocrocite suspension was equilibrated with aqueous Fe(II) and sodium hydroxide to pH 8 as reported above. During these strictly anaerobic addition steps the formation of a brownish or blackish precipitate could be observed. The freshly formed iron mineral phase showed magnetic behavior which indicated that possibly magnetite was formed. For identification of the freshly formed iron mineral, μ-XRD and Mössbauer measurements were performed. The spectrum of the μ-XRD measurement

(Figure 3.5, top) shows that the new iron mineral phases could be identified as magnetite. Due to an overlapping of the main signals of the two iron minerals and the relatively low content of magnetite on the surface of lepidocrocite, it was difficult to verify this assumption. However with Mössbauer spectroscopy the secondary mineral formation could be clearly identified as small amounts of magnetite (Figure 3.5, bottom).
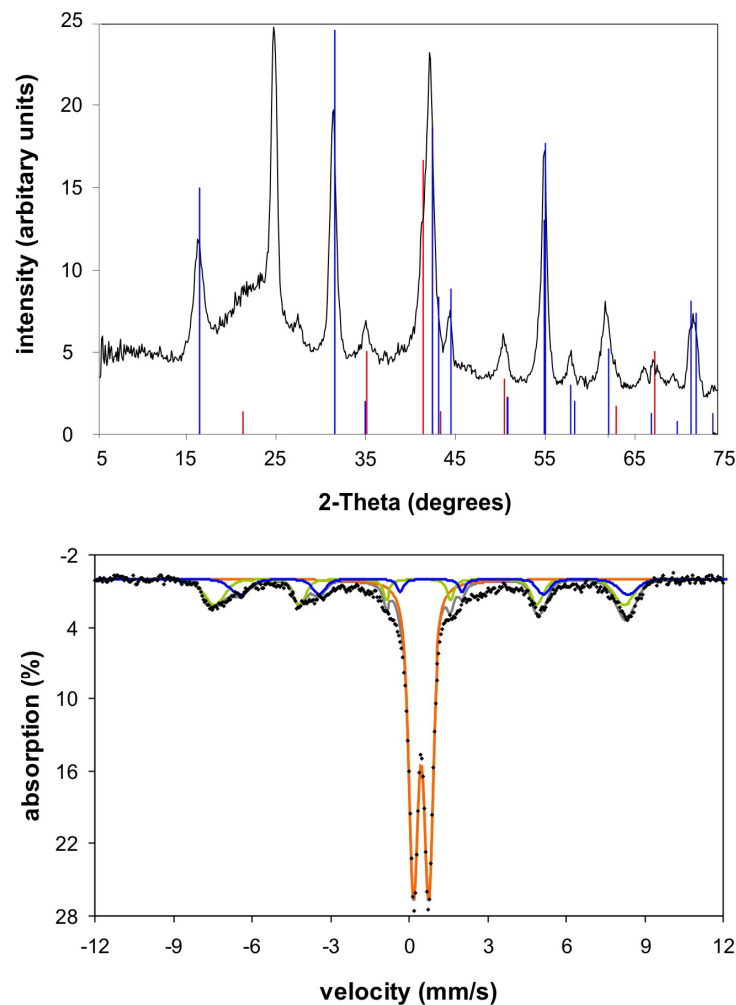
Figure 3.5: µ-XRD (top) and Mössbauer spectra (bottom) of lepidocrocite and a second iron mineral phase after the addition of Fe(II) at pH 8; top: blue and red lines in XRD spectra indicate reference lines of lepidocrocite (card 190629) and magnetite (card 441415); bottom: Mössbauer spectra at 140 K, data (black), overall fit (grey line), lepidocrocite (orange) and magnetite with tetrahedral iron sites (green) and octahedral iron sites (blue).

Lepidocrocite shows a doublet whereas magnetite splits into two sextets at 140 K. One sextet represents the tetrahedral iron sites and one the octahedral iron sites. Secondary iron mineral formation on iron oxides was also reported by Larese-Casanova and co-workers (Larese-Casanova et al., 2009). It can be concluded that the newly formed magnetite, coating the lepidocrocite particles, is the reactive phase for the transformation of CCl_4 on the mineral surface at pH 8.

3.4.4 Investigations of the non reactive magnetite towards CCl_4

Due to the observation that magnetite exposed to Fe(II) will not reduce CCl_4 at pH 8 after several weeks, the properties of the magnetite were further investigated. First the oxidant CCl_4 was replaced by 2-chloronitrobenzene, a more reactive oxidant than CCl_4 which was often used by Larese-Casanova (Larese-Casanova et al., 2009). But even 2-chloronitrobenzene was not transformed by the magnetite/Fe(II) system after 7 days. Klausen and others (Klausen et al., 1995) reported that 4-chloronitrobenzene was rapidly reduced in a magnetite/Fe(II) system at pH 7.

Furthermore Mössbauer measurements were carried out with the magnetite and the magnetite/Fe(II) suspension. The Mössbauer spectra of pure magnetite showed an expected sextet at 140 K (Larese-Casanova, 2006). However the magnetite treated with Fe(II) revealed nearly an identical spectrum (Figure 3.6). Additionally iron signals like a ferrous iron doublet could not be observed in the Mössbauer spectra.
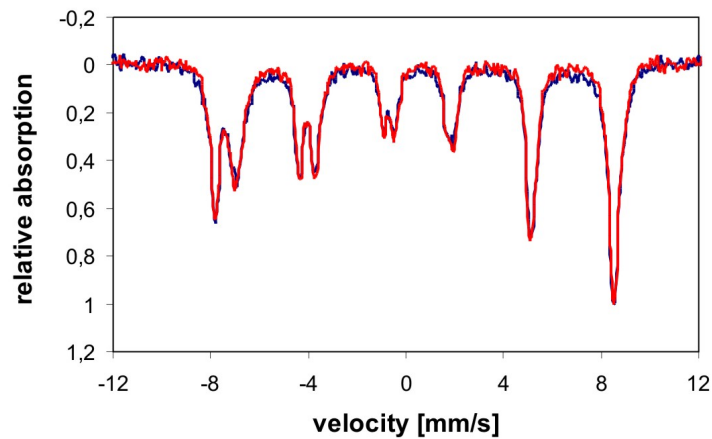
Figure 3.6: Comparison of normalized Mössbauer spectra of magnetite before and after the addition of Fe(II) at pH 8; overall fit of magnetite (blue) and magnetite/Fe(II) (red) at 140 K.

Based on the observations above the composition of ferrous and ferric iron in the magnetite structure was calculated (Table 3.2). The percentage of total Fe(II) in both samples was nearly the same (~ 28%) and the ratio of Fe(II)/Fe(III) was determined to 37.6/39.5% which means that both samples are under-stoichiometric compared to stoichiometric magnetite (Fe(II)/Fe(III) = 0.5) (Table 3.2).

Table 3.2: Calculations of the ratio of Fe(II) and Fe(III) in magnetite and magnetite/Fe(II) systems.

	magnetite	magnetite + Fe(II)	stoichiometric magnetite[1]
tetrahedral Fe(III) [%]	45.4	43.4	
octahedral Fe(II) & Fe(III) [%]	54.6	56.6	
total Fe(III) [%]	72.7	71.7	
total Fe(II) [%]	27.3	28.3	
Fe(II)/Fe(III) ratio [%]	37.6	39.5	50.0[1]
Fe(II)/(Fe(II)+Fe(III)) ratio [%]	27.3	28.3	33.0[1]

[1] theoretical values of stoichiometric magnetite

In conclusion all Fe(II) that sorbed on the mineral surface became part of the magnetite structure. Some of that sorbed Fe(II) was probably transformed to octahedral Fe(II) and/or some of that sorbed Fe(II) was oxidized within the structure and became tetrahedral or octahedral Fe(III). Additionally octahedral Fe(III) could be reduced to octahedral Fe(II) during the partial oxidation of sorbed Fe(II) (Gorski and Scherer, 2009). The single Mössbauer spectra with the tetrahedral and octahedral iron sites of magnetite and magnetite exposed to Fe(II) are attached in the Appendix for further information (Figure A3.2).

However two different processes are possible with "normal" magnetite. Magnetite can donate electrons within its structure and can be reactive or present aqueous Fe(II) can still interact with the surface of magnetite and create a transient Fe(II) phase which can reduce contaminants. The magnetite used in this study was not undergoing these two processes and was not reducing the contaminants CCl_4 and 2-chloronitrobenzene. Gorski and Scherer (Gorski and Scherer, 2009) showed that non-stoichiometric magnetite reduced nitrobenzene with a much slower rate than stoichiometric magnetite. Therefore it is reasonable that the used under-stoichiometric magnetite alone would not be able to reduce nitrobenzene or CCl_4. However the batch experiment contained a lot of Fe(II) and this aqueous Fe(II) should be able to interact with the surface of magnetite as described above. Especially since Gorski and Scherer (Gorski and Scherer, 2009) observed an Fe(II) uptake on a similar non-stoichiometric magnetite (Fe(II)/Fe(III) = 0.31) until nearly stoichiometric magnetite was reached in the excess of aqueous Fe(II).

Explanations for the non-typical behavior of the studied magnetite could be found in the particle size of the magnetite and possible passivation of the mineral surface through other particles. The investigated magnetite particles are between 300-600 nm which is relatively huge compared with the small magnetite particles (~ 11 nm) used in the study of Gorski and Scherer.

Maybe the total oxidation of Fe(II) and the electron transfer in these particles are not possible. Another possible reason could be identified in the passivation of the mineral surface by present silica oxides which were proven in small amounts by X-ray fluorescence.

3.5 Conclusion

The presented study demonstrates that the transformation of CCl₄ was affected by various pH values and the type of the mineral. Due to the potential of goethite as the most reactive mineral in this study, the iron mineral goethite was selected for further investigations with regard to several effects of further environmental factors on the oxidation of sorbed Fe(II).

3.6 References

Amonette, J. E., Workman, D. J., Kennedy, D. W., Fruchter, J. S. and Gorby, Y. A., Dechlorination of Carbon Tetrachloride by Fe(II) Associated with Goethite. *Environ. Sci. Technol.* **2000,** *34*, (21), 4606-4613.

Christensen, T. H., Kjeldsen, P., Bjerg, P. L., Jensen, D. L., Christensen, J. B., Baun, A., Albrechtsen, H.-J. and Heron, G., Biogeochemistry of landfill leachate plumes. *Applied Geochemistry* **2001,** *16*, (7-8), 659-718.

Coughlin, B. R. and Stone, A. T., Nonreversible Adsorption of Divalent Metal Ions (MnII, CoII, NiII, CuII, and PbII) onto Goethite: Effects of Acidification, FeII Addition, and Picolinic Acid Addition. *Environ. Sci. Technol.* **1995,** *29*, (9), 2445-2455.

Elsner, M., Haderlein, S. B., Kellerhals, T., Luzi, S., Zwank, L., Angst, W. and Schwarzenbach, R. P., Mechanisms and products of surface-mediated reductive dehalogenation of carbon tetrachloride by Fe(II) on goethite. *Environ Sci Technol* **2004,** *38*, (7), 2058-66.

Elsner, M., Schwarzenbach, R. P. and Haderlein, S. B., Reactivity of Fe(II)-bearing minerals toward reductive transformation of organic contaminants. *Environ Sci Technol* **2004,** *38*, (3), 799-807.

Gorski, C. A. and Scherer, M. M., Influence of Magnetite Stoichiometry on FeII Uptake and Nitrobenzene Reduction. *Environmental Science & Technology* **2009,** *43*, (10), 3675-3680.

Gupta, S. K., Über die Phosphat-Elimination in den Systemen HPO-γ-FeO(OH) und HPO-FeCl und die Eigenschaften von Klärschlamm-Phosphat. *Dissertation* **1976,** *Universität Bern*, 138pp.

Heijman, C. G., Grieder, E., Holliger, C. and Schwarzenbach, R. P., Reduction of Nitroaromatic Compounds Coupled to Microbial Iron Reduction in Laboratory Aquifer Columns. *Environ. Sci. Technol.* **1995,** *29*, (3), 775-783.

Hiemstra, T. and van Riemsdijk, W. H., Adsorption and surface oxidation of Fe(II) on metal (hydr)oxides. *Geochimica et Cosmochimica Acta* **2007,** *71*, (24), 5913-5933.

Hofstetter, T. B., Heijman, C. G., Haderlein, S. B., Holliger, C. and Schwarzenbach, R. P., Complete Reduction of TNT and Other (Poly)nitroaromatic Compounds under Iron-Reducing Subsurface Conditions. *Environ. Sci. Technol.* **1999,** *33*, (9), 1479-1487.

Klausen, J., Troeber, S. P., Haderlein, S. B. and Schwarzenbach, R. P., Reduction of Substituted Nitrobenzenes by Fe(II) in Aqueous Mineral Suspensions. *Environ. Sci. Technol.* **1995,** *29*, (9), 2396-2404.

Larese-Casanova, P., Heterogeneous ferrous iron reactions on subsurface environments: A [57]Fe Mössbauer spectroscopy investigation. *University of Iowa* **2006**, PhD thesis.

Larese-Casanova, P., Kappler, A. and Haderlein, S. B., Heterogeneous oxidation of Fe(II) on iron oxides: Controls on Fe(III) product formation. *Geochimica et Cosmochimica Acta* **2009**, in preparation.

Larese-Casanova, P. and Scherer, M. M., Fe(II) Sorption on Hematite: New Insights Based on Spectroscopic Measurements. *Environ. Sci. Technol.* **2007,** *41*, (2), 471-477.

Lee, W. and Batchelor, B., Abiotic reductive dechlorination of chlorinated ethylenes by iron-bearing soil minerals. 1. Pyrite and magnetite. *Environ Sci Technol* **2002,** *36*, (23), 5147-54.

Liu, C., Zachara, J. M., Foster, N. S. and Strickland, J., Kinetics of Reductive Dissolution of Hematite by Bioreduced Anthraquinone-2,6-disulfonate. *Environ. Sci. Technol.* **2007,** *41*, (22), 7730-7735.

McCormick, M. L. and Adriaens, P., Carbon Tetrachloride Transformation on the Surface of Nanoscale Biogenic Magnetite Particles. *Environ. Sci. Technol.* **2004,** *38*, (4), 1045-1053.

Pecher, K., Haderlein, S. B. and Schwarzenbach, R. P., Reduction of polyhalogenated methanes by surface-bound Fe(II) in aqueous suspensions of iron oxides. *Environ Sci Technol* **2002,** *36*, (8), 1734-41.

Rugge, K., Hofstetter, T. B., Haderlein, S. B., Bjerg, P. L., Knudsen, S., Zraunig, C., Mosbaek, H. and Christensen, T. H., Characterization of Predominant Reductants in an Anaerobic Leachate-Contaminated Aquifer by Nitroaromatic Probe Compounds. *Environ. Sci. Technol.* **1998,** *32*, (1), 23-31.

Schmidt, T. C., Zwank, L., Elsner, M., Berg, M., Meckenstock, R. U. and Haderlein, S. B., Compound-specific stable isotope analysis of organic contaminants in natural environments: a critical review of the state of the art, prospects, and future challenges. *Anal Bioanal Chem* **2004,** *378*, (2), 283-300.

Stookey, L. L., Ferrozine - a new spectrophotometric reagent for iron. *Anal. Chem.* **1970,** *42*, (7), 779-781.

Stumm, W. and Sulzberger, B., The cycling of iron in natural environments: Considerations based on laboratory studies of heterogeneous redox processes. *Geochimica et Cosmochimica Acta* **1992,** *56*, (8), 3233-3257.

Williams, A. G. and Scherer, M. M., Spectroscopic evidence for Fe(II)-Fe(III) electron transfer at the iron oxide-water interface. *Environ Sci Technol* **2004,** *38*, (18), 4782-90.

Zhang, Y., Charlet, L. and Schindler, P. W., Adsorption of protons, Fe(II) and Al(III) on lepidocrocite ([gamma]-FeOOH). *Colloids and Surfaces* **1992,** *63*, (3-4), 259-268.

Zwank, L., Elsner, M., Aeberhard, A., Schwarzenbach, R. P. and Haderlein, S. B., Carbon isotope fractionation in the reductive dehalogenation of carbon tetrachloride at iron (hydr)oxide and iron sulfide minerals. *Environ Sci Technol* **2005,** *39*, (15), 5634-41.

3.7 Appendix

The appendix contains further information regarding a GC-IRMS chromatogram (Figure A3.1), the adsorption of Fe(II) on different mineral surfaces (Table A3.1) and Mössbauer spectra of magnetite before and after the adsorption of Fe(II) (Figure A3.2).
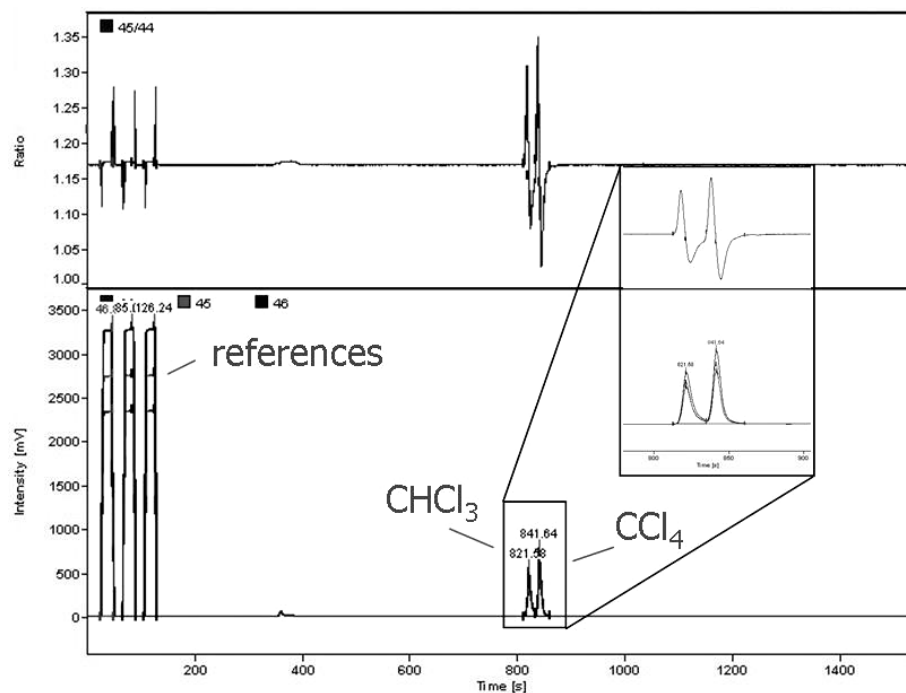
Figure A3.1: GC-IRMS chromatogram (bottom) and isotope swings (top) of a sample from a kinetic batch experiment with goethite. The two peaks belong to the substrate CCl₄ and the product CHCl₃ in similar concentrations. The enlargement shows the baseline separation of the peaks and the isotope swings (S-shaped ratio of mass 45/44) used as an indicator for a good chromatographic performance.

Table A3.1: Adsorption of aqueous Fe(II) on different mineral surfaces at pH 5-8.

pH [a]	Fe(II)$_{ads}$ [μmol/m²]			
	goethite	hematite	magnetite	lepidocrocite
5	6.882	n.d. [b]	n.d. [b]	n.d. [b]
6	12.014	7.571	6.622	5.195
7	20.842	9.209	12.365	6.462
8	37.496	15.588	19.232	11.298

[a] pH of 5.1 ± 0.05 for example
[b] not determined
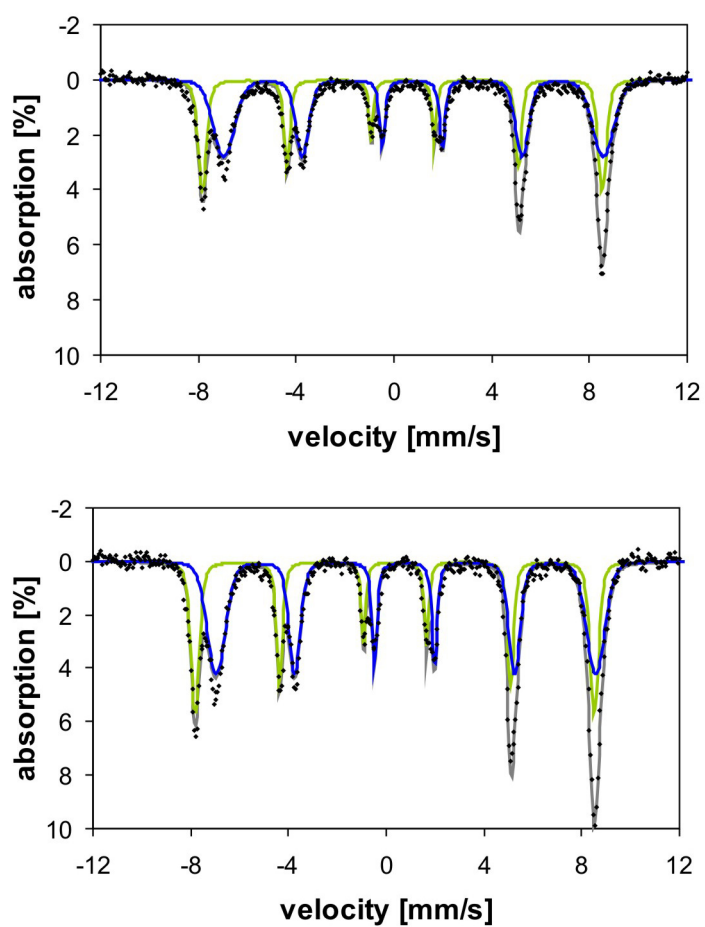
Figure A3.2: Mössbauer spectra of magnetite and magnetite/Fe(II) (bottom) at pH 8 measured at 140 K: data (black), overall fit (grey), tetrahedral iron sites (green) and octahedral iron sites (blue).

4. Effect of environmental factors on the oxidation of Fe(II) at goethite monitored by carbon isotope fractionation of CCl$_4$

4.1 Abstract

Iron minerals support electron cycles and facilitate redox reactions in the anoxic subsurface. The high affinity of iron oxides for dissolved ferrous iron leads to accelerated oxidation of Fe(II) upon sorption involving changes in reactivity and structure of the mineral surface. Carbon tetrachloride CCl$_4$ was used as a model oxidant for an indirect method to trace these changes based on its carbon isotope fractionation (CSIA). Variations in pH, amount of oxidant and sorption time of Fe(II) were studied under well-defined conditions (50 m^2/L goethite, 1 mM Fe(II)$_{aq}$) in batch experiments to elucidate surface reactivity of Fe(II) and the effects of environmental factors on its oxidation at goethite. After only a small fraction of sorbed Fe(II) was oxidized by CCl$_4$, Fe(II) surface species changed significantly as demonstrated by changes (i) in the product distribution (yield of chloroform), (ii) in reaction rate constants and (iii) in carbon isotope fraction of CCl$_4$. The isotope enrichment factors, ε, suggest that two different "types" of reactive Fe(II) surface species were present. A small fraction of highly reactive Fe(II) species (ε = -10 to -15‰) which is readily depleted by oxidation and a larger but sustaining fraction of less reactive Fe(II) species ($\varepsilon \sim$ -25‰), formed by readsorption of Fe(II) and/or further surface remodelling processes. The presence of these two different Fe(II) species could be further supported by Mössbauer spectroscopy. Our work demonstrates that the dynamic surface properties of minerals (here goethite) play a decisive role for determining the reactivity of surface bound Fe(II) and thus the redox conditions in heterogeneous Fe(II)/Fe(III)-systems.

4.2 Introduction

Understanding transformation pathways of contaminants and the impact of different environmental conditions on these pathways has been a major focus of biogeochemical and environmental research (Bjerg et al., 1995; Christensen et al., 2000; Postma and Jakobsen, 1996; Schmidt et al., 2004). Especially the importance of ferrous iron in groundwater systems (Jensen et al., 1998; Stumm and Sulzberger, 1992), its interactions with minerals (Coughlin and Stone, 1995; Hofstetter et al., 2003; Jeon et al., 2001; Rugge et al., 1998; Zhang et al., 1992) and its versatile redox behavior such as oxidation by contaminants or reduction by microbiological processes is widely discussed (Curtis and Reinhard, 1994; Hofstetter et al., 1999; Klausen et al., 1995; McCormick and Adriaens, 2004). A key finding of these studies is that oxidation of Fe(II) processes can be drastically enhanced by sorption at mineral surfaces as compared to dissolved state.

Several groups investigated the oxidation of Fe(II) on iron mineral surfaces (Amonette et al., 2000; Elsner et al., 2004; Elsner et al., 2004; Pecher et al., 2002; Zwank et al., 2005). Amonette and co-workers (Amonette et al., 2000) found that the surface of goethite promoted the oxidation of Fe(II) by CCl_4. Pecher and others (Pecher et al., 2002) proposed the formation of several different iron species at the goethite surface that reacted with halogenated methanes depending on sorption time, surface density of Fe(II)$_{aq}$ and the type of iron oxide surface. They could also show that the mechanism of electron transfer between Fe(II) and the halogenated oxidants is not correlated with the observed reaction rate constants. Controlling factors for an initial one vs. two electron transfer were the type of mineral surface and especially the type of Fe(II) species sorbed (Pecher et al., 2002). Elsner et al. (Elsner et al., 2004; Elsner et al., 2004) focused on the reactivity of Fe(II) at different minerals and the mechanisms of Fe(II) using isotope fractionation of CCl_4 as model oxidant. They postulated that, depending on the mineral

and solution conditions, a one or two electron transfer may occur and that C-Cl-bond cleavage is involved in the rate limiting step. Trichloromethyl radicals were postulated as central intermediate species for both possible further reaction pathways to yield either $CHCl_3$ or CO. Carbon isotope fractionation of CCl_4 at iron oxides and sulphides with Fe(II) was also studied by Zwank et al. (Zwank et al., 2005). At given reaction conditions (pH 7, 1 mM dissolved Fe(II)) the oxidation of Fe(II) on various iron oxides turned out to be a strongly fractionating process whereas on iron sulphides only weak carbon isotope fractionation occurred. However, the properties of sorbed Fe(II) was not further investigated regarding the influence of different geochemical conditions like pH or the surface density of Fe(II) monitored by the isotope fractionation of CCl_4. We expect that different Fe(II) species would react differently with CCl_4 and produce different carbon isotope enrichment factors. Therefore, compound specific isotope analysis (CSIA) can be a tool for probing the different reactive Fe(II) species associated with goethite

Recently, Hiemstra et al.(Hiemstra and van Riemsdijk, 2007) discussed various sorption processes of Fe(II) on the goethite surface. They postulated two major types of Fe(II) species corresponding to ferrous iron with or without electron transfer to the interior Fe(III) lattice of the mineral. That such an electron transfer during Fe(II) adsorption occurs on iron minerals was previously proven by Williams and Scherer (Williams and Scherer, 2004) and Larese-Casanova et al. (Larese-Casanova and Scherer, 2007), by Mössbauer spectroscopy in several iron oxide systems.

In this work we investigated the influence of environmentally relevant conditions on the oxidation of Fe(II) at goethite by varying pH values, initial CCl_4 concentrations and sorption time periods of aqueous Fe(II). CCl_4 was chosen as model oxidant as its single carbon atom facilitates the interpretation of carbon isotope fractionation obtained from CSIA. The major goals of this study were (i) to identify the effect of these

environmental factors on the oxidation of Fe(II) by considering reaction rate constants, product formation and carbon isotope fractionation, (ii) to gain further insight into the pathways and dynamics involved in the oxidation of Fe(II) and (iii) to obtain further information on the surface properties of goethite during Fe(II) oxidation by Mössbauer spectroscopy.

4.3   Material and Methods

4.3.1   Chemicals

Carbon tetrachloride CCl_4 (99+%) and tetrachloroethylene C_2Cl_4 (99.9+%) were purchased from Aldrich (Steinheim, Germany), chloroform $CHCl_3$ (≥99.5%) from Fluka (Buchs, Switzerland) respectively. Sodium hydroxide (1 M), hydrochloric acid (1 M) and metal iron Fe(0) were obtained from Merck. The ferrozine solution was made with 0.1% (w/v) 3-(2-pyridyl)-5-6-diphenyl-1,2,4-triazine-p,p′-disulfonic acid in 50% (w/v) ammonium acetate (Acros, ≥98.0%). All stock solutions or dilutions were prepared using Millipore water.

4.3.2   Goethite

The iron mineral goethite (α-FeOOH) was purchased from Lanxess Germany GmbH (Bayferrox 920 Z) (see Table 4.1). The storage was dry and cool under lab atmosphere. The goethite was characterized determining specific surface area (BET measurement), purity (X-ray diffraction), crystal form and particle size (scanning electron microscopy), total organic carbon and pH_{pzc} (Liu et al., 2007). The properties of the goethite were in the expected range but the pH_{pzc} was 6.5 (6.1-9.5; literature values) after washing the mineral twice for sulphate removal (for more details see Appendix, Figure A4.1).

4.3.3 Fe(II) Stock Solution

The preparation of the iron stock solution using metal iron Fe(0) and 1 M HCl was performed following the procedure of Elsner et al. (Elsner et al., 2004). The exact content of Fe(II) was determined photometrically (562 nm) by the ferrozine assay (Stookey, 1970) (for more details see Appendix).

4.3.4 pH and Fe(II)$_{aq}$ in goethite suspension

All preparation steps in which Fe(II) was involved, were conducted in a glove box (Unilab, Braun, Garching, Germany) to work under strictly anoxic conditions and avoid any oxidation of Fe(II). The general procedure preparing a mineral/Fe(II) suspension is described by Zwank et al. (Zwank et al., 2005) and is also attached in the supporting information. The mineral suspension was adjusted with NaOH/HCl to a considered pH, Fe(II) stock solution was added and after an equilibration time of 18 hours the Fe(II)$_{aq}$ concentration was determined by the ferrozine assay (Stookey, 1970). If necessary these steps were repeated to reach a Fe(II)$_{aq}$ concentration of 1 mM and a considered pH after a total equilibration time of at least 48 hours. Instead of organic buffers, the intrinsic buffer capacity of goethite was used to stabilize the suspension (Elsner et al., 2004), since the influence of organic buffers on the transformation of contaminants is discussed controversially and was studied separately.

The pH dependent experiments were carried out at pH 5.01, 6.01, 7.01 and 8.01 ± 0.05. For experiments with different initial CCl$_4$ concentration or longer exposure times of Fe(II), the pH was set 7.01 or 8.01 ± 0.05 (indicated there).

4.3.5 Batch Experiments

First aqueous stock solutions of carbon tetrachloride (CCl$_4$) and tetrachloroethylene (C$_2$Cl$_4$, internal standard) were prepared. Serum bottles

with 100 mL of Millipore water closed with butyl rubber stoppers were flushed with N_2 for 30 minutes through a syringe needle before aliquots of the pure chemicals were added to obtain carbon tetrachloride concentrations between 5 to 70 μM. Before adding the pure chemicals the rubber stoppers were quickly opened and afterwards replaced by Viton stoppers during a gentle nitrogen stream in the headspace of the vials (removal of any oxygen while adding) and immediately transferred into the glove box.

The equilibrated and stirred mineral/Fe(II) suspension was divided in 42 mL aliquots within 50 mL serum bottles inside the glove box. The reaction was started by adding 6 mL of the aqueous stock solution. The serum bottles were immediately closed with Viton stoppers. Serum bottles with 42 mL water instead of the goethite/Fe(II) suspension were prepared and treated in the same way as the samples to analyze the total concentration of CCl_4 and C_2Cl_4 at the initial and final sample point. The serum bottles were placed on a horizontal shaker (140 rpm, 25°C, in the dark) outside the glove box. All experiments were carried out in duplicates.

4.3.6 Sampling

For each sampling campaign the serum bottles closed with Viton stoppers (duplicates) were centrifuged (Hermle Z320, Hermle, Gosheim, Germany) at 2000 rpm for 10 minutes, individually opened and the supernatant was quickly divided for GC-MS and GC-IRMS measurements. For GC-IRMS measurements a threefold dilution was necessary (for concentrations < 10 μM CCl_4 once) due to the limited linear range of the instrument. These steps were repeated for each sampling point and the interval of each sampling campaign ranged from hours to days depending on reaction conditions.

4.3.7 Mössbauer spectroscopy

The mineral/Fe(II) suspension was prepared the same way described above using ^{57}Fe(II) instead of ^{NA}Fe(II). After starting the experiment with 55 µM CCl$_4$ samples were taken after 1 and 6 days (low and high Fe(II) oxidation) by filtering the suspension and preparing it for Mössbauer measurements (Larese-Casanova and Scherer, 2007). The instrument was a MB-500 with a ^{57}Co Mössbauer source (Wissenschaftliche Elektronik GmbH, Starnberg, Germany) operated in transmission mode with a Janis cryostat. Spectra were calibrated against a spectrum of α-Fe(0) foil.

4.3.8 Analytical Methods

For quantitative analyses of CCl$_4$, CHCl$_3$ and C$_2$Cl$_4$ a TraceGC 2000 gas chromatograph coupled to a TraceDSQ single quadrupole mass spectrometric detector (ThermoFinnigan) was used. The injection was performed with a 2.5 mL headspace syringe (CTC-CombiPAL autosampler) and a split ratio of 1:50. To separate of the compounds an Rtx-VMS capillary column (60 m ×0.32 mm I.D., 1.8 µm film thickness, Restek) was installed. The temperature of the column was initially hold at 40°C for 4 min, heated up to 100°C with a rate of 7°C/min and maintained at 150°C for another 5 min.

The compound-specific isotope ratios (δ^{13}C values) were determined using a Trace gas chromatograph coupled to a combustion interface (GC Combustion III) maintained at 940°C and an isotope ratio mass spectrometer (DeltaPLUS XP; all Thermo Finnigan). As extraction technique a solid phase microextraction (SPME) with an 85 µm Carboxen™/PDMS Stable Flex™ fiber (Supelco) was used. The extraction time was 20 min at 35°C and the following desorption time was 0.5 min at 270°C. An Rtx-VMS capillary column (same as above) and as carrier gas Helium 5.0 (Air Liquide) were used at several column and split flows. The baseline separation of the compounds were reached using a temperature profile

(40°C for 2 min, 100°C for 1 min and 200°C for 5 min to avoid any carry over). Isotopic ratios were determined to a referenced CO_2 standard relative to Vienna Pee Dee Belemnite (VPDB). Reoxidation of the catalyst was carried out regularly after 40-50 measurements. All samples were run in triplicates with standards in between to exclude variability of the instrument (for more details see Appendix).

4.4   Results and Discussion

The reactive species of surface mediated processes and the reaction mechanism of the transformation of CCl_4 on goethite/Fe(II) surfaces were investigated by Pecher et al. (Pecher et al., 2002) and Elsner et al. (Elsner et al., 2004). A modified reaction pathway of CCl_4 is illustrated in Figure 4.1. Sorption of Fe(II)$_{aq}$ on the mineral surface leads to surface remodeling by electron transfer between the sorbed Fe(II) and the mineral (Hiemstra and van Riemsdijk, 2007) providing a reactive mineral/Fe(II) surface for CCl_4 sorption.

A one electron transfer from a reactive Fe(II)$_{sorb}$ species to CCl_4 results in a reactive trichloromethyl radical intermediate which can react further by different pathways on the mineral surface. Either by a hydrogen radical transfer that delivers chloroform as final product or by a second electron transfer resulting in a trichloromethylene anion. Pecher et al. (Pecher et al., 2002) showed with the help of deuterated water that the trichloromethylene anion was not present in solution to form deuterochloroform. The anion may decompose to a highly reactive dichlorocarbene that rapidly undergoes hydrolysis to form instable HCOCl and finally the completely dechlorinated products formate and its anhydrite CO. The desorption of the trichloromethyl radical from the mineral surface and the following

oxidation of Fe(II) in solution seems to be not very likely due to the lower reactivity of aqueous Fe(II) compared to sorbed Fe(II).
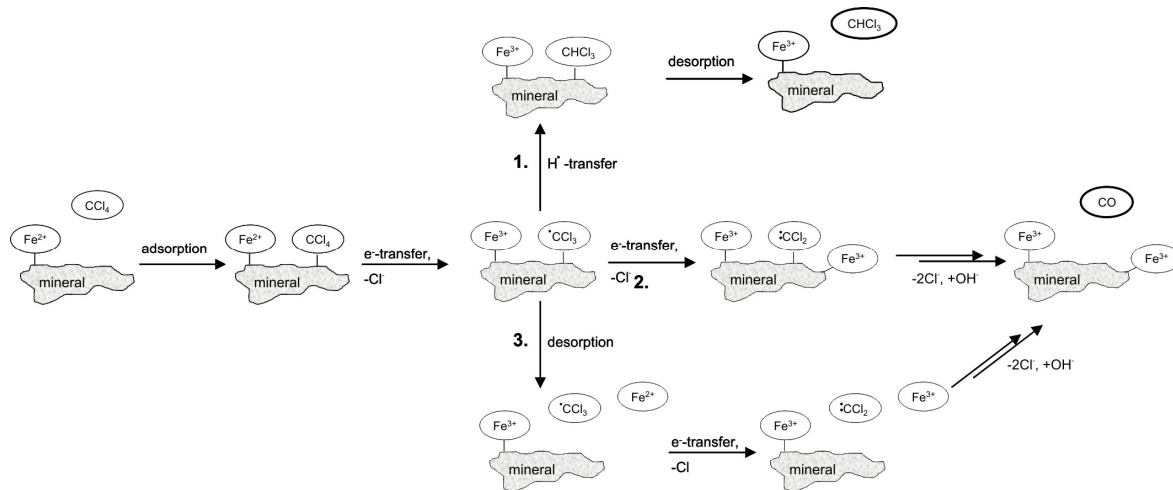
Figure 4.1: Schematic reaction pathway of the oxidation of Fe(II) and transformation of CCl₄: after reductive dehalogenation of CCl₄ to a trichloromethyl radical ˙CCl₃ (shown in the box) on the mineral surface 3 pathways are possible: 1. transfer of hydrogen radical or 2. further dehalogenation and hydrolysis or 3. desorption and following e-transfer in the suspension (modified from (Elsner et al., 2004)).

Based on the preliminary investigations by Pecher et al. (Pecher et al., 2002) and Elsner et al. (Elsner et al., 2004) we performed batch experiments studying important environmental conditions like different pH values, amounts of oxidized Fe(II) and sorption times of Fe(II)$_{aq}$. We suppose to gain further insights on the electron transfer and the reactive species present at the mineral surface by examining the product distribution, reaction kinetics and isotope fractionation in these systems.

4.4.1   *Effect of pH and amount of Fe(II)$_{sorb}$*

The point of zero charge of iron minerals is essential for the adsorption of ferrous iron. For our goethite the pH$_{pzc}$ was determined by titration and electrophoretic mobility measurements to be 6.5 which is unusually low (Cornell and Schwertmann, 2003). Consequently, the pristine goethite surface was positively charged at pH values below 6.5 resulting in

electrostatic repulsion of Fe(II)$_{aq}$ whereas at circumneutral and higher pH values the negative surface charge promoted Fe(II) sorption. Adsorption of ferrous iron to iron oxides can occur with or without electron transfer to the ferric iron centers in the mineral lattice (Hiemstra and van Riemsdijk, 2007; Williams and Scherer, 2004). With regard to its redox properties adsorbed Fe(II) may be divided into two classes (Scheme 2): non reactive Fe(II) species including electrostatically bound Fe(II), ^{ie}Fe(II)$_{sorb}$ (Hofstetter et al., 2003), and oxidized Fe(II) through the underlying goethite, ^{ox}Fe(II)$_{sorb}$ (Williams and Scherer, 2004), as opposed to reactive Fe(II) species including various fractions of sorbed Fe(II), such as ferrous iron surface complexes ^{react}Fe(II)$_{sorb}$, or sorbed Fe(II) after surface remodeling processes, ^{remod}Fe(II)$_{sorb}$.

Scheme 2:
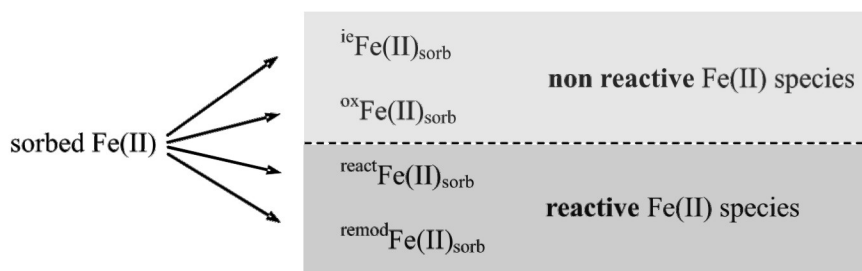
In conclusion it can be expected that electron transfer reactions of surface bound ferrous iron to increase the sorption of aqueous Fe(II), promote the surface remodeling of goethite and to enhance reaction rate constants at higher pH values. Previous work (Amonette et al., 2000; Elsner et al., 2004; Liger et al., 1999) has demonstrated that both the adsorption of Fe(II) on iron minerals and the reactivity of sorbed iron species at different minerals varied considerably.

We conducted our experiments at four pH values in the range of 5-8 (for experimental details see Table 4.1).

Table 4.1: Properties of goethite and the experimental conditions at different pH values in this study.

Properties of goethite

Formula	α-FeOOH		
XRD	pure	SEM: particle size [µm]	0.6 - 0.9
BET [m²/L]	9.2	crystal form	needles
TOC [%]	0.013	pH_{pzc}	5.5 ± 0.4

Experimental conditions

expected				
pH	5.1 ± 0.05	6.1 ± 0.05	7.1 ± 0.05	8.1 ± 0.05
$Fe(II)_{aq}$ [mM]		1.00 ± 0.05		
added to suspension				
mineral [g/L]		5.43		
Fe(II) [mL]	1.9	2.3	2.9	4.0
0.1 M NaOH [mL]	1.4	2.8	6.7	11.0
measured				
pH	5.08	6.13	7.05	8.09
$Fe(II)_{aq}$ [mM]	1.00	1.03	0.98	1.01
calculated				
$Fe(II)_{ads}$ [mM]	0.34	0.60	1.04	1.88
$Fe(II)_{ads}$ [µmol/m²]	6.88	12.01	20.84	37.50

The amount of sorbed ferrous iron, $Fe(II)_{sorb}$, was calculated from the concentration difference after 48 hours between dissolved ferrous iron, $Fe(II)_{aq}$, and total Fe(II) added initially to the system. $Fe(II)_{ads}$ varied systematically with pH. At the lowest pH value the amount of $Fe(II)_{sorb}$ was six times less compared to the highest pH value and half as much as one pH unit higher (Table 4.1 and Figure 4.2a).
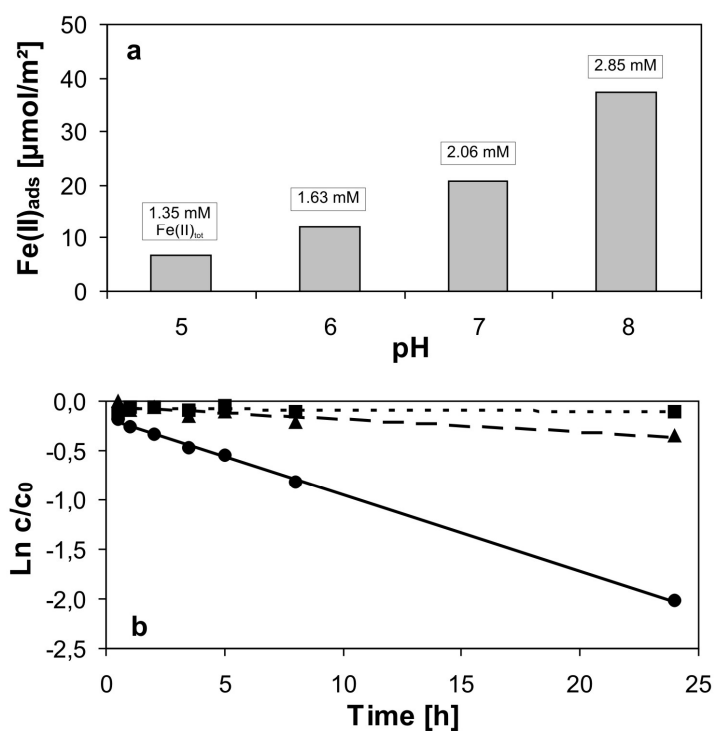
Figure 4.2: (a) Adsorption of Fe(II) to the goethite surface (Fe(II)$_{aq}$ = 1 mM, surface concentration of goethite 50 m²/L, 5.43 g/L respectively) in dependency of pH; (b) Kinetics of CCl₄ transformation at different pH values: (■) pH 6; (▲) pH 7; (●) pH 8.

The oxidation of Fe(II) followed pseudo-first order kinetics (Figure 4.2b). At pH 7 the reaction rate constant k'$_{obs}$ (normalized to the total surface concentration of 50 m²/L) was 5.3×10^{-4} h⁻¹m⁻²L). In former works (Elsner et al., 2004; Pecher et al., 2002; Zwank et al., 2005) similar reaction rate constants have been observed ranging from 1.5×10^{-4}-6.4×10^{-4} h⁻¹m⁻²L. These studies were performed under similar conditions: pH 7, 1 mM Fe(II)$_{aq}$ (1 mM Fe(II)$_{tot}$, Pecher et al.) and CCl₄ as model oxidant. However, the properties of the goethite were different. Besides a higher specific surface area (17 vs. 9 m²/g), although k'$_{obs}$ were normalized to surface areas, the pH$_{pzc}$ differed by one unit (7.5-7.8 vs. 6.5). Thus, at pH 7 the goethite surface in our study was negatively charged whereas as opposed to the previous studies. Although the amount of sorbed Fe(II) was two times higher in our study this additional fraction of surface associated Fe(II) is probably only loosely bound by electrostatic attraction and thus not reactive. At pH 8 the

amount of previously sorbed Fe(II) was only 2x higher compared to pH 7 but the k'$_{obs}$ was 6.5x greater (3.4×10^{-3} h^{-1}m^{-2}L) at pH 8. Similar observations were made with the transformation of RDX in a magnetite/Fe(II) system by Gregory and co-workers (Gregory et al., 2004). This suggest that more complexed ferrous iron was adsorbed leading to an increase in the fraction of reactive Fe(II) surface species.

As described by Pecher et al. (Pecher et al., 2002) and Elsner et al. (Elsner et al., 2004) the main products of the transformation of CCl$_4$ were chloroform, carbon monoxide and formate. These products occurred in different proportions depending on conditions. Here we focused on the quantification of chloroform assuming that the remaining fraction of the mass balance was made up by the fully dehalogenated products. The presence of CO was exemplarily proven in several batch reactors. With increased pH value a decrease of the relative CHCl$_3$ formation from 45% (pH 7) to 32% (pH 8) was observed. Zwank et al. (Zwank et al., 2005) and Elsner et al. (Elsner et al., 2004) reported CHCl$_3$ formation between 30 and 33% for similar conditions at pH 7, however the properties of their goethite differ in pH$_{pzc}$, specific surface area and particle size. At low pH values (5-6) we did not find significant reactivity of CCl$_4$ and thus oxidation of Fe(II) in our systems. which contrast findings of Amonette and co-workers (Amonette et al., 2000), who observed little transformation of CCl$_4$ on a goethite/Fe(II) surface. Unfortunately the properties of their goethite, especially the pH$_{pzc}$, are partly unknown to us which hinders further discussions. Our findings are in line with the assumption that at higher pH conditions more highly reactive surface sites of Fe(II) are present. Consequently, more electrons were transferred to the sorbed CCl$_4$ before the products of CCl$_4$ could desorb (see below).

The isotope fractionation data of CCl$_4$ suggest that two different kinds of reactive Fe(II) surface species predominate as a function of pH. The carbon isotope enrichment factor ε was -21.9‰ at pH 7 which is in accordance with

results of Zwank et al. (Zwank et al., 2005) and Elsner et al. (Elsner et al., 2004) with ε of -26.1‰ and -26.5‰ at pH 7. At pH 7 the abundance of the highly reactive Fe(II) species, ^{react}Fe(II)$_{sorb}$, is much lower compared to higher pH values and therefore the surface remodeling and readsorption of aqueous Fe(II), ^{remod}Fe(II)$_{sorb}$, is more significant during the progress of the reaction. Thus, the isotope enrichment factor is in the range of -25‰ for ^{remod}Fe(II)$_{sorb}$ species. However at pH 8 the carbon isotope enrichment factor was different with ε of -13.8‰ and remains in the initial low range (ε = -10 to -15‰) which is characteristic for the class of highly reactive Fe(II) surface sites. The highly reactive Fe(II) species, ^{react}Fe(II)$_{sorb}$, are present initially and the significance of surface remodeling and formation of less reactive readsorbed Fe(II) is diminished. For an experimental overview see Appendix (Table A4.1).

4.4.2 *Effect of the amount of oxidized Fe(II)*

Initial carbon tetrachloride concentrations between 5 and 70 μM were used to oxidize variable amounts of Fe(II) on goethite surface. At pH 7 the product distribution of CCl$_4$ depended on the amount of oxidized Fe(II) (Figure 4.3). Two different domains of relative chloroform formation could be identified after more than 90% CCl$_4$ transformation. In the first domain (initial CCl$_4$ below 10 μM) carbon tetrachloride was almost quantitatively transformed to chloroform (c$_{CHCl3}$ = 97.0 ± 2.8%) whereas in the second domain (initial CCl$_4$ above 10 μM) much more fully dehalogenated products were formed and chloroform made up for only 41.7 ± 3.5% of the mass balance (additional information see Appendix, Figure A4.2). These findings are comparable to those of Elsner et al. (Elsner et al., 2004), where a CHCl$_3$ yield of 44% with at initial CCl$_4$ concentrations of 40-50 μM was obtained. The abstraction of hydrogen radicals to form chloroform on the mineral surface depended on the initial CCl$_4$ concentration with a quantitative yield of CHCl$_3$ at lower oxidant concentrations. In contrast to the first domain, a

steady formation of chloroform formation occurred with time in the second domain. Since the ratio of reactive Fe(II) surface species was identical at initial conditions in all experiments, additional reactive Fe(II) surface species, ^{remod}Fe(II)$_{sorb,}$ must have formed on the mineral predominately in domain two leading to different product ratios and isotope fractionation. An intermediate storage of the trichloromethyl radical can be excluded due to the fact that the radical would immediately react by hydrogen abstraction or undergo further electron transfer.
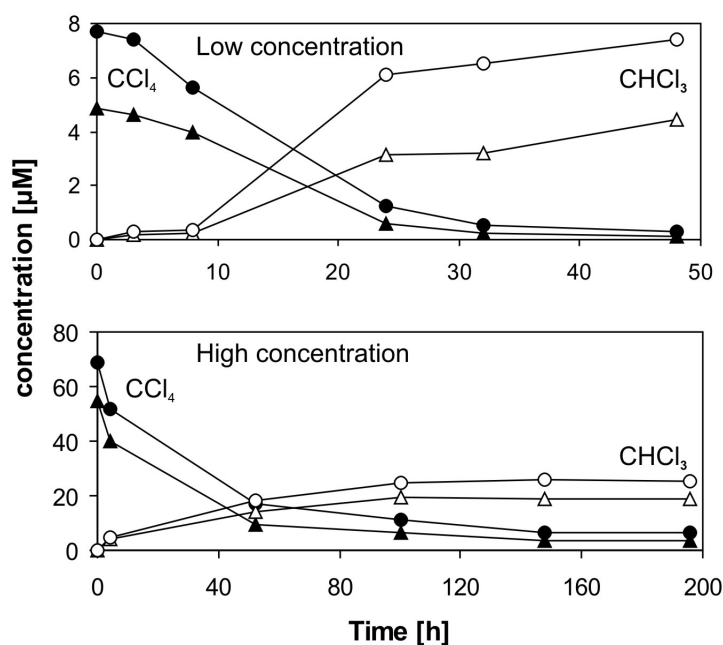
Figure 4.3: Transformation of CCl$_4$ and formation of CHCl$_3$ (goethite, 1mM Fe(II)$_{aq}$, pH 7). *Low concentration:* **CCl$_4$: (▲) 5 μM; (●) 7.5 μM; corresponding CHCl$_3$: (△) and (○); *High concentration:* CCl$_4$: (▲) 55 μM; (●) 70 μM; corresponding CHCl$_3$: (△) and (○).**

For further insights into the effect of different amounts of oxidized Fe(II), the reaction rate constants and enrichment factors were calculated at pH 7. Again two domains below and above 10 μM initial CCl$_4$ were evident in the reaction rate constants as well as in the enrichment factor (Figure 4.4). The reaction followed a pseudo-first order kinetic only at low amounts of oxidized Fe(II) with 1.1-1.2×10^{-3} h^{-1}m^{-2}L for 5 μM and 7.5 μM CCl$_4$. At higher

oxidation levels of Fe(II) k'_{obs} decreased to $5.6\text{-}2.4 \times 10^{-4}\,h^{-1}m^{-2}L$ and the reaction kinetics clearly changed compared to low amounts of Fe(II) oxidation. These two domains can be rationalized by a change of the reactive sorbed Fe(II) concentration already after little amounts of oxidized Fe(II) either by a depletion of reactive iron surface complexes or further surface remodeling.

Also, the enrichment factors were in the characteristic range of the highly reactive $^{react}Fe(II)_{sorb}$ species for little oxidation of Fe(II) ($\varepsilon = \text{-}12.1 \pm 3.2‰$) and of the less reactive $^{remod}Fe(II)_{sorb}$ species for much oxidation of Fe(II) ($\varepsilon = \text{-}25.4 \pm 3.2‰$) for pH 7. Apparently, these findings illustrate that the surface speciation of Fe(II) at goethite changed significantly after only a small fraction of Fe(II) sites being oxidized, as indicated by the change in the product formation, in the reaction rate constants and in the carbon isotope fractionation.
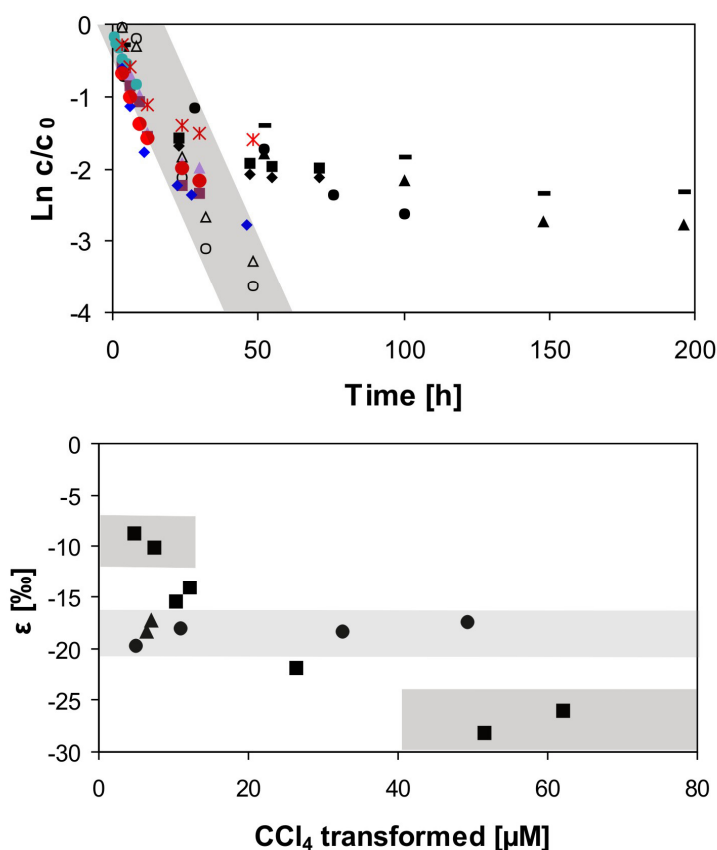
Figure 4.4: Reactivity and isotope fractionation of CCl4 in a goethite/Fe(II) system at pH 7; (top) Reaction kinetics at different initial CCl4 concentrations; black symbols: pH 7, (open symbols: < 10 μM, filled symbols: > 10 μM); colored symbols: pH 8; red symbols: pH 8, long sorbed Fe(II). (bottom) Carbon isotope enrichment factors ε at different amounts of transformed CCl4: pH 7 (■), pH 8 (●), pH 8, long sorbed Fe(II) (▲).

At pH 8 a distinction between two domains of reactive Fe(II) surface sites was not evident. The product distribution of chloroform was steady during the progress of the reaction and ranged between 83-56% (low to high initial concentrations of CCl4). These results indicate that the abstraction of hydrogen radicals was again more favoured at low initial CCl4 concentrations. Moreover the reaction rate constants followed first pseudo-first order kinetics with a decline only at the very end of the reaction probably caused by limitation of reactive iron surface species and/or by the steady decrease of pH (0.5 pH units) during the progress of the reaction. However the aqueous Fe(II) concentration was below the Fe(OH)$_2$ solubility. The isotope enrichment factors of ε = -18.2 ± 1.2‰ are also in line with the

interpretation that at pH 8 more highly reactive Fe(II) species were present at the mineral surface diminishing the significance of different initial CCl_4 concentrations as compared to pH 7. The parallel reaction of CCl_4 with high and low reactivity sites leads to an observed isotope enrichment factor that is in-between the ones of the two classes of the two ferrous iron surface species (Figure 4.4).

4.4.3   *Effect of the exposure time of Fe(II) at goethite*

As the effect of highly reactive Fe(II) species on the mineral surface, which are responsible for the faster reaction rate of CCl_4, was very pronounced, we investigated the influence of different sorption time periods of aqueous Fe(II) on the mineral surface. As short term contact time periods (up to 48 hours) were already studied in detail by Pecher et al. (Pecher et al., 2002) we investigated the effects on redox processes for long term ferrous iron equilibration times of 10 and 30 days. The total amount of sorbed Fe(II) was equal within 2 and 10 days as the sorption maxima already occurred after 2 days (Pecher et al., 2002). Iron sorption data, however, do not reveal if the type of sorbed Fe(II) , i.e. the fraction of reactive Fe(II) species, $^{react}Fe(II)_{sorb}$, changed with longer exposure times at goethite. Experiments with initial CCl_4 concentration below 10 μM were performed to address this question. The formation of chloroform decreased significantly to 30% in comparison to ~ 80% of sorbed Fe(II) after 2 days and a pH drop of 0.3 pH units could be observed. Previous experiments, however, demonstrated that a slight pH drop is not relevant for the product formation. Further surface remodeling processes and the formation of more $^{remod}Fe(II)_{sorb}$ species after longer exposure times could be responsibly for the relative low percentage of chloroform yield. The reaction rate constants were in the same range whereas a slower reaction rate could be observed at the endpoint of the redox reaction (Figure 4.4). Thus the fraction of highly reactive iron sites, $^{remod}Fe(II)_{sorb}$, might be subject to further reorganized during the aging of the

system. The isotope enrichment factor kept almost constant with $\varepsilon = -17.7‰$ (Figure 4.4).

The same goethite/Fe(II) suspension was also studied after 30 days, after complete mixing of Fe(II) and goethite occurred probably due to remodeling processes (Handler et al., 2009). Whereas the enrichment factor changed slightly with $\varepsilon = -18.3‰$ (Figure 4.4), the chloroform formation and the reaction rate constant showed noticeable changes (39% $CHCl_3$, slower k'_{obs}; Figure 4.4). The pH dropped from initially pH 8 over the days of further equilibration time and/or aging of the mineral suspension to 7.2 and after the redox reaction to 7.1. However, desorption of $Fe(II)_{ads}$ could not be recognized assuming that the Fe(II) species were irreversible sorbed to the mineral surface and were exposed to different remodeling processes. In conclusion our data suggest that prolonged aging of goethite/Fe(II) suspensions had only minor effects on the distribution of Fe(II) species on the mineral surface, product formation and reaction kinetics and on the isotope fractionation of CCl_4.

4.4.4   Surface dynamics of goethite/Fe(II)

Using $^{57}Fe(II)$ and Mössbauer spectroscopy we further investigated the dynamics, speciation and sorption behaviour of reactive Fe(II) on goethite. Three $^{57}Fe(II)$ experiments were carried out (at low, high and without oxidation of $^{57}Fe(II)$ which gave similar results with regard reaction rate constants and product distribution compared to natural abundance ferrous iron, $^{NA}Fe(II)_{sorb}$. At 77 K the Mössbauer spectra showed a sextet of ^{57}Fe in goethite due to a combination of the natural abundant ^{57}Fe and partially oxidized added $^{57}Fe(II)$ (Williams and Scherer, 2004) and an associated doublet of the relatively small quantity of sorbed $^{57}Fe(II)$ (see Appendix, Figure A4.3). This Fe(II) doublet is similar to the $^{57}Fe(II)$ found to form on aluminium oxide (Williams and Scherer, 2004) and on ^{56}hematite at aqueous

[57]Fe(II) concentrations (Larese-Casanova and Scherer, 2007). This doublet represents an Fe(II) species that did not get oxidized by the underlying goethite and may be a reductant for CCl$_4$. The relative peak area of the Fe(II) doublet which is considered as ^{react}Fe(II)$_{sorb}$, decreased with the onset of initial oxidation of Fe(II) and further declined with continued ferrous iron oxidation. The amount of oxidized [57]Fe(II) was calculated considering an one electron transfer for chloroform and a two electron transfer for CO formation. The values were compared to a sorption experiment of Fe(II) in the absence of CCl$_4$. The results indicate that the freshly sorbed Fe(II) was directly involved in the electron transfer reaction with CCl$_4$. Secondary mineral phases could not be observed suggesting that the new mineral phase is identical to the supporting goethite. That goethite could form as secondary mineral phase was demonstrated previously by the oxidation of [57]Fe(II) on [56]hematite by chloronitrobenzene and the subsequent formation of [57]goethite on [56]hematite (Larese-Casanova et al., 2009). In summary, these results confirm that the type of reactive Fe(II) species at the goethite surface and also the reaction mechanism changed after only an initial amount of Fe(II) was oxidized.

4.5   Environmental significance

In this study several factors including pH dependency, amount of surficial oxidized Fe(II) and sorption times of Fe(II) were investigated with respect to the reactivity of Fe(II) at goethite as monitored by reaction rate constants, product distribution and enrichment factors of the model oxidant CCl$_4$. Our work demonstrates that the surface properties of minerals (here goethite) are highly dynamic due to oxidation and re-adsorption of Fe(II) and play a decisive role for determining the redox conditions in heterogeneous Fe(II)/Fe(III)-systems. It could be shown that at least two

Fe(II) species of different reactivity exist on the goethite surface and that their formation is a highly dynamic process. A small fraction of total surface bound ferrous is initially present as highly reactive Fe(II) species at the goethite surface which is preferentially consumed by oxidation reactions. Re-adsorption of Fe(II)$_{aq}$ and/or concomitant surface remodelling sustains a second population of less reactive Fe(II)-species. The occurrence of two different reactive Fe(II) surface sites could be confirmed by Mössbauer spectroscopy and corresponds to different carbon isotope fractionation patterns of the probe oxidant CCl$_4$. Thus isotope fractionation of CCl$_4$ can provide indirect information about transient Fe(II) species present at iron minerals. It is important to note that the dynamic surface remodelling processes at goethite may influence subsequent redox reactions with regard to reaction rates and product distribution, e.g., in the case of CCl$_4$ the potential formation of toxic chloroform vs. harmless CO.

Given the considerable surface dynamics of reactive Fe(II) species and the sensitivity of surface mediated redox reactions of Fe(II) on the actual surface chemistry one can expect significant effects of other sorbates such as natural organic matter (NOM) and other ligands in natural environments. Further investigations are currently in progress in our laboratories regarding such effect of organic ligands on the oxidation of Fe(II) at goethite and other iron minerals.

4.6 References

Amonette, J. E., Workman, D. J., Kennedy, D. W., Fruchter, J. S. and Gorby, Y. A., Dechlorination of Carbon Tetrachloride by Fe(II) Associated with Goethite. *Environ. Sci. Technol.* **2000,** *34*, (21), 4606-4613.

Bjerg, P. L., Ruegge, K., Pedersen, J. K. and Christensen, T. H., Distribution of redox-sensitive groundwater quality parameters downgradient of a landfill (Grindsted, Denmark). *Environ. Sci. Technol.* **1995,** *29*, (5), 1387-1394.

Christensen, T. H., Bjerg, P. L., Banwart, S. A., Jakobsen, R., Heron, G. and Albrechtsen, H.-J., Characterization of redox conditions in groundwater contaminant plumes. *Journal of Contaminant Hydrology* **2000,** *45*, (3-4), 165-241.

Cornell, R. M. and Schwertmann, U., The iron oxides. *Wiley-VCH Verlag GmbH & Co. KGaA, Weinheim* **2003,** *second, completely revised and extended edition*, 664 pp.

Coughlin, B. R. and Stone, A. T., Nonreversible Adsorption of Divalent Metal Ions (MnII, CoII, NiII, CuII, and PbII) onto Goethite: Effects of Acidification, FeII Addition, and Picolinic Acid Addition. *Environ. Sci. Technol.* **1995,** *29*, (9), 2445-2455.

Curtis, G. P. and Reinhard, M., Reductive Dehalogenation of Hexachloroethane, Carbon Tetrachloride, and Bromoform by Anthrahydroquinone Disulfonate and Humic Acid. *Environ. Sci. Technol.* **1994,** *28*, (13), 2393-2401.

Elsner, M., Haderlein, S. B., Kellerhals, T., Luzi, S., Zwank, L., Angst, W. and Schwarzenbach, R. P., Mechanisms and products of surface-mediated reductive dehalogenation of carbon tetrachloride by Fe(II) on goethite. *Environ Sci Technol* **2004,** *38*, (7), 2058-66.

Elsner, M., Schwarzenbach, R. P. and Haderlein, S. B., Reactivity of Fe(II)-bearing minerals toward reductive transformation of organic contaminants. *Environ Sci Technol* **2004,** *38*, (3), 799-807.

Gregory, K. B., Larese-Casanova, P., Parkin, G. F. and Scherer, M. M., Abiotic Transformation of Hexahydro-1,3,5-trinitro-1,3,5-triazine by FeII Bound to Magnetite. *Environmental Science & Technology* **2004,** *38*, (5), 1408-1414.

Handler, R. M., Beard, B. L., Johnson, C. M. and Scherer, M. M., Atom exchange between aqueous Fe(II) and goethite: an Fe isotope tracer study. *Environ Sci Technol* **2009,** *43*, (4), 1102-7.

Hiemstra, T. and van Riemsdijk, W. H., Adsorption and surface oxidation of Fe(II) on metal (hydr)oxides. *Geochimica et Cosmochimica Acta* **2007,** *71*, (24), 5913-5933.

Hofstetter, T. B., Heijman, C. G., Haderlein, S. B., Holliger, C. and Schwarzenbach, R. P., Complete Reduction of TNT and Other (Poly)nitroaromatic Compounds under Iron-Reducing Subsurface Conditions. *Environ. Sci. Technol.* **1999,** *33*, (9), 1479-1487.

Hofstetter, T. B., Schwarzenbach, R. P. and Haderlein, S. B., Reactivity of Fe(II) species associated with clay minerals. *Environ Sci Technol* **2003,** *37*, (3), 519-28.

Jensen, D. L., Boddum, J. K., Redemann, S. and Christensen, T. H., Speciation of Dissolved Iron(II) and Manganese(II) in a Groundwater Pollution Plume. *Environ. Sci. Technol.* **1998,** *32*, (18), 2657-2664.

Jeon, B.-H., Dempsey, B. A., Burgos, W. D. and Royer, R. A., Reactions of ferrous iron with hematite. *Colloids and Surfaces A: Physicochemical and Engineering Aspects* **2001,** *191*, (1-2), 41-55.

Klausen, J., Troeber, S. P., Haderlein, S. B. and Schwarzenbach, R. P., Reduction of Substituted Nitrobenzenes by Fe(II) in Aqueous Mineral Suspensions. *Environ. Sci. Technol.* **1995,** *29*, (9), 2396-2404.

Larese-Casanova, P., Kappler, A. and Haderlein, S. B., Heterogeneous oxidation of Fe(II) on iron oxides: Controls on Fe(III) product formation. *Geochimica et Cosmochimica Acta* **2009**, in preparation.

Larese-Casanova, P. and Scherer, M. M., Fe(II) Sorption on Hematite: New Insights Based on Spectroscopic Measurements. *Environ. Sci. Technol.* **2007,** *41*, (2), 471-477.

Liger, E., Charlet, L. and Van Cappellen, P., Surface catalysis of uranium(VI) reduction by iron(II). *Geochimica et Cosmochimica Acta* **1999,** *63*, (19-20), 2939-2955.

Liu, C., Zachara, J. M., Foster, N. S. and Strickland, J., Kinetics of Reductive Dissolution of Hematite by Bioreduced Anthraquinone-2,6-disulfonate. *Environ. Sci. Technol.* **2007,** *41*, (22), 7730-7735.

McCormick, M. L. and Adriaens, P., Carbon Tetrachloride Transformation on the Surface of Nanoscale Biogenic Magnetite Particles. *Environ. Sci. Technol.* **2004,** *38*, (4), 1045-1053.

Pecher, K., Haderlein, S. B. and Schwarzenbach, R. P., Reduction of polyhalogenated methanes by surface-bound Fe(II) in aqueous suspensions of iron oxides. *Environ Sci Technol* **2002,** *36*, (8), 1734-41.

Postma, D. and Jakobsen, R., Redox zonation: Equilibrium constraints on the Fe(III)/SO4-reduction interface. *Geochimica et Cosmochimica Acta* **1996,** *60*, (17), 3169-3175.

Rugge, K., Hofstetter, T. B., Haderlein, S. B., Bjerg, P. L., Knudsen, S., Zraunig, C., Mosbaek, H. and Christensen, T. H., Characterization of Predominant Reductants in an Anaerobic Leachate-Contaminated Aquifer by Nitroaromatic Probe Compounds. *Environ. Sci. Technol.* **1998,** *32*, (1), 23-31.

Schmidt, T. C., Zwank, L., Elsner, M., Berg, M., Meckenstock, R. U. and Haderlein, S. B., Compound-specific stable isotope analysis of organic contaminants in natural environments: a critical review of the state of the art, prospects, and future challenges. *Anal Bioanal Chem* **2004,** *378*, (2), 283-300.

Stookey, L. L., Ferrozine - a new spectrophotometric reagent for iron. *Anal. Chem.* **1970,** *42*, (7), 779-781.

Stumm, W. and Sulzberger, B., The cycling of iron in natural environments: Considerations based on laboratory studies of heterogeneous redox processes. *Geochimica et Cosmochimica Acta* **1992,** *56*, (8), 3233-3257.

Williams, A. G. and Scherer, M. M., Spectroscopic evidence for Fe(II)-Fe(III) electron transfer at the iron oxide-water interface. *Environ Sci Technol* **2004,** *38*, (18), 4782-90.

Zhang, Y., Charlet, L. and Schindler, P. W., Adsorption of protons, Fe(II) and Al(III) on lepidocrocite ([gamma]-FeOOH). *Colloids and Surfaces* **1992,** *63*, (3-4), 259-268.

Zwank, L., Elsner, M., Aeberhard, A., Schwarzenbach, R. P. and Haderlein, S. B.,
Carbon isotope fractionation in the reductive dehalogenation of carbon
tetrachloride at iron (hydr)oxide and iron sulfide minerals. *Environ Sci
Technol* **2005,** *39*, (15), 5634-41.

4.7 Appendix

The appendix contains a SEM image and an X-ray diffractogram of goethite (Figure A4.1); additional information of "material and methods"; experimental overview (Table A4.1); Mössbauer spectra (Figure A4.2).
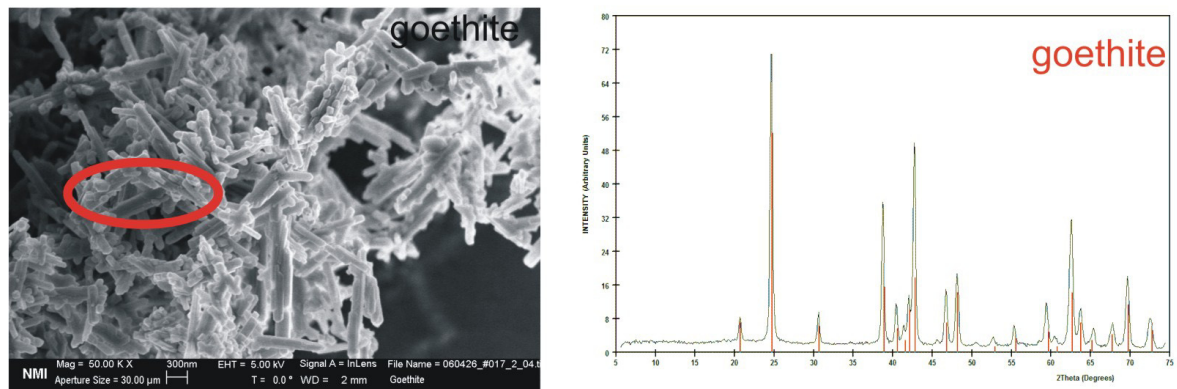
Figure A4.1: Scanning electron microscopy picture and X-ray diffractogram (XRD) of goethite (Bayferrox 920Z); SEM image shows as crystal forms needles with a length of 0.6-0.9 µM, XRD indicates goethite without impurities (red lines correspond to a standard of goethite).

4.7.1 Material and Methods

Goethite

The iron mineral goethite (α-FeOOH) was purchased from Lanxess Germany GmbH under the name Bayferrox 920 Z. The storage was dry and cool as received under lab atmosphere. The specific surface area was investigated by N_2 adsorption with a Gemini 2375 Surface Area Analyzer. The BET surface was 9.2 m^2/g using the multi point BET measurement. X-ray diffraction (µ-XRD, Bruker-D8 with GADDS) showed that the sample did not contain impurities. Furthermore the crystal form and the particle size were determined by scanning electron microscopy (LEO 1550 VP) after sputter deposition on a thin gold layer and showed pure needle shaped crystals. The particle size ranged between 0.6 and 0.9 µm in length. The TOC (total organic carbon) content was with 0.01% near the detection limit (Hariba P100 with TOC Boat Sampler, detection limit 0.006%). The point of zero charge (pH_{pzc}) was determined with 6.5 ± 0.4 (Liu et al., 2007). The properties of the goethite were in the expected range but the pH_{pzc} was 6.5 (6.1-9.5; literature values) after washing the mineral twice due to sulphate removal.

Fe(II) Stock Solution

The preparation of the iron stock solution was performed by adding 3.63 g (0.065 mmol) metal iron (Fe(0)) to 100 mL of a 1 M HCl solution in a serum bottle. The 1 M HCl solution was made anoxic before the experiments by bubbling nitrogen through a rubber stopper in the solution for 30 min (gas outlet for pressure release). The suspension was heated up to 80°C while gently stirring. After 2 hours no more hydrogen evolution was observed. The suspension was filtered within the glove box with a 0.2 µm PTFE filter to remove any residual metal iron. The exact content of Fe(II) was determined photometrically (562 nm) by the ferrozine assay (Stookey, 1970).

pH and Fe(II)$_{aq}$ in goethite suspension

All following preparation steps in which Fe(II) was involved were conducted in a glove box (Unilab with a PLC control panel Siemens Simatic OP7, Braun, Garching, Germany) to work strictly under anoxic conditions and avoid any oxidation of Fe(II). The mineral suspensions were prepared by adding 5.43 g of goethite to a 1 L bottle filled with Millipore water to reach a total specific surface of 50 m^2/L (Zwank et al., 2005). The suspensions were shaken in an overhead shaker for 24 hours to remove any sorbed impurities from the mineral surface and then washed twice with Millipore water. Afterwards the suspensions were purged with nitrogen for 90 min and transferred into the glove box.

The suspensions were always stirred during additions or equilibration time. Before adding Fe(II) to the goethite suspension the pH was adjusted with 0.2 M NaOH or with 0.2 M HCl (pH 5 only) to the required pH value. After an equilibration time of 18 hours the Fe(II)$_{aq}$ concentration was determined by the ferrozine assay (Stookey, 1970). If necessary these steps were repeated to reach a Fe(II)$_{aq}$ concentration of 1 mM and a considered pH after a total equilibration time of at least 48 hours. Instead of organic buffers the intrinsic buffer capacity of goethite was used to stabilize the suspension (Elsner et al., 2004) since the influence of organic buffers on the transformation of contaminants are discussed controversially and were studied separately.

The pH dependent experiments were carried out at pH 5.01, 6.01, 7.01 and 8.01 ± 0.05. For experiments with different initial CCl$_4$ concentration or longer exposure times of Fe(II), the pH was set 7.01 or 8.01 ± 0.05 (indicated there).

Analytical Methods

For quantitative analyses of CCl$_4$, CHCl$_3$ and C$_2$Cl$_4$ a TraceGC 2000 (ThermoFinnigan, Milano, Italy) gas chromatograph coupled to a TraceDSQ single quadrupole mass spectrometric detector (ThermoFinnigan, Austin,

TX, US) was used. The injection was performed with a headspace method using a 2.5 mL gastight syringe (CTC-CombiPAL autosampler) and a split ratio of 1:50. For separation of the compounds an Rtx-VMS capillary column (60 m × 0.32 mm I.D., 1.8 μm film thickness, Restek Corp., Bellefonte, PA, US) was installed. The temperature of the column was initially hold at 40°C for 4 min, heated up to 100°C with a rate of 7°C/min and maintained at 150°C for another 5 min. For the mass spectrometer the electron impact ionization mode (EI) at 70 eV, a source temperature of 220°C and transfer line temperature of 250°C were applied. The scan mode was a full scan (m/z = 50-300). To avoid carry over, a gentle nitrogen stream was used to clean the syringe for 5 min after each injection. Data acquisition and processing were carried out using Xcalibur Data System Version 1.3 (ThermoFinnigan, Austin, TX, US).

The compound-specific isotope ratios ($\delta^{13}C$ values) were determined using a Trace gas chromatograph (ThermoFinnigan, Milan, Italy) coupled to a combustion interface (GC Combustion III; Thermo-Finnigan MAT) maintained at 940°C and an isotope ratio mass spectrometer (DeltaPLUS XP; Thermo Finnigan MAT, Bremen, Germany). A programmable temperature vaporizer (PTV) injector (Optic 3; ATAS GL International B.V., Veldhoven, The Netherlands) was connected upstream of the gas chromatograph. As extraction technique a solid phase microextraction (SPME) with an 85 μm Carboxen™/PDMS Stable Flex™ fiber (Supelco, Germany) in a CombiPal autosampler was used. The extraction time was 20 min at 35°C and the following desorption time in the injector was 0.5 min at 270°C. An Rtx-VMS capillary column (same as above) and as carrier gas Helium 5.0 (Air Liquide, Düsseldorf, Germany) at a column flow of 2.0 mL/min in the first minute and then decreased to a constant flow of 1.5 mL/min were used. The split flow increased to 15 mL/min after the decreasing of the column flow.

The baseline separation of the compounds were reached starting with a temperature of 40 °C for 2 min, ramped it with 4°C to 100°C, maintained

there for 1 min and went quickly up to 200°C for 5 min to avoid any carry over. Isotopic ratios were determined to a referenced CO_2 standard relative to Vienna Pee Dee Belemnite (VPDB). The IRMS instrument was tuned to maximum linearity. Reoxidation of the NiO/CuO/Pt catalyst was carried out regularly after 40-50 measurements. All samples were run in triplicates with standards in between to avoid any variability of the instrument. The isotope compositions of CCl_4, $CHCl_3$ and C_2Cl_4 were determined by EA-IRMS measurements.

Table A4.1: Overview of the experiments carried out and results of relative formation of CHCl₃, ration rate constants k′obs and enrichment factors ε.

pH[1]	CCl_4 concentration [μM]	Fe(II) sorption [days]	rel. formation $CHCl_3$ [%][2]	k'obs [h*(m²/L))$^{-1}$]	ε [‰][3]
5.1			n.d.[4]	n.d.[4]	n.d.[4]
6.1	30.0	2	n.d.[4]	n.d.[4]	n.d.[4]
7.1			44.8	5.3×10^{-4}	-21.9
8.1			31.8	3.4×10^{-3}	-13.8
	5.0		94.1	1.2×10^{-3}	-8.8
	7.5		99.9	1.1×10^{-3}	-10.1
7.1	12.5	2	43.4	5.6×10^{-4}	-15.5
	15.0		43.4	6.0×10^{-4} [5]	-14.1
	55.0		36.1	2.8×10^{-4} [5]	-28.2
	70.0		40.6	2.4×10^{-4} [5]	-26.0
	5.0		83.8	1.3×10^{-3} [5]	-19.8
8.1	12.5	2	71.1	1.7×10^{-3} [5]	-17.4
	55.0		56.2	1.2×10^{-3} [5]	-17.4
8.1	7.5	10	30.0	1.4×10^{-3} [5]	-17.7
7.2 [6]	7.5	30	39.2	6.7×10^{-4} [5]	-18.3

[1] deviation of pH values ± 0.05

[2] relativ formation of CHCl3 means (CHCl3)t/((CCl4)0-CCl4)t)

[3] with a standard variation of 0.5‰ for isotope measurements

[4] n.d. = not determined due to no reaction took place

[5] not a pseudo-first order reaction, values are single point determinations after > 90% transformation of CCl4

[6] pH value dropped from 8.1 during the time period from 10 to 30 days
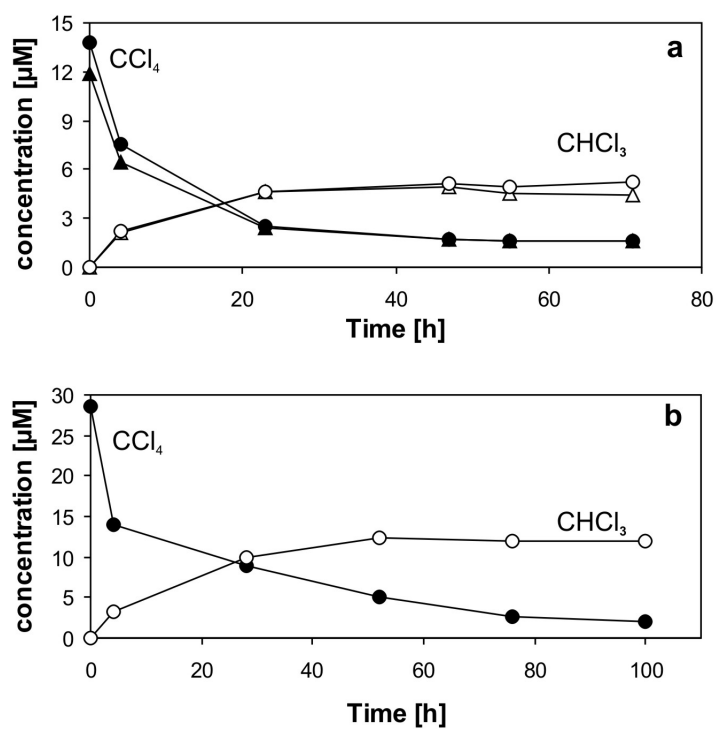
Figure A4.2: Transformation of CCl₄ and formation of CHCl₃ (goethite, 1 mM Fe(II)ₐq, pH 7): (a) CCl₄: (▲) 12.5 µM; (●) 15 µM; corresponding CHCl₃: (△) and (○), (b) CCl₄: (●) 30 µM; corresponding CHCl₃: (○).
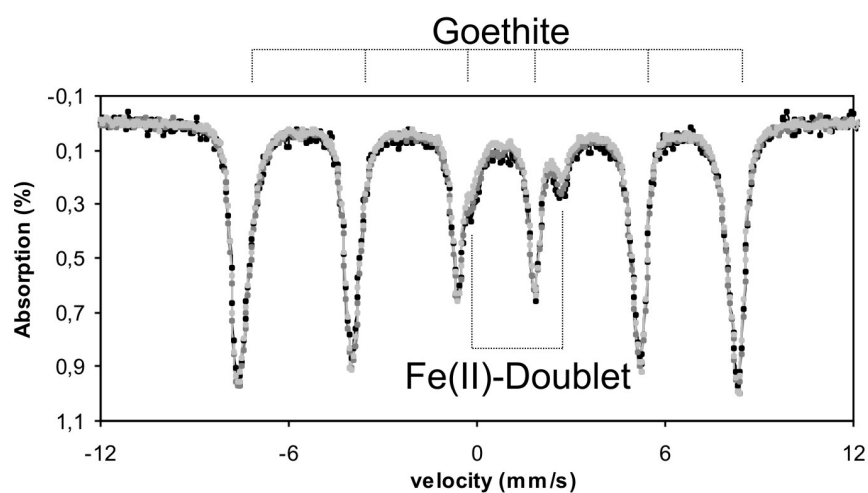
Figure A4.3: Normalized Mössbauer spectra at 77 K of goethite/^{57}Fe(II)$_{sorb}$ (black), goethite/^{57}Fe(II)$_{sorb}$ after little oxidized ^{57}Fe(II) by CCl$_4$ (dark grey) and goethite/^{57}Fe(II)$_{sorb}$ after progressive oxidized ^{57}Fe(II) by CCl$_4$ (light grey).

References

Elsner, M., Haderlein, S. B., Kellerhals, T., Luzi, S., Zwank, L., Angst, W. and Schwarzenbach, R. P., Mechanisms and products of surface-mediated reductive dehalogenation of carbon tetrachloride by Fe(II) on goethite. *Environ Sci Technol* **2004,** *38*, (7), 2058-66.

Liu, C., Zachara, J. M., Foster, N. S. and Strickland, J., Kinetics of Reductive Dissolution of Hematite by Bioreduced Anthraquinone-2,6-disulfonate. *Environ. Sci. Technol.* **2007,** *41*, (22), 7730-7735.

Stookey, L. L., Ferrozine - a new spectrophotometric reagent for iron. *Anal. Chem.* **1970,** *42*, (7), 779-781.

Zwank, L., Elsner, M., Aeberhard, A., Schwarzenbach, R. P. and Haderlein, S. B., Carbon isotope fractionation in the reductive dehalogenation of carbon tetrachloride at iron (hydr)oxide and iron sulfide minerals. *Environ Sci Technol* **2005,** *39*, (15), 5634-41.

5. Effects of organic buffers on the sorption and oxidation of ferrous iron at goethite

5.1 Abstract

The oxidation of Fe(II) on iron minerals is controlled by various factors including pH in aqueous systems. Therefore many environmental based studies include Good's buffers to control reaction conditions although the application of these buffers is discussed controversially in terms of their potential effects on reaction conditions. The effects of the widely used zwitterionic amine buffers 3-morpholinopropane-1-sulfonic acid (MOPS) and 4-(2-hydroxyethyl)-1-piperazineethanesulfonic acid (HEPES) on the oxidation of Fe(II) at goethite were studied in batch experiments at various concentrations (1-50 mM) using CCl_4 as model oxidant. The adding of these organic buffers caused desorption of previously sorbed Fe(II) from the goethite surface (up to -53.3/-47.9% at 50 mM MOPS/HEPES). Significant sorption of the organic buffers to goethite occurred only in the presence of sorbed Fe(II) (MOPS more than HEPES) but not on a pure goethite surface. The results suggest that an interaction of the organic sorbates and Fe(II) occurred.

These desorption-sorption-processes of buffers and Fe(II) had various effects on the oxidation of Fe(II) by CCl_4; i.e., slower reaction rate constants and higher yield of chloroform with increasing organic sorbate concentrations. To elucidate the type of interaction between MOPS and HEPES and Fe(II) in terms of electrostatic and steric effects we studied the competitive effects of model compounds like calcium as cation and two different sulfonic acids as anions. Neither desorption of Fe(II) nor significant sorption of Ca^{2+} or the sulfonic acids were observed. We therefore hypothesize that a complex between the organic buffers and Fe(II) forms

involving the free electron pair of the nitrogen in the heterocyclic ring. *In situ* ATR-FTIR spectroscopy showed that C-H or C-C bonds are not involved in this interaction. Our data showed for the first time that the frequently used zwitterionic organic buffers may interfere significantly with redox reactions at the goethite/Fe(II) surface. Thus, you should take care when interpreting mechanistic or kinetic data obtained in such systems.

5.2   Introduction

In the anoxic subsurface, one of the major redox sensitive metal species is ferrous iron which is a driving force in transformation processes of pollutants (Heron et al., 1994). Several studies investigated the influence of different geochemical conditions on degradation processes which occur in the environment (Cervini-Silva et al., 2001; Christensen et al., 2001). The adsorption of Fe(II) to different minerals (Charlet et al., 1998; Liger et al., 1999; Williams and Scherer, 2004), the oxidation of Fe(II) by contaminants or the reduction of Fe(III) by bacteria (Heijman et al., 1995; McCormick et al., 2002) are widely discussed. Due to the lack of *in situ* spectroscopic techniques the oxidation of surface-bound Fe(II) on iron mineral surfaces is commonly investigated by studying the reaction of model oxidants or reductants such as dechlorination processes in batch experiments (Amonette et al., 2000; Elsner et al., 2004; Pecher et al., 2002; Zwank et al., 2005). Although the presence of organic sorbates like natural organic matter or organic buffers may strongly affect the reactivity and transformation of contaminants in batch and field experiments, organic buffers were used to control the experimental systems. The so-called Good's buffers like 3-morpholinopropane-1-sulfonic acid (MOPS), 4-(2-hydroxyethyl)-1-piperazineethanesulfonic acid (HEPES) and piperazine-N,N'-bis(2-ethanesulfonic acid) (PIPES) were commonly used for

this approach. However the potential effect of organic buffers on reaction conditions, i.e., affinity to metal ions and formation of complexes is discussed controversially.

Good and co-workers (Good et al., 1966) did not see evidence for complex formation of the zwitterionic amino acids like HEPES with the metal ions Mg^{2+}, Ca^{2+}, Mn^{2+} and Cu^{2+}. Ferrous iron, however, was not investigated in this study. Evans et al. (Evans and Wood, 1987) recognized complexes between the amine buffer PIPES and soluble bivalent copper ions by an electron spin resonance (ESR) study. Similar observations were gained by Simpson et al. (Simpson et al., 1988) where a complex between HEPES and soluble Cu^{2+} was measured, while the formation of a complex between HEPES and iron salts could not be detected.

Nearly 30 years later Yu et al. (Yu et al., 1997) studied again the possible formation of complexes between various tertiary amine buffers and divalent copper ions. They recommended the three buffers MES, MOPS, PIPES as non-complexing buffers, which contrast with former observations (Evans and Wood, 1987). HEPES was not recommended, due to its possibility of forming weak complexes with copper ions as indicated by ultraviolet spectroscopy. The different behavior of the amine buffers was explained by Yu and co-workers (Yu et al., 1997) with the side chain of the buffer molecules. HEPES was the only compound with a hydroxyl group in a side chain and a complex between this hydroxyl group and copper ions would be more likely. Additionally, studies were performed by Mash et al. (Mash et al., 2003) in which even a stronger complexation of HEPES and copper ions was observed. They assumed that this stronger complexation may be induced by an impurity of HEPES without alkanesulfonate side chain (0.5% of total mass). Furthermore weak complex formation of MOPSO (similar to MOPS) and copper ions could also be observed by Mash and co-workers. In contrast to the complexation studies above Danielsen et al. (Danielsen et al., 2005) investigated the influence of amine buffers on the

reductive dechlorination of carbon tetrachloride by magnetite. The presence of amine buffers (TEEN, TEA and TRIS) had different effects on the oxidation of Fe(II), i.e., complexing metal ions, dissolving surface iron sites and acting as a hydrogen radical source.

In this paper we investigated systematically and for the first time the influence of selected Good's buffers and model compounds on the oxidation of Fe(II) by the model oxidant CCl_4 as these buffers are frequently used in environmental studies to control pH, presumably without interfering with redox sensitive metals. Our study focused on the following aspects: (i) to gain insights on interactions of the two organic buffers with the goethite/Fe(II) surface, (ii) to get more information about the influence of the organic sorbates on product distribution and reaction rate constants including changes in the reaction mechanism during the transformation of CCl_4, and (iii) to assess the type of interactions between organic sorbates and goethite/Fe(II) systems using model compounds and ATR-FTIR spectroscopy.

5.3   Material and Methods

5.3.1   Chemicals

Carbon tetrachloride CCl_4 (99+%) and tetrachloroethylene C_2Cl_4 (99.9+%) were purchased from Aldrich (Steinheim, Germany), chloroform $CHCl_3$ ($\geq$ 99.5%) from Fluka (Buchs, Switzerland) respectively. Sodium hydroxide (1 M), hydrochloric acid (1 M) and metal iron (Fe(0)) were obtained from Merck (Darmstadt). The zwitterionic buffers 3-(N-morpholino)propane-1-sulfonic acid (MOPS) and 4-(2-hydroxyethyl)-1-piperazine ethanesulfonic acid (HEPES) with pK_a values of 7.2 (MOPS) and 7.5 (HEPES) were ordered from Roth or Sigma ($\geq$ 99.5%). $CaCl_2$ x 2 H_2O ($\geq$ 98.0%) and benzenesulfonic

acid (98%), Sodium 2-bromoethanesulfonate (98%) were purchased from Fluka and Aldrich (Figure 5.1). The ferrozine solution was made with 0.1% (w/v) 3-(2-Pyridyl)-5-6-diphenyl-1,2,4-triazine-p,p'-disulfonic acid in 50% (w/v) ammonium acetate (Acros organics, ≥ 98.0%). All stock solutions or dilutions were prepared using Millipore water.
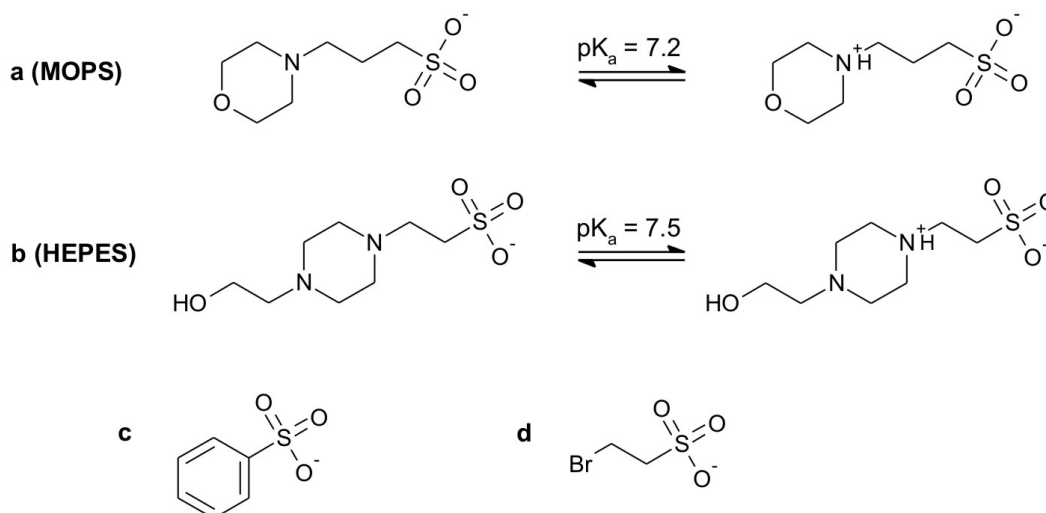
Figure 5.1: Structure of the zwitterionic tertiary amine buffers with pK$_a$ values at pH 7: (a) 3-(N-morpholino) propane-1-sulfonic acid (MOPS) and (b) 4-(2-hydroxyethyl)-1-piperazineethanesulfonic acid (HEPES) and model compounds: (c) benzenesulfonic acid and (d) 2-Bromoethanesulfonic acid.

5.3.2   *Goethite*

The iron mineral goethite (α-FeOOH) was purchased from Lanxess Germany GmbH as Bayferrox 920 Z. The storage was dry and cool as received under lab atmosphere. The goethite was characterized determining specific surface area (BET measurement), purity (X-ray diffraction), crystal morphology and particle size (scanning electron microscopy), total organic carbon and point of zero charge pH$_{pzc}$ (Liu et al., 2007) (more details see Appendix).

5.3.3   Fe(II) Stock Solution

The preparation of the iron stock solution using metal iron Fe(0) and 1 M HCl was performed following the procedure of Elsner and co-workers (Elsner et al., 2004). The exact content of Fe(II) was determined photometrically (562 nm) by the ferrozine assay (Stookey, 1970) (more details see Appendix).

5.3.4   Goethite/Fe(II) Suspension

All preparation steps in which Fe(II) was involved were conducted in a glove box (Unilab, Braun, Garching, Germany) to maintain strictly anoxic conditions avoiding any oxidation of Fe(II). The general procedure preparing a mineral/Fe(II) suspension follows the description of Zwank et al. (Danielsen et al., 2005; Zwank et al., 2005) and is also documented in the supporting information. For all experiments a pH of 7.0-7.1 was chosen. After an equilibration time of 18 hours the $Fe(II)_{aq}$ concentration was determined by the ferrozine assay (Stookey, 1970). If necessary these steps were repeated to reach 1 mM $Fe(II)_{aq}$ and pH of 7 after a total equilibration time of at least 48 hours. Afterwards MOPS or HEPES buffers were added in different amounts (1, 10, 25, 50 mM) to cover the concentration range of Good's buffers described in the literature (0.4-25 mM) for transformation experiments on iron oxides (Elsner et al., 2004; Larese-Casanova and Scherer, 2007; Pecher et al., 2002). The aqueous Fe(II) concentration was measured again after an equilibration time of 24 hours. In some of the experiments instead of buffers a cation (Ca^{2+}) or one of the anions (2-bromethanesulfonic acid, benzenesulfonic acid) were used.

5.3.5 DOC and AAS Measurements

The adsorption of the organic sorbates or the sulfonic acids to the mineral or the mineral/Fe(II) surface was determined by measuring the DOC content in the aqueous phase after 24 h with a HighTOC-analysator® (Elementar Analysensysteme GmbH, Hanau, Germany) and subtracting it from the total amount of added compounds. The aqueous concentration of calcium was detected with atomic absorption spectroscopy (AAS 1100, PerkinElmer, Waltham, MA) after 24 hours.

5.3.6 Batch Experiments

First anoxic aqueous stock solutions of carbon tetrachloride (CCl_4) and tetrachloroethylene (C_2Cl_4, internal standard) were prepared. Serum bottles with 100 mL of Millipore water closed with butyl rubber stoppers were flushed with N_2 for 30 minutes through a syringe needle before aliquots of the pure solutes (CCl_4/C_2Cl_4) were added to obtain a carbon tetrachloride concentration of 30 µM. Before adding the pure solutes the rubber stoppers were quickly opened and afterwards replaced by Viton stoppers during a gentle nitrogen stream in the headspace of the vials (removal of any oxygen while the additions) and immediately transferred into the glove box.

In the glove box, 42 mL aliquots of the equilibrated and stirred mineral/Fe(II) suspension were transferred to 50 mL serum bottles inside the glove box after the organic buffers or model compounds were added. The reaction was started by adding 6 mL of the stock solution of CCl_4 and C_2Cl_4. The serum bottles were immediately closed with Viton stoppers. Control experiments without goethite were carried out in parallel. The serum bottles were placed on a horizontal shaker (140 rpm, 25°C, in the dark) outside the glove box. All experiments were carried out in duplicates.

5.3.7 Sampling

For each sampling campaign duplicates of each experiment were centrifuged (Eppendorf Z320, BHG Hermle) at 2000 rpm for 10 minutes, individually opened and quickly transferred to the vials for GC-MS measurements.

5.3.8 Analytical Method

For quantitative analyses of CCl_4, $CHCl_3$ and C_2Cl_4 a TraceGC 2000 gas chromatograph coupled to a TraceDSQ single quadrupole mass spectrometric detector (ThermoFinnigan) was used. The injection was performed with a 2.5 mL headspace syringe (CTC-CombiPAL autosampler) and a split ratio of 1:50. For separation of the compounds an Rtx-VMS capillary column (60 m $\times$ 0.32 mm I.D., 1.8 µm film thickness, Restek) was installed. The temperature of the column was initially hold at 40°C for 4 min, heated up to 100°C with a rate of 7°C/min and maintained at 150°C for another 5 min. For further information see Appendix.

5.4   Results and Discussion

5.4.1   Influence of organic buffers on the oxidation of Fe(II)

Our batch experiments showed that after $100\,h$ about 92% of CCl_4 was transformed in the absence of organic sorbates while in the presence of organic sorbates only 26.2/39.2% of CCl_4 was transformed ($50\,mM$ MOPS/HEPES) (Figure 5.2).
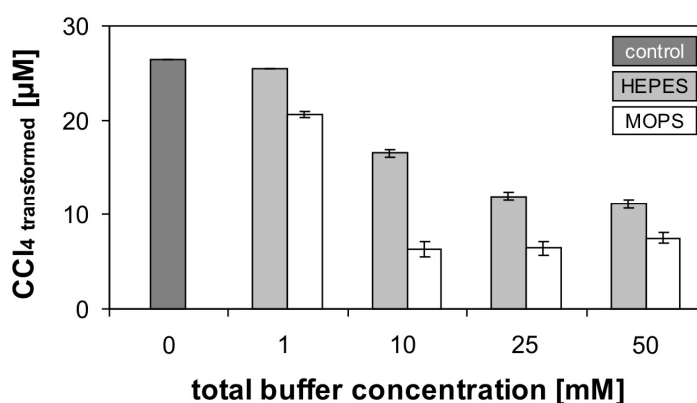
Figure 5.2: Effect of organic sorbates on the oxidation of Fe(II) at goethite at pH 7; transformation of CCl_4 after 100 h without organic sorbates (dark grey), with HEPES (light grey), MOPS (white).

The decrease of CCl_4 was more pronounced with MOPS than with HEPES. The total concentration of the organic buffers generally had strong effects on the transformation of CCl_4. It could be concluded that the organic buffers showed also strong effects on the oxidation of Fe(II) on the mineral surface due to the simultaneous oxidation of Fe(II) and transformation of CCl_4 as redox couple (Elsner et al., 2004; Pecher et al., 2002). Based on this phenomenon further experiments were carried out to determine which factors - interaction of organic buffers with Fe(II) and/or goethite, sorption processes or complex formation – are responsible for decreased transformation of CCl_4 and simultaneous oxidation of Fe(II).

5.4.2   Organic sorbates and goethite/Fe(II) suspension

The behavior of Fe(II) in the goethite suspension was monitored during the addition of organic buffers. Before one of the organic buffers was added to the system about half of the total Fe(II) was sorbed to the goethite surface (1.06 mM) in equilibration with aqueous Fe(II) (1.08 mM) at pH 7. The buffers induced a desorption of Fe(II) resulting in an increase of aqueous Fe(II) in the range of 23.3% (1 mM) to 52.0% (50 mM) for MOPS and of 15.2% (1 mM) to 46.7% (50 mM) for HEPES respectively. Effects of pH change on this desorption process can be excluded since the goethite/Fe(II) suspension and the organic buffer solutions had the same pH of 7 (Table 5.1).

Table 5.1: Desorption of Fe(II) and sorption of organic sorbates on goethite or goethite/Fe(II) systems.

system	$Fe(II)_{aq}$ [mM]	$Fe(II)_{sorb}$ [mM][a]	$Fe(II)_{desorb}$ [mM][b]	$\Delta Fe(II)_{aq}$ [%]	sorption of organic sorbates [mM][c]	
					goethite	goethite/Fe(II)
goethite/Fe(II)	1.08	1.06	0	0	-	-
+ 1 mM MOPS	1.34	0.81	0.25	23.3	0.00	0.20
+ 10 mM MOPS	1.58	0.57	0.49	45.5	0.18	1.97
+ 25 mM MOPS	1.60	0.54	0.52	47.8	0.41	4.06
+ 50 mM MOPS	1.65	0.49	0.56	52.0	0.76	7.51
+ 1 mM HEPES	1.25	0.89	0.17	15.2	0.00	0.26
+ 10 mM HEPES	1.44	0.71	0.35	32.5	0.00	1.72
+ 25 mM HEPES	1.53	0.62	0.44	40.8	0.35	3.27
+ 50 mM HEPES	1.59	0.55	0.51	46.7	0.43	4.47

[a] calculated by the difference of total Fe(II) ($Fe(II)_{aq}$ + $Fe(II)_{sorb}$ = 2.14 mM) and aqueous Fe(II) in the system.

[b] = $\Delta Fe(II)_{sorb}$; calculated by the difference of sorbed Fe(II) before and after organic sorbate addition.

[c] determined by DOC measurements; calculated by the difference of added organic sorbates and aqueous organic sorbates.

Furthermore the sorption behavior of the organic sorbates to the goethite and goethite/Fe(II) surface was investigated. The sorption of MOPS and HEPES on the goethite surface was very low while in the presence of sorbed Fe(II) much higher sorption of these organic buffers (10 times higher) occurred (Table 5.1). At all concentration levels the sorption of MOPS was more pronounced compared to HEPES (see sorption isotherms in the Appendix, Figure A5.1). The relationship between desorbed Fe(II) and

sorbed organic buffers is illustrated in Figure 5.3a. Enhanced desorption of Fe(II)$_{sorb}$ occurred along with increased sorption of MOPS compared to HEPES.
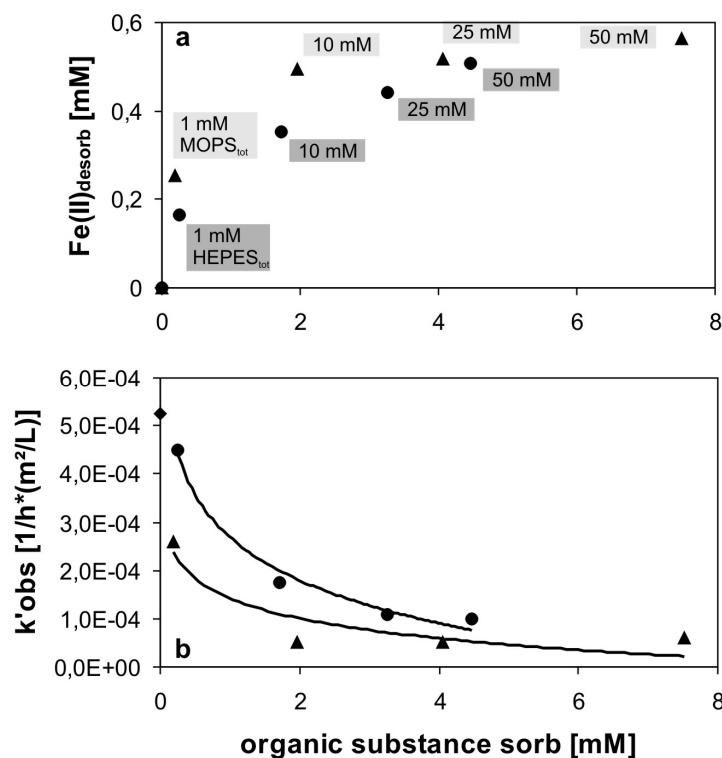
Figure 5.3: Effect of organic sorbates on the goethite/Fe(II) system; relationship between (a) sorption of organic sorbates and desorption of Fe(II) and (b) reaction rate constants k'$_{obs}$ and organic substance$_{sorb}$; (◆) without organic sorbates, (●) with HEPES, (▲) MOPS.

Consistent with the extent of sorption of the buffers to goethite/Fe(II) the decrease of CCl$_4$ transformation was more pronounced with MOPS than with HEPES and in each case with increasing buffer concentrations. The reaction rate constants, k'$_{obs}$, decreased in the presence of MOPS/HEPES from $2.6 \times 10^{-4}/4.5 \times 10^{-4}$ h^{-1}m^{-2}L (1 mM) to $6.1 \times 10^{-5}/9.9 \times 10^{-5}$ h^{-1}m^{-2}L (50 mM) (Figure 5.3b). The decrease of CCl$_4$ transformation and reaction rate constants can be rationalized by desorption of reactive Fe(II) species from the mineral surface induced by the simultaneous sorption of the organic sorbates.

5.4.3 Product distribution during transformation of CCl₄

Also the product distribution of CCl₄ was affected by the presence of organic sorbates. The fraction of CHCl₃ formation by the oxidation of Fe(II)ₛₒᵣᵦ ranged from 65.4/49.3% to 2.6/3.8% (1 mM to 50 mM MOPS/HEPES) after 100 hours. Even low concentrations of organic buffers (1 mM) showed an influence on the product distribution (Figure 5.4). The chloroform formation did not show any clear trend about the reaction time in all batch experiments (see Appendix, Table A5.1). Therefore three domains of chloroform formation might be distinguished.
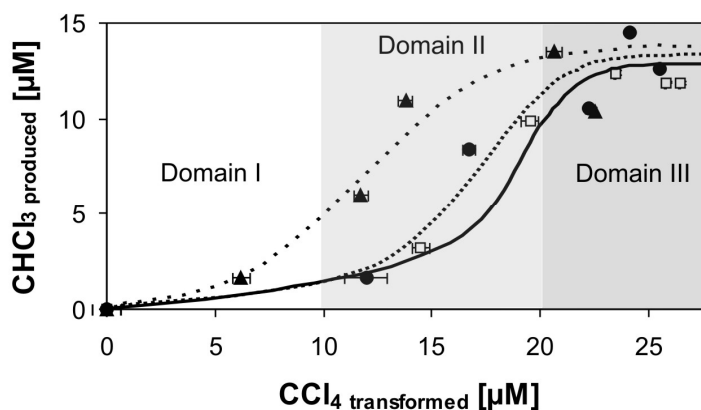
Figure 5.4: Effect of organic sorbates on the product distribution of CCl₄ at goethite at pH 7; Yield of CHCl₃: (□) without organic sorbates; (●) 1 mM HEPES; (▲) 1 mM MOPS.

In general, the surface-mediated transformation of CCl₄ on iron minerals follows an irreversible one-electron transfer to a trichloromethyl radical as intermediate and either by further reductive dechlorination of a second-electron transfer to carbon monoxide or by the abstraction of a hydrogen radical to chloroform as product (Danielsen et al., 2005; Elsner et al., 2004; Pecher et al., 2002). Additionally, either these organic buffers desorbed or blocked reactive Fe(II) species and/or interacted as hydrogen radical donor to the intermediate trichloromethyl radical after sorption to the mineral/Fe(II) surface (Lewis and Crawford, 1999). For detailed information on the mechanistic pathway see Appendix (Figure A5.2).

At the beginning chloroform was hardly found till 10 µM of transformed CCl$_4$, probably due to products binding to the surface at the beginning of the oxidation of Fe(II) (Figure 5.4, domain I). Sufficient reactive Fe(II) species were apparently present at the mineral surface even in the presence of organic buffers to promote a second electron transfer to direct product formation towards carbon monoxide. Subsequently, an increased formation of CHCl$_3$ during further oxidation of Fe(II) (10-20 µM transformed CCl$_4$) was observed with a higher chloroform yield in the presence of organic sorbates (Figure 5.4, domain II). Additionally more chloroform was produced in the presence of MOPS than of HEPES which is consistent with the observation that more MOPS than HEPES sorbed to the mineral surface. After the initial consumption of sorbed Fe(II), less reactive Fe(II) at the mineral surface was left and further surface remodeling took place which affected the further reaction of the trichloromethyl radical to chloroform. Especially the experiments with organic sorbates showed that the decrease of reactive Fe(II) species (-23.9/-15.6% 1 mM MOPS/HEPES) and the sorption of organic sorbates as hydrogen radical donor played a significant role in the system. Finally, in the third domain of the transformation of CCl$_4$ equal amounts of CHCl$_3$ and CO were observed in all experiments, probably due to the reactivity of freshly sorbed Fe(II) species and surface remodeling processes (Figure 5.4, domain III).

5.4.4 *Electrostatic and steric effects of model compounds on goethite/Fe(II) surfaces*

The interaction of MOPS and HEPES with the goethite/Fe(II) surface was further investigated using model compounds mimicking certain properties of these buffers. Due to the pK$_a$ of the tertiary amine buffers (pK$_a$ (MOPS) = 7.2 and pK$_a$ (HEPES) = 7.5) the organic sorbates are present in a zwitterionic form at pH 7. Such zwitterionic compounds have the potential to sorb to the mineral/Fe(II) surface by electrostatic attraction.

Since the goethite surface is little charged at pH 7 (pH_{pzc} = 6.5) and aqueous Fe(II) sorbs strongly to the mineral surface, it might be assumed that the positive and/or negative part of the zwitterionic organic buffers were involved during the sorption processes at the mineral surface. Lorphensri et al. (Lorphensri et al., 2006) demonstrated that anionic and zwitterionic pharmaceuticals containing a piperazinyl group like in HEPES showed greater sorption to positively than to negatively charged surfaces at pH 7. Therefore experiments with calcium (Ca^{2+}) were performed to evaluate the significance of cation exchange. Our data clearly show that the influence of Ca^{2+} ions on the amount of sorbed Fe(II) at the goethite surface was neglectible (Table 5.2). Furthermore, no sorption of Ca^{2+} ions could be observed on the goethite/Fe(II) surface at pH 7 (Table 5.2). Batch experiments with a goethite/Fe(II) suspension and CCl_4 showed exactly the same results with regard to product distribution and reaction rate constants of CCl_4 in the absence or presence of 10 mM or 50 mM calcium (data not shown here). Therefore calcium did not show an effect on the amount of reactive sorbed Fe(II) species and did not promote hydrogen radical formation. In addition the anionic (sulfonic acid) part of the organic sorbates could be responsible for the electrostatic processes. To investigate this hypothesis, sorption experiments of structure analogues of MOPS and HEPES were carried out using two different kinds of sulfonic acids, 2-bromoethanesulfonic acid and benzenesulfonic acid (Figure 5.1). After the addition of sulfonic acids, previously sorbed Fe(II) did not desorb from the mineral surface. Sorption of sulfonic acids was very low (< 1.5% of the total sulfonic acid content) at the highest concentration level. Additionally, the sorption behavior of the two sulfonic acids was not affected by different molecule structures (aromatic vs. aliphatic) (Table 5.2).

Table 5.2: Changes of aqueous Fe(II) and sorption of model compounds on goethite or goethite/Fe(II) mineral surfaces.

goethite/Fe(II)	Fe(II)$_{aq}$ [mM]	ΔFe(II)$_{aq}$ [%][a]	sorption of organic sorbates [mM][b]	
			goethite	goethite/Fe(II)
+ 0 mM Ca^{2+}	1.00	0	-	-
+ 1 mM Ca^{2+}	1.03	3.1	0	0.06
+ 10 mM Ca^{2+}	0.98	-2.0	0	0
+ 25 mM Ca^{2+}	0.99	-0.5	0	0
+ 50 mM Ca^{2+}	0.97	-2.6	0	0
+ 0 mM Bromoethanesulfonic acid	1.12	0	-	-
+ 1 mM Bromoethanesulfonic acid	1.14	1.7	0	0
+ 10 mM Bromoethanesulfonic acid	1.13	0.7	0.15	0
+ 25 mM Bromoethanesulfonic acid	1.14	1.8	0	0
+ 50 mM Bromoethanesulfonic acid	1.16	3.8	0.51	0.73
+ 0 mM Benzenesulfonic acid	1.11	0	-	-
+ 1 mM Benzenesulfonic acid	1.11	-0.6	0	0
+ 10 mM Benzenesulfonic acid	1.14	2.1	0	0
+ 25 mM Benzenesulfonic acid	1.13	1.7	0	0
+ 50 mM Benzenesulfonic acid	1.17	5.2	0.71	0

[a] calculated by the difference of aqueous Fe(II) without and with model compound addition, all values are averages of duplicated experiments;standard variation of ± 5%.

[b] determined by AAS for Ca^{2+} and DOC measurements for the sulfonic acids; calculated by the difference of added model compound and aqueous model compound

An overview of the sorption behavior of the organic sorbates and the discussed model compounds is shown at a concentration of 50 mM (Figure 5.5). Whereas the organic sorbates sorbed strongly to the goethite/Fe(II) surface, less sorption to goethite surface could be observed. The fact, that Fe(II) and Fe(III) species are present in a goethite/Fe(II) system, may have a strong effect on the sorption behaviour of zwitterionic molecules. Calcium showed no sorption in any of these systems. The sulfonic acids showed only very little sorption in these systems indicating that the goethite surface does not offer electrostatic interactions in the absence and in the presence of sorbed Fe(II).
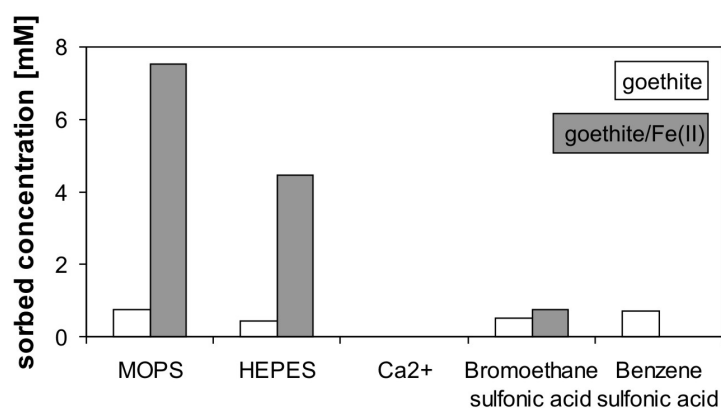
Figure 5.5: Sorption of organic sorbates, Ca^{2+} or sulfonic acids (total concentration 50 mM in each case) on goethite (grey) or goethite/Fe(II) (white) at pH 7.

In conclusion the fraction of electrostatic and steric effect of anionic or cationic charged molecules can be neglected in the progress of desorption of surface-sorbed Fe(II) and the sorption of these molecules. Therefore other interactions are likely to be responsible for the sorption of organic buffers MOPS and HEPES and the subsequent desorption of Fe(II).

The sorption of zwitterionic pharmaceuticals to minerals is influenced by the compound structure investigated by Carrasquillo and co-workers (Carrasquillo et al., 2008). Enhanced zwitterionic sorption occurred with increasing distance of positively and negatively charged parts of the molecule. In our case, the distance between the anionic amine group and the cationic sulfonic acid group within a molecule was different to the two zwitterionic buffers MOPS and HEPES. MOPS contains a propyl group whereas HEPES has an ethyl group in-between (Figure 5.1). If this fact significantly contributes to the sorption behavior of the two organic sorbates, it was in concordance with our findings that the sorption of MOPS was more pronounced than the sorption of HEPES. In the presence of amine buffers (TRIS, TEEN, TEA), Danielsen and co-workers (Danielsen et al., 2005) showed an increased transformation of CCl$_4$ in a magnetite system. However the chemical structure of these amine buffers is different compared to MOPS and HEPES. While TRIS has three hydroxyl groups next

to an amine group, TEEN and TEA contain of one and two amine groups as functional groups. However at pH 7, these buffers do not exist as zwitterionic molecules suggesting that the zwitterionic character may play a key role in the sorption of MOPS and HEPES to the goethite/Fe(II) surface. The sorption of the organic buffers TRIS, TEEN and TEA to iron mineral phases was not investigated in this study.

5.4.5 *Complex of organic sorbates and Fe(II)*

The interaction of the zwitterionic amine buffers MOPS and HEPES and Fe(II) was further investigated. Yu and co-workers (Yu et al., 1997) showed the existence of a complex containing Cu(II) ion and HEPES by ultraviolet spectroscopy. The reason for the complexation of aquatic Cu(II) with HEPES and not with MOPS was attributed to the hydroxyl group of the side chain in the HEPES molecule (Figure 5.1). Note that sorption of MOPS was higher than HEPES and caused more desorption of Fe(II) than HEPES in our experiments. The determination of a complex between MOPS/HEPES and Fe(II) was not possible with ultraviolet spectroscopy due to the lack of chromophores.

In situ ATR-FTIR spectroscopy showed, however, that C-H or C-C bonds are not involved in the interaction of any complexes between aqueous Fe(II) and MOPS/HEPES (1:1; 1:2 or 1:3 Fe(II)-buffer complexes) (see Appendix, Figure A5.3). As no precipitation of a complex from solution could be observed, we conclude that the complex forms only on the mineral surface at significant extent. Consequently, the complex formation of the organic buffers on the mineral/Fe(II) surface involves both sorbed Fe(II) and Fe(III) of the mineral structure. So far, the isolation of these complexes on the mineral surface is not feasible with ATR-FTIR spectroscopy.

Furthermore the tertiary amine in the heterocyclic ring of both molecules also could undergo a complex formation with Fe(II) involving the free electron pair at the nitrogen atom. Furthermore, the oxygen atom containing two free electron pairs in MOPS and a further nitrogen atom (one electron pair) or the hydroxyl group in the side chain of HEPES could foster a complex formation between these molecules and ferrous iron. Complexes between Fe(II) and a piperazinyl ring containing molecules were found by Ostermeier and co-workers (Ostermeier et al., 2006). They investigated the complex formation of 1,4-bis(2-pyridyl-methyl)piperazine and Fe(II) or Fe(III) by single crystal X-ray diffraction. It turned out that Fe(II) tends to form poly- and oligomeric structures by chair or boat configurations of the piperazinyl ring.

In analogues, one can postulate a complex formation through the free electron pair of the nitrogen (and oxygen) containing heterocyclic ring by a boat configuration and of the aliphatic hydroxyl group in HEPES according to the cited literature (Figure 5.6).
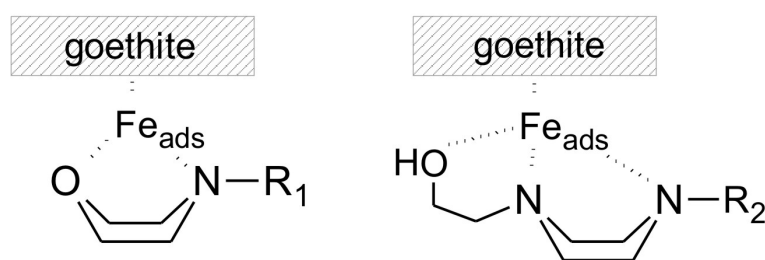
Figure 5.6: Postulated complex formation of MOPS (left) and HEPES (right) with adsorbed Fe(II).

5.5   Environmental significance

The results of this study indicate that the influence of organic amine buffers should carefully be evaluated before using them to control pH conditions. Especially, great care should be taken if batch studies are carried out to simulate environmental conditions (Doong and Lai, 2006; Elsner et al., 2004; Pecher et al., 2002). In contrast to our results, Danielsen and co-workers (Danielsen et al., 2005) observed increased transformation of CCl_4 in a magnetite system in the presence of amine buffers (TRIS, TEEN, TEA), while the chemical composition of these amine buffers have no zwitterionic structure at pH 7. Our results demonstrated clearly that the effects of amine buffers could be even more pronounced in these buffered transformation systems than reported so far. It could be shown that the sorption of these organic buffers to goethite/Fe(II) surfaces has a strong effect on the product distribution and reaction rate constants of CCl_4. The product distribution and thus the reaction pathway could be changed as the organic amine buffers could facilitate the transfer of hydrogen radicals on the surface-mediated transformation of pollutants and lead to a loss of reactive Fe(II) on the mineral surface. Subsequently little transformation of contaminants can be observed. As an alternative to organic buffers, the intrinsic buffer capacity of the studied iron minerals should be determined and used if possible for batch experiments. Our data further suggest that the influence of organic sorbates, especially even more complex organic molecules (NOM) may play a key role in environmental systems and is currently further investigated in our laboratories.

5.6 References

Amonette, J. E., Workman, D. J., Kennedy, D. W., Fruchter, J. S. and Gorby, Y. A., Dechlorination of Carbon Tetrachloride by Fe(II) Associated with Goethite. *Environ. Sci. Technol.* **2000,** *34*, (21), 4606-4613.

Carrasquillo, A. J., Bruland, G. L., MacKay, A. A. and Vasudevan, D., Sorption of Ciprofloxacin and Oxytetracycline Zwitterions to Soils and Soil Minerals: Influence of Compound Structure. *Environ. Sci. Technol.* **2008,** *42*, (20), 7634-7642.

Cervini-Silva, J., Larson, R. A., Wu, J. and Stucki, J. W., Transformation of Chlorinated Aliphatic Compounds by Ferruginous Smectite. *Environ. Sci. Technol.* **2001,** *35*, (4), 805-809.

Charlet, L., Silvester, E. and Liger, E., N-compound reduction and actinide immobilisation in surficial fluids by Fe(II): the surface =Fe^{III}OFe^{II}OH° species, as major reductant. *Chemical Geology* **1998,** *151*, (1-4), 85-93.

Christensen, T. H., Kjeldsen, P., Bjerg, P. L., Jensen, D. L., Christensen, J. B., Baun, A., Albrechtsen, H.-J. and Heron, G., Biogeochemistry of landfill leachate plumes. *Applied Geochemistry* **2001,** *16*, (7-8), 659-718.

Danielsen, K. M., Gland, J. L. and Hayes, K. F., Influence of Amine Buffers on Carbon Tetrachloride Reductive Dechlorination by the Iron Oxide Magnetite. *Environ. Sci. Technol.* **2005,** *39*, (3), 756-763.

Doong, R. A. and Lai, Y. L., Effect of metal ions and humic acid on the dechlorination of tetrachloroethylene by zerovalent iron. *Chemosphere* **2006,** *64*, (3), 371-8.

Elsner, M., Haderlein, S. B., Kellerhals, T., Luzi, S., Zwank, L., Angst, W. and Schwarzenbach, R. P., Mechanisms and products of surface-mediated reductive dehalogenation of carbon tetrachloride by Fe(II) on goethite. *Environ Sci Technol* **2004,** *38*, (7), 2058-66.

Elsner, M., Schwarzenbach, R. P. and Haderlein, S. B., Reactivity of Fe(II)-bearing minerals toward reductive transformation of organic contaminants. *Environ Sci Technol* **2004,** *38*, (3), 799-807.

Evans, D. F. and Wood, D., An Electron Spin Resonance Study of Frozen Aqueous Solutions containing 5,10,15,20-Tetrakis(N-methyl-4'-pyridinio)porphyrinato cobalt(II). *Dalton Transactions* **1987**, (12), 3099-3101.

Good, N. E., Winget, G. D., Winter, W., Connolly, T. N., Izawa, S. and Singh, R. M. M., Hydrogen Ion Buffers for Biological Research. *Biochemistry* **1966,** *5*, (2), 467-477.

Heijman, C. G., Grieder, E., Holliger, C. and Schwarzenbach, R. P., Reduction of Nitroaromatic Compounds Coupled to Microbial Iron Reduction in Laboratory Aquifer Columns. *Environ. Sci. Technol.* **1995,** *29*, (3), 775-783.

Heron, G., Crouzet, C., Bourg, A. C. M. and Christensen, T. H., Speciation of Fe(II) and Fe(III) in Contaminated Aquifer Sediments Using Chemical Extraction Techniques. *Environ. Sci. Technol.* **1994,** *28*, (9), 1698-1705.

Larese-Casanova, P. and Scherer, M. M., Fe(II) Sorption on Hematite: New Insights Based on Spectroscopic Measurements. *Environ. Sci. Technol.* **2007,** *41*, (2), 471-477.

Lewis, T. A. and Crawford R. L., In Novel Approaches for Bioremediation of Organic Pollution. *Fass, Ed.; Kluwer Academic: New York* **1999**, 1-11pp.

Liger, E., Charlet, L. and Van Cappellen, P., Surface catalysis of uranium(VI) reduction by iron(II). *Geochimica et Cosmochimica Acta* **1999,** *63*, (19-20), 2939-2955.

Liu, C., Zachara, J. M., Foster, N. S. and Strickland, J., Kinetics of Reductive Dissolution of Hematite by Bioreduced Anthraquinone-2,6-disulfonate. *Environ. Sci. Technol.* **2007,** *41*, (22), 7730-7735.

Lorphensri, O., Intravijit, J., Sabatini, D. A., Kibbey, T. C., Osathaphan, K. and Saiwan, C., Sorption of acetaminophen, 17alpha-ethynyl estradiol, nalidixic acid, and norfloxacin to silica, alumina. and a hydrophobic medium. *Water Res* **2006,** *40*, (7), 1481-91.

Mash, H. E., Chin, Y. P., Sigg, L., Hari, R. and Xue, H., Complexation of Copper by Zwitterionic Aminosulfonic (Good) Buffers. *Anal. Chem.* **2003,** *75*, (3), 671-677.

McCormick, M. L., Bouwer, E. J. and Adriaens, P., Carbon Tetrachloride Transformation in a Model Iron-Reducing Culture: Relative Kinetics of Biotic and Abiotic Reactions. *Environ. Sci. Technol.* **2002,** *36*, (3), 403-410.

Ostermeier, M., Limberg, C., Ziemer, B., The Coordination Chemistry of Iron with the 1,4-Bis(2-pyridyl-methyl)piperazine Ligand. *Zeitschrift für anorganische und allgemeine Chemie* **2006,** *632*, (7), 1287-1292.

Pecher, K., Haderlein, S. B. and Schwarzenbach, R. P., Reduction of polyhalogenated methanes by surface-bound Fe(II) in aqueous suspensions of iron oxides. *Environ Sci Technol* **2002,** *36*, (8), 1734-41.

Simpson, J. A., Cheeseman, K. H., Smith, S. E. and Dean, R. T., Free-radical generation by copper ions and hydrogen peroxide. Stimulation by Hepes buffer. *Biochem J* **1988,** *254*, (2), 519-23.

Stookey, L. L., Ferrozine - a new spectrophotometric reagent for iron. *Anal. Chem.* **1970,** *42*, (7), 779-781.

Williams, A. G. and Scherer, M. M., Spectroscopic evidence for Fe(II)-Fe(III) electron transfer at the iron oxide-water interface. *Environ Sci Technol* **2004,** *38*, (18), 4782-90.

Yu, Q., Kandegedara, A., Xu, Y. and Rorabacher, D. B., Avoiding interferences from Good's buffers: A contiguous series of noncomplexing tertiary amine buffers covering the entire range of pH 3-11. *Anal Biochem* **1997,** *253*, (1), 50-6.

Zwank, L., Elsner, M., Aeberhard, A., Schwarzenbach, R. P. and Haderlein, S. B., Carbon isotope fractionation in the reductive dehalogenation of carbon tetrachloride at iron (hydr)oxide and iron sulfide minerals. *Environ Sci Technol* **2005,** *39*, (15), 5634-41.

5.7 Appendix

The appendix contains additional information of the Material and Methods section, sorption isotherm of MOPS and HEPES (Figure A5.1), schematic reaction pathway of the oxidation of Fe(II) (Figure A5.2), ATR-FTIR spectra (Figure A5.3), overview of the transformation of CCl_4 (Table A5.1).

5.7.1 Material and Methods

Goethite

The iron mineral goethite (α-FeOOH) was purchased from Lanxess Germany GmbH as Bayferrox 920 Z. The storage was dry and cool as received under lab atmosphere. The goethite was characterized determining specific surface area (BET measurement), purity (X-ray diffraction), crystal morphology and particle size (scanning electron microscopy), total organic carbon and point of zero charge pH_{pzc} (Liu et al., 2007). The specific surface area was investigated by N_2 adsorption with a Gemini 2375 Surface Area Analyzer. The BET surface was $9.2\ m^2/g$ using the multi point BET measurement. X-ray diffraction (μ-XRD, Bruker-D8 with GADDS) showed that the sample did not contain impurities. Furthermore the crystal form and the particle size were determined by scanning electron microscopy (LEO 1550 VP) after sputter deposition on a thin gold layer and showed pure needle shaped crystals. The particle size ranged between 0.6 and 0.9 μm in length. The TOC (total organic carbon) content was with 0.01% near the detection limit (Hariba P100 with TOC Boat Sampler, detection limit 0.006%). The point of zero charge (pH_{pzc}) was determined with 6.5 ± 0.4 (Liu et al., 2007). The properties of the goethite were in the expected range except for the pH_{pzc} (lower than literature values).

Fe(II) Stock Solution

The preparation of the iron stock solution was performed by adding 3.63 g (0.065 mmol) metal iron (Fe(0)) to 100 mL of a 1 M HCl solution in a serum bottle (Zwank et al., 2005). The 1 M HCl solution was made anoxic before the experiments by bubbling nitrogen through a rubber stopper in the solution for 30 min (gas outlet for pressure release). The suspension was heated up to 80°C while gently stirring. After 2 hours no more hydrogen evolution was observed. The suspension was filtered within the glove box with a 0.2 μm PTFE filter to remove any residual metal iron. The exact content of Fe(II) was determined photometrically (562 nm) by the ferrozine assay (Stookey, 1970).

Analytical Methods

For quantitative analyses of CCl_4, $CHCl_3$ and C_2Cl_4 a TraceGC 2000 (ThermoFinnigan, Milano, Italy) gas chromatograph coupled to a TraceDSQ single quadrupole mass spectrometric detector (ThermoFinnigan, Austin, TX, US) was used. The injection was performed with a headspace method using a 2.5 mL gastight syringe (CTC-CombiPAL autosampler) and a split ratio of 1:50. For separation of the compounds an Rtx-VMS capillary column (60 m × 0.32 mm I.D., 1.8 μm film thickness, Restek Corp., Bellefonte, PA, US) was installed. The temperature of the column was initially hold at 40°C for 4 min, heated up to 100°C with a rate of 7°C/min and maintained at 150°C for another 5 min. For the mass spectrometer the electron impact ionization mode (EI) at 70 eV, a source temperature of 220°C and transfer line temperature of 250°C were applied. The scan mode was a full scan (m/z = 50-300). To avoid carry over, a gentle nitrogen stream was used to clean the syringe for 5 min after each injection. Data acquisition and processing were carried out using Xcalibur Data System Version 1.3 (ThermoFinnigan, Austin, TX, US).

Figure A5.1: Sorption isotherm of (▲) MOPS and (●) HEPES on goethite/Fe(II) surface at pH 7.
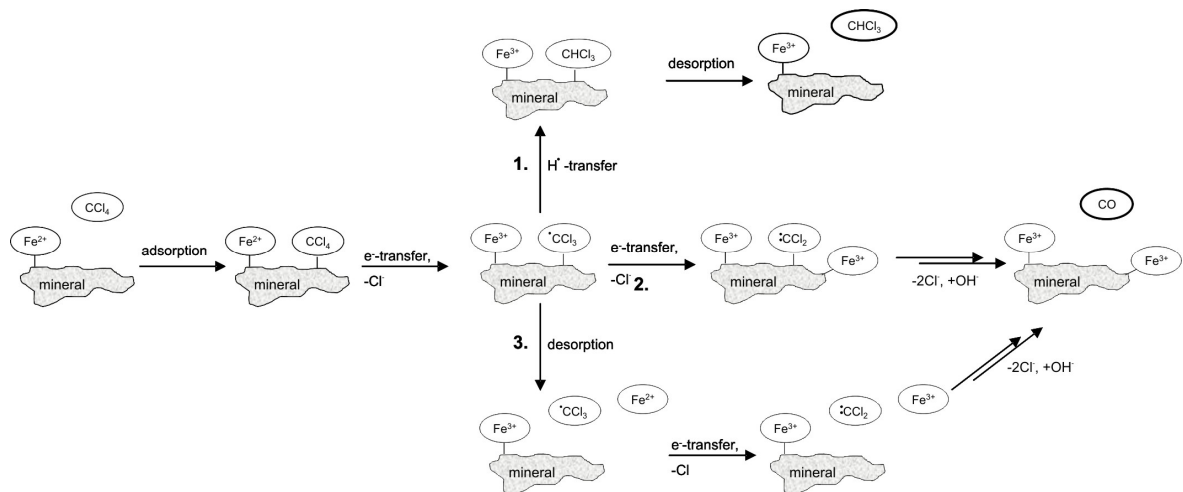
Figure A5.2: Schematic reaction pathway of the oxidation of Fe(II) and transformation of CCl₄: after reductive dehalogenation of CCl₄ to a ·CCl₃ radical (shown in the middle of the figure) on the mineral surface three pathways are possible: 1. transfer of a hydrogen radical or 2. further dehalogenation and hydrolysis or 3. desorption and following e-transfer in the suspension modified from Elsner and co-workers (Elsner et al., 2004).
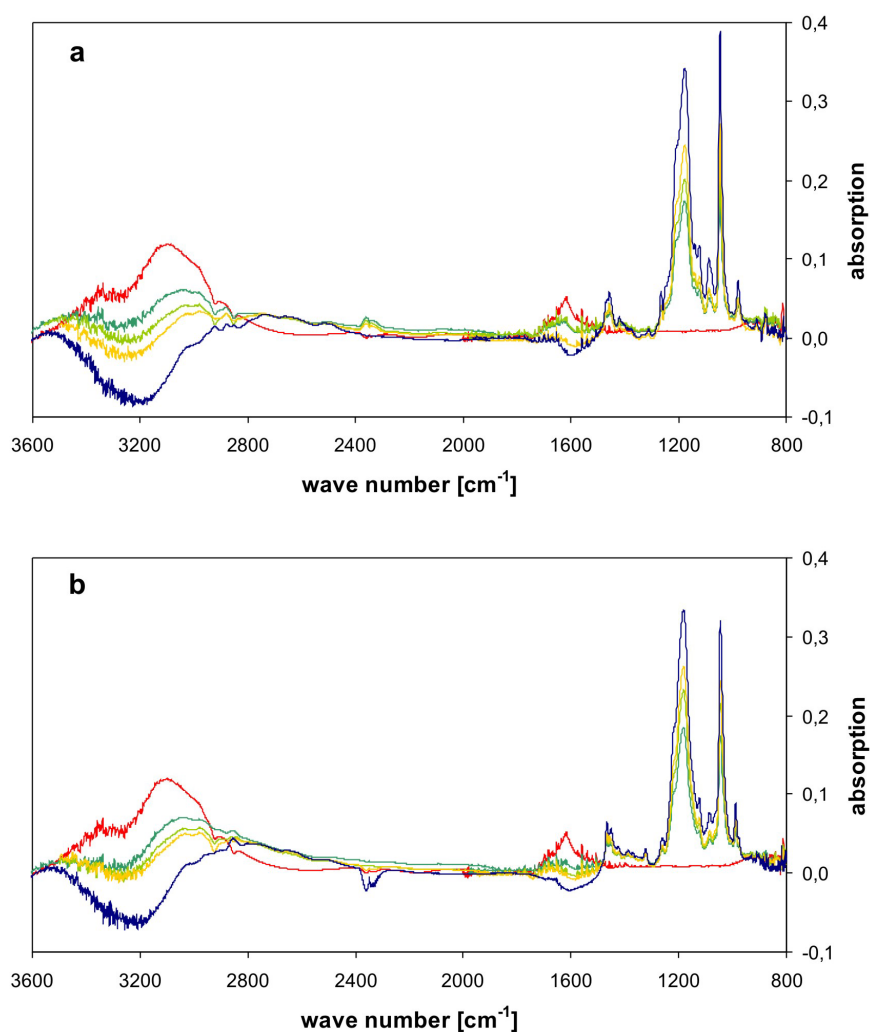
Figure A5.3: ATR-FTIR spectra of (a) MOPS (blue), complexes between Fe and MOPS: 1:1 (green), 1:2 (light green) and 1:3 (yellow) and Fe(II) (red); (b) HEPES (blue), complexes between Fe and HEPES: 1:1 (green), 1:2 (light green) and 1:3 (yellow) and Fe(II) (red). Relevant parts of the spectra are located between 2820 and 2760 cm^{-1} for N-CH$_2$ stretching and between 1300 and 1000 cm^{-1} for CN stretching. These spectra were obtained by subtracting a huge water background and were tricky for interpretation due to possible small changes of the samples.

Table A5.1: Overview of the relative formation of CHCl₃ and ration rate constants k′obs in the presence of the organic sorbates MOPS and HEPES.

system[a]	rel. formation $CHCl_3$ [%][b]	k'obs $[h*(m^2/L))^{-1}]$
goethite/Fe(II)	44.8	5.3×10^{-4}
+ 1 mM MOPS	65.4	2.6×10^{-4}
+ 10 mM MOPS	21.1	5.0×10^{-5}
+ 25 mM MOPS	4.4	5.1×10^{-5}
+ 50 mM MOPS	2.6	6.1×10^{-5}
+ 1 mM HEPES	49.3	4.5×10^{-4}
+ 10 mM HEPES	21.4	1.7×10^{-4}
+ 25 mM HEPES	8.7	1.1×10^{-4}
+ 50 mM HEPES	3.8	9.9×10^{-5}

[a] pH value of 7.05 ± 0.05
[b] relativ formation of $CHCl_3$ means $(CHCl_3)_t/((CCl_4)_0-CCl_4)_t)$ after 100 hours

References

Elsner, M., Haderlein, S. B., Kellerhals, T., Luzi, S., Zwank, L., Angst, W. and Schwarzenbach, R. P., Mechanisms and products of surface-mediated reductive dehalogenation of carbon tetrachloride by Fe(II) on goethite. *Environ Sci Technol* **2004,** *38*, (7), 2058-66.

Liu, C., Zachara, J. M., Foster, N. S. and Strickland, J., Kinetics of Reductive Dissolution of Hematite by Bioreduced Anthraquinone-2,6-disulfonate. *Environ. Sci. Technol.* **2007,** *41*, (22), 7730-7735.

Stookey, L. L., Ferrozine - a new spectrophotometric reagent for iron. *Anal. Chem.* **1970,** *42*, (7), 779-781.

Zwank, L., Elsner, M., Aeberhard, A., Schwarzenbach, R. P. and Haderlein, S. B., Carbon isotope fractionation in the reductive dehalogenation of carbon tetrachloride at iron (hydr)oxide and iron sulfide minerals. *Environ Sci Technol* **2005,** *39*, (15), 5634-41.

6. General Conclusion and Outlook

The main goal of the present work was to gain an improved understanding of heterogeneous redox reactions and phase transformation processes taking place at iron minerals in anoxic environments. In details the main objectives were (i) to monitor electron transfer processes at iron minerals by developing and applying the reactive isotope tracer approach, (ii) to characterize and investigate various iron minerals with respect to the oxidation of sorbed Fe(II) on the mineral surfaces and (iii) to evaluate the effects of geochemical conditions (pH, sorption time of Fe(II), organic sorbates) on the oxidation of Fe(II) on goethite surfaces and the isotope fractionation of the model oxidant CCl_4. The results may provide further insights into the occurrence and the dynamics of surface bound Fe(II) species involved in the redox reactions.

The analytical methods for the quantification and the compound specific isotope analysis (CSIA) used in this study were developed and could be further refined. For the quantification of the probe oxidant CCl_4 and the product $CHCl_3$, a GC-MS method was established and the sampling was improved using a headspace technique compared to liquid-liquid extraction with organic solvents (Elsner et al., 2004). Enrichment of the samples was necessary for isotope analysis and was performed by headspace-solid phase micro extraction (SPME) technique. This technique is known as fast, non-fractionating enrichment method for CSIA (Jochmann et al., 2006) and enables improved baseline separation of the compounds in comparison to liquid-liquid extraction (Elsner et al., 2004) and the purge & trap method (Zwank et al., 2005). Former studies (Elsner et al., 2004; Zwank et al., 2005) and the measurements in this thesis with the developed instrumental set-up implicated that the indirect method, the so-called "reactive isotope tracer

approach", seemed to be a suitable tool to characterize the properties and the dynamics of reactive iron species coating the mineral surfaces.

Batch experiments with various iron minerals suggested that the properties of iron minerals may have an influence on the oxidation of surface bound Fe(II) and subsequently on the product distribution and reaction rate constants of CCl_4. Well defined conditions (pH 7, 1 mM Fe(II)$_{aq}$, total surface area of minerals 50 m^2/L) were chosen for the batch experiments and the reaction rate constants decreased in the following order: goethite > hematite > magnetite/lepidocrocite as well as the product distribution changed comparing the goethite with the hematite system. Similar experiments were performed by Zwank et al. (Zwank et al., 2005) with regard to the total surface area of the goethite, the aqueous Fe(II) concentration and the pH. However, the amount of sorbed Fe(II) and the reactivity of surface bound Fe(II) differed. Due to different specific surface areas and pH$_{pzc}$, the surface site density might be one factor determining the initial surface reactivity of iron minerals. It could also be shown that the purity of the iron mineral phase may affect the reactivity of the experiments. The detection of highly reactive goethite impurities (5-10%) in the lepidocrocite system of Zwank et al. (Zwank et al., 2005) indicated a higher reactivity in this batch compared to the presented study. Therefore it is really essential to characterize the iron minerals carefully before using them in any experiments.

The pH dependency in a goethite system showed that enhanced Fe(II) adsorption occurred at higher pH values and resulted in a higher surface site density. Additionally further insights on the oxidation of surface bound Fe(II) were gained by using different oxidant concentrations at pH 7. The surface speciation of Fe(II) species changed significantly after only a small amount of sorbed Fe(II) species had been oxidized by CCl_4. This could be demonstrated by changes in (i) the product distribution of the transformation of CCl_4 by changes of the reaction mechanism, (ii) reaction rate constants of CCl_4 and (iii) isotope fractionation factors of CCl_4.

Furthermore the isotope fractionation factor as well as Mössbauer measurements indicted that two different classes of surface bound Fe(II) species were present on the mineral surface. Therefore the fractionation factors of probe oxidants like CCl4 seem to be a very sensitive tool for a better detection and understanding of the dynamics and nature of electron transfer and surface remodeling processes *in situ*.

The influence of organic buffers was investigated on the sorption and oxidation of surface bound Fe(II) species due to these buffers were commonly used to stabilize reaction conditions. While sorption of the organic buffers MOPS and HEPES was observed, simultaneously desorption of sorbed Fe(II) species could be verified. It can be concluded that the organic buffers may have a direct effect on the redox reaction of surface bound Fe(II) and contaminants (CCl4). The product distribution, reaction rate constants and the isotope fractionation of CCl4 on the iron mineral surface were also affected. Further investigations of the interaction between the organic buffers and the Fe(II)-iron mineral surface suggested that a complex formation took place only with the sorbed Fe(II) species on the mineral surface.

In summary, the hypothesis that distinct fractionation factors of CCl4 are characteristic for certain geochemical conditions, could not be proven. Even more, the oxidation of surface bound Fe(II) showed that the dynamic of iron mineral surfaces is higher than expected. Therefore the practical application of the experimentally gained fractionation factors for predicting geochemical conditions in the field is very limited or not feasible at all. Additionally, the potential effect of organic buffers on the electron transfer processes at iron mineral surfaces could be demonstrated. As these buffers are commonly used to stabilize reaction conditions in batch experiments, the results described here should be considered in future studies. Further investigations on the oxidation of surface bound Fe(II) are necessary

to obtain detailed information in more complex systems as they can be found in the environment. Therefore the influence of organic matter (NOM) and model compounds (Quinones) on the electron transfer at heterogeneous redox reaction should be further investigated in iron mineral systems.

6.1 References

Elsner, M., Haderlein, S. B., Kellerhals, T., Luzi, S., Zwank, L., Angst, W. and Schwarzenbach, R. P., Mechanisms and products of surface-mediated reductive dehalogenation of carbon tetrachloride by Fe(II) on goethite. *Environ Sci Technol* **2004,** *38*, (7), 2058-66.

Elsner, M., Schwarzenbach, R. P. and Haderlein, S. B., Reactivity of Fe(II)-bearing minerals toward reductive transformation of organic contaminants. *Environ Sci Technol* **2004,** *38*, (3), 799-807.

Jochmann, M. A., Kmiecik, M. P. and Schmidt, T. C., Solid-phase dynamic extraction for the enrichment of polar volatile organic compounds from water. *J Chromatogr A* **2006,** *1115*, (1-2), 208-16.

Zwank, L., Elsner, M., Aeberhard, A., Schwarzenbach, R. P. and Haderlein, S. B., Carbon isotope fractionation in the reductive dehalogenation of carbon tetrachloride at iron (hydr)oxide and iron sulfide minerals. *Environ Sci Technol* **2005,** *39*, (15), 5634-41.

List of Figures and Tables

List of Abbreviations

‰	permil
BET	Developed by *B*runauer, *E*mmett and *T*eller
CHC	Chlorinated hydrocarbons
CSIA	Compound specific isotope analysis
CT (CCl_4)	Tetrachloromethane (Carbon tetrachloride)
EA	Elementar analyzer
f	Fraction of remained contaminant
Fe(II)	Ferrous iron
Fe(III)	Ferric iron
Fe_2O_3	Hematite
Fe_3O_4	Magnetite
GC	Gas chromatography
HCl	Hydrochloric acid
HEPES	4-(2-hydroxyethyl)-1-piperazineethanesulfonic acid
IRMS	Isotope ratio mass spectrometry
K	Kelvin
k'_{obs}	Reaction rate constant
MOPS	3-(N-morpholino) propane-1-sulfonic acid
^{NA}Fe	Natural abundant iron
NaOH	Sodium hydroxide
PCE (C_2Cl_4)	Tetrachloroethane
pH_{pzc}	Point of zero charge
PTFE	Polytetrafluoroethylene (Teflon)
rpm	Rounds per minute
SEM	Scanning electron microscopy
SPME	Solid-phase microextraction
TCM ($CHCl_3$)	Trichloromethane (Chloroform)

TOC	Total organic carbon
VPDB	Vienna Pee Dee Belemnite
XRD	X-ray diffraction
α	Fractionation factor
α-FeOOH	Goethite
γ-FeOOH	Lepidocrocite
ε	Enrichment factor

Curriculum Vitae

Persönliche Daten

Name	Anke Buchholz, geb. Schmidt
Geburtsdatum	6. Oktober 1980
Geburtsort	Saulgau

Ausbildung

1987 – 1991	Berta Hummel-Grundschule in Saulgau
1991 – 2000	Störck-Gymnasium in Bad Saulgau, Abitur (28. Juni 2000)
2000 – 2005	Studium der Chemie in Tübingen
10/2002	Vordiplom in Chemie (07. Oktober 2002)
06/2005 – 12/2005	Diplomarbeit, Abteilung Bioanalytik und Pharmakologie, Titel: „Massenspektrometrische Untersuchungen zum Metabolismus von Piritramid durch LC-MS-Kopplung", Betreuer: Prof. C. Gleiter und Dr. B. Kammerer
12/2005	Diplom in Chemie mit Wahlpflichtfach „Pharmakologie und Toxikologie" (15. Dezember 2005)
02/2001 – 03/2001	Praktikum bei Labor Dr. Gärtner in Weingarten
10/2002 – 07/2004	wissenschaftliche Hilfskraft an der Universität Tübingen, Fakultät für Chemie, Betreuung von Praktika
09/2004 – 10/2004	Praktikum bei Boehringer Ingelheim in Biberach an der Riss, Abteilung Drug Metabolism and Pharmacokinetics
2006 – 2009	Promotion am Zentrum für Angewandte Geowissenschaften (ZAG), Bereich Umweltmineralogie und Umweltchemie in Tübingen, Betreuer: Prof. S. Haderlein

Veröffentlichungen

2007	Schmidt A., Haderlein S.B., Characterization of redox reactions and phase transformation processes at iron minerals surfaces. *EMU Summer School*, München, Posterpräsentation.
	Schmidt A., Haderlein S.B., Effect of pH on the reaction rates and isotope enrichment factors of redox reactions at iron mineral surfaces using compound-specific isotope analysis. *Workshop "Biogeochemical processes in groundwater systems"*, München, Posterpräsentation.
	Schmidt A., Haderlein S.B., Compound specific isotope analysis as a tool to investigate redox reactions and reactive surface species at iron mineral surfaces. *Stable Isotope Conference*, Ascona, Schweiz, Posterpräsentation.
2008	Schmidt A., Haderlein S.B., Influence of pH and organic buffers on the oxidation of Fe(II) by CCl_4 at iron mineral surfaces studied by compound specific isotope analysis. *Workshop "Electron transfer processes at biogeochemical gradients"*, Leipzig, Posterpräsentation.
	Schmidt A., Haderlein S.B., Oxidation of Fe(II) by CCl_4 at iron mineral surfaces influenced by pH and organic buffers: a compound specific isotope analysis study. *EGU General Assembly*, Wien, Österreich, Posterpräsentation.
2009	Schmidt A., Haderlein S.B., Oxidation of Fe(II) by CCl_4 at iron mineral surfaces studied by compound specific isotope analysis. *ACS Spring 2009 National Meeting*, Salt Lake City, Utah, USA, Vortrag.

2009 (Forts.)   Buchholz A., Haderlein S.B., Effect of environmental factors on the oxidation of Fe(II) at goethite monitored by carbon isotope fractionation of CCl_4. *Environmental Science & Technology*, eingereicht.

                       Buchholz A., Laskov C., Haderlein S.B., Effects of organic buffers on the sorption and oxidation of ferrous iron at goethite. *Environmental Science & Technology*, eingereicht.